THE UNIVERSITY OF ALBERTA

MECHANISMS OF RAPID ADAPTATION IN AN INSECT MECHANORECEPTOR NEURON

by

© PÄIVI HELENA TORKKELI

A thesis submitted to the Faculty of Graduate Studies and Research in partial fulfilment of the requirements fc. the degree of **Doctor of Philosophy**.

DEPARTMENT OF PHYSIOLOGY

EDMONTON, ALBERTA

SPRING 1995

ISBN   0-612-01767-2

Canada

UNIVERSITY OF ALBERTA

RELEASE FORM

NAME OF AUTHOR: Päivi Helena Torkkeli

TITLE OF THESIS: Mechanisms of rapid adaptation in an insect

                        mechanoreceptor neuron

DEGREE: Doctor of Philosophy

YEAR THIS DEGREE GRANTED: Spring 1995
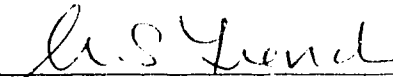
Päivi H. Torkkeli
Dalhousie University
Department of Physiology and Biophysics
Halifax, Nova Scotia
B3H 4H7
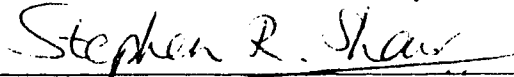
Date _25 October 1994_

THE UNIVERSITY OF ALBERTA

FACULTY OF GRADUATE STUDIES AND RESEARCH
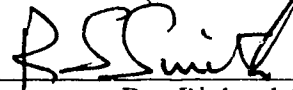
The undersigned certify that they have read, and recommend to the Faculty of Graduate Studies and Research, for acceptance, a thesis entitled **MECHANISMS OF RAPID ADAPTATION IN AN INSECT MECHANORECEPTOR NEURON** submitted by PÄIVI HELENA TORKKELI in partial fulfilment of the requirements for the degree of DOCTOR OF PHILOSOPHY.
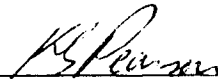
_____
Dr. Andrew S. French (Supervisor)
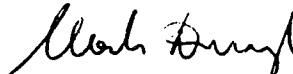
_____
Dr. Stephen R. Shaw (External examiner)
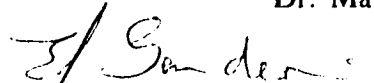
_____
Dr. Richard S. Smith

_____
Dr. Keir G. Pearson

_____
Dr. Marek Duszyk

_____
Dr. Esmond J. Sanders (Chairman)

Date: 20 Sept 1994

This thesis is dedicated to the memory of my father, Reino.

ABSTRACT

The femoral tactile spine of cockroach (*Periplaneta americana*) belongs to a group of insect mechanosensilla that have a bipolar sensory neuron, the dendritic part associated with the cuticle. Previous research described the rapidly adapting response of this neuron as an example of power-law behaviour.

In this thesis the original extracellular experiments with mechanical stimulation were repeated using long observation times and a log-binning method that was originally developed to study the distribution of ion channel dwell times. This examination indicated, that adaptation in the tactile spine neuron actually follows a multiple exponential time course.

The location of electrical excitability in the tactile spine neuron was studied by measuring the threshold for electrical stimulation as a function of spatial position in the spine lumen. The spine was then fixed and serially sectioned for computer-aided reconstruction. Alignment of threshold measurements with reconstructions produced maps of excitability around the neuron. The lowest threshold was always found close to the sensory dendrite or the adjacent soma, but the electrode could not be located near the axon. These results indicated that the intracellular recordings are done in the soma or basal part of the dendrite.

The ionic mechanisms underlying rapid adaptation in the tactile spine neuron were studied using the discontinuous single-electrode current- and voltage-clamp methods. These techniques did not allow an investigation of the inward currents, but when the inward currents were blocked by TTX it was possible to record the outward currents in the soma. This examination revealed three types of K^+-currents, each of which plays an important role in the behaviour of the neuron. A delayed rectifier type of K^+-current was the sole component of action potential repolarization while an A-type K^+-current had an important function in the regulation of the intervals between action potentials during moderate stimulation. A Ca^{2+}-sensitive K^+-current was the most important component of adaptation, increasing in effectiveness during stronger depolarizations.

ACKNOWLEDGEMENTS

INDEX

Chapter

LIST OF TABLES

LIST OF FIGURES

Chapter 6.

Appendix

LIST OF SYMBOLS

Units

ap/s	rate; action potentials/second
C	charge; coulombs
°C	temperature; degrees Celsius
h	time; hours
Hz	frequency; Hertz
K	temperature; Kelvin
kHz	frequency; kilohertz
M	concentration; molar
min	time; minutes
mm	length; millimeters
mm^2	area; square millimeters
mM	concentration; millimolar
ms	time; milliseconds
mV	voltage; millivolts
$M\Omega$	resistance; megohms
nA	current; nanoamperes
pA	current; picoamperes
nm	length; nanometers
μm	length; micrometers
μm^2	area; square micrometers
μm^3	volyme; cube micrometers
μM	concentration; micromolar
Ωcm^2	resistivity; ohms times centimeters squared
pF	capacitance; picofarads
pS	conductance; picosiemens
s	time; seconds
μs	time; microseconds
μV	voltage; microvolts
V	voltage; volts

Acronyms

A1 and A2	amplifiers in dSEVC and dSECC
AHP	After hyperpolarization
4-AP	4-aminopyridine
AX	axon
Bit	binary digit
BB	basal body
BK-channels	large-conductance Ca^{2+}-sensitive K^+-channels

.

CCS	controlled current source in dSEVC
Choline-Cl	Choline chloride
CTX	charybdotoxin
DC	direct current
dSECC	discontinuous single-electrode current-clamp method
dSEVC	discontinuous single-electrode voltage-clamp method
DS	dendritic sheath
DUM-neuron	dorsal unpaired median neuron
GL	glial cell
IK-channel	intermediate-conductance Ca^{2+}-sensitive K^+-channel
K_{Ca}-channel	Ca^{2+}-sensitive K^+-channel
LU	spine lumen
MOPS	morpholinopropanesulfonic acid
PBS	phosphate buffered saline
RLC	Receptor lymph cavity
SA	socket attachment
SH1	sample-and-hold device
S1	switch between the voltage-recording and current-passing modes of dSEVC and dSECC
S2	switch between voltage- and current-clamp in dSEVC
S.D.	standard deviation
SO	soma
SK-channels	small-conductance Ca^{2+}-sensitive K^+-channels
TB	tubular body
TEA	tetraethylammonium chloride
TEP	transepithelial potential
TP	terminal plug
TS	tactile spine
TTL	transistor transistor logic
TTX	tetrodotoxin

Other symbols

α	relative amplitude of two inactivation components
a	initial rate (ap/s); constant related to the sensitivity of the neuron
b	integral of the action potentials over time
β	$\ln(\tau)$
c	constant of integration
d	a fractional exponent of time
d.f.	degree of freedom (number of experiments minus 2 in correlation analysis)
e	elementary charge $(1.602 \times 10^{-19}C)$
e	exponential

E_{rev}	reversal potential of a current
f_e	upper cut-off frequency of the electrode
f_f	upper cut-off frequency of the low-pass filter used in current recording in dSEVC and dSECC
f_m	upper cut-off frequency of the membrane
f_s	sampling frequency of the data collection system in dSEVC and dSECC
f_{sw}	switching frequency of dSEVC and dSECC
$G(x)$	log bin distribution function
g_T	gain of CCS in dSEVC
g	conductance
$g(x)$	log bin rate function
g_0	log bin generic function
g_{max}	maximum conductance
I	current
I_0	current flowing into the cell via microelectrode in dSEVC
I_A	transient outward current, A-current
I_K	delayed rectifier potassium current
$I_{K(Ca)}$	calcium activated potassium current
I_{leak}	leakage current
I_{Na}	sodium current
I_∞	current level expected in the absence of inactivation in Boltzmann equation
k	Boltzmann's constant ($1.382 \times 10^{-23} VCK^{-1}$)
$[K^+]_{in}$	intracellular K^+-concentration
$[K^+]_{out}$	extracellular K^+-concentration
m	integer exponent in exponential power equation
n	constant
Na^+-pump	electrogenic sodium pump
p	probability
pH	acidity
r	correlation coefficient
R_m	membrane resistance
T	absolute temperature ($273.16\ °C = K$)
s	slope factor
t	time
Δt	time interval
τ	time constant
τ_1	activation time constant of a current
τ_2 and τ_3	inactivation time constants of a current
V_{50}	membrane potential at half maximal activation or inactivation
V_{ave}	average value of V_{ms} in the dSEVC
V_c	command voltage in dSEVC
V_e	electrode potential

V_H	holding potential
V_1	command voltage in dSECC
V_m	membrane potential
V_{ms}	sampled voltage in dSEVC
x	$\ln(t)$
y	action potential rate
z	valency of the equivalent gating charge
z	$x - \beta$

1. GENERAL INTRODUCTION

The detection of external or internal mechanical stimuli is not only crucial to clearly sensory functions, like hearing, balance and touch, but also to various other physiological mechanisms that lead to behavioral activities, including locomotion, posture, feeding, orientation and mating. For example, muscle contraction, joint rotation, cardiovascular and gastro-intestinal functions all use mechanically sensitive cells to detect mechanical changes in their environment.

The mechanoreceptor cell itself and its surrounding tissues are the sites of the three major components of mechanotransduction: **1.** Mechanical deformations are coupled to the receptor cell (**mechanical coupling**) and **2.** converted to changes in ionic conductance in the cell membrane that produce the receptor or generator potential (**transduction**). Mechanoelectric transduction is believed to be mediated by specialized ion channels that open in response to deformation of the cell membrane. **3.** Opening of these stretch-activated channels depolarizes the cell locally and this depolarization spreads to the site where the conducted action potentials are initiated (**encoding**). Modification of the time course of the final signal (**adaptation**) could be due to dynamic processes in any of these three stages.

Although some mechanoreceptors respond continuously to a maintained stimulus, most demonstrate some reduction of response. Many show strong reduction in action

1

potential firing after a step change in deformation and some cease firing completely unless the stimulus is changed. This phasic behavior, or adaptation could serve several purposes. In some cases, the receptor may only be used to detect novel stimuli, in others only rapidly changing stimuli, such as vibration may be of interest. Finally, adaptation can be used to adjust the sensitivity of a receptor to a range of stimulus amplitudes.

In the work described here, I examined the adaptation mechanisms of one mechanoreceptor cell, the cockroach tactile spine neuron. This neuron is one of the mechanoreceptors in the insect exoskeleton that makes it possible for the animal to perceive its external mechanical environment, in spite of the hard cuticle forming the outermost surface. The functions of tactile spines have not yet been established. Their sensory role is probably to act as perimeter detectors, because they surround the outside of the animal during its normal postures. However, they may also serve a purely mechanical function. Their positions and angles of articulation would favour forward movement of the animal and oppose reverse movements. This could be useful in moving through confined spaces or in resisting predators that try to remove them from such places.

The tactile spine neuron has been classified as a phasic mechanoreceptor because of its ability to adjust rapidly to a constant stimulus, indicating that it functions to detect changes in its immediate environment, that do not need to be observed after their initial occurrence. In the remaining part of this introductory chapter, I describe the different

types of insect mechanosensilla (section 1.1), outline the three processes leading to mechanoreception (section 1.2) and review present models of adaptation (section 1.3) in mechanoreceptor cells. In section 1.4, I briefly review previous research concerning the structure and function of the tactile spine neuron, and in section 1.5 I outline the original research that forms the main subject of this thesis.

1.1. Insect mechanosensilla

Insect mechanoreceptors can be divided into two main groups **Type I** and **Type II** (McIver 1985). Type I receptors are bipolar neurons with ciliary structures in their dendrites, which are associated in some way with the cuticle. Their dendritic region is separated from the hemolymph and bathed in a fluid whose composition is controlled by specialized epithelial cells, the sheath cells, surrounding the dendrite. Type II neurons are multipolar and they do not have a visible ciliary structure in the dendrites. Their dendrites are exposed to hemolymph and they are usually associated with connective tissue, the inner surface of the body wall, muscles, or the walls of the alimentary canal, but not the cuticle (McIver 1985). The widely studied crayfish abdominal stretch receptors belong to the latter group.

The three basic sub-classes of Type I sensilla are **chordotonal organs**, **campaniform sensilla** and **trichoid sensilla**. They may occur singly, in small groups or in large groups that function as specialized organs. However, they are all basically holes

3

in the cuticle covered by a membrane to which the sensory dendrite is attached. The various cuticular auxiliary structures provide a high sensitivity to deformation, even in response to very small forces (Barth 1981, McIver 1985). The trichoid and campaniform sensilla are regarded as cuticular mechanoreceptors, because both of them have clear external cuticular components (McIver and Siemicki 1975). The chordotonal organs lack a cuticular component, but they are connected to the cuticle by supporting cells. Chordotonal organs can be simple single-cell structures like the cuticular sensilla, but they often form highly developed organs such as the Johnston's or tympanal organs, that detect vibration and function as the "ears" of insects (McIver 1985). The trichoid sensilla have a cuticular part that can take the form of a hair, scale, filament or peg and they may function solely as a mechanosensillum or be associated with chemosensilla. Campaniform sensilla usually appear as a small cuticular cap surrounded by a ring of raised cuticle and they function as proprioceptors responding to strains in the exoskeleton (McIver 1985).

Two or more non-neural sheath cells surround the neurons of cuticular mechanosensilla. They are named according to their morpho-genetic function of secreting certain parts of the cuticular apparatus of the sensillum: The trichogen cell produces the dendritic sheath during development and also creates the shaft of the hair or equivalent structure as well as the "cup" and "strut" which are important in the spatial orientation of the dendrite. The tormogen cell generates the socket region (McIver 1985). These non-neural cells of a sensillum delimit a cavity beneath the cuticle into which the ciliary outer segment(s) of the sensory cell(s) protrude. This fluid-filled extracellular space, the

4

receptor lymph cavity (RLC), is separated from the hemolymph space (Nicklaus et al. 1967).

1.2. Information processing in mechanoreceptors

Mechanical coupling

A movement stimulus is coupled to the membrane of the neuron by mechanical components. In all mechanoreceptors, amplification or reduction of the primary signal is achieved by some kind of physical coupling of the sensory cell to the site of stimulation. For example, the hairs on human skin provide a leverage that makes it possible for the receptor cells at the base of the hairs to detect small movements of the tip of the hair (Mountcastle et al. 1972). The specialization of different insect mechanosensilla to detect different kind of stimuli arises from the great variety of external structures associated with the sensory cells (French 1988).

In all types of insect mechanosensilla, the sensory dendrite is believed to be deformed in response to mechanical stimuli and only 1 - 10 nm deformation is required to produce activity (Thurm 1965; French 1988; French 1992). A dense arrangement of microtubules in the tips of these dendrites probably functions as a rigid cytoskeleton (Rice et al. 1973). However, the idea that microtubules are crucial to transduction (Moran and Varela 1971; Schafer and Reagan 1981) was proved inaccurate when

5

mechanotransduction and even the dynamic behavior of these receptors remained

unchanged after microtubules were removed (Erler 1983, Kuster et al. 1983).

Transduction

The process by which the mechanical stimulus is converted to an electrical

response in the form of a receptor or generator potential is called transduction (McIver

1985, French 1988). In insect cuticular mechanosensilla, the microvilli on the apical

membranes of the tormogen cells transport potassium so that the K^+-concentration rises

and generates a positive potential in the extracellular space surrounding the sensory

dendrite. This **transepithelial potential** difference (TEP) lies between 20 and 80 mV,

with the cuticular side positive. It decreases with adequate stimulation and is very

dependent on oxidative metabolism. For example, the K^+-concentration of the RLC of

campaniform sensilla on the fly haltere is thirteen times higher than that of the

hemolymph (Küppers 1974). This arrangement produces a very small potassium ion

concentration gradient across the nerve cell membrane but its transmembrane potential

is about 140 mV (if the intracellular potential with respect to the hemolymph is -70 mV).

Under these conditions, the opening of potassium-selective mechanically-activated ion

channels in the dendrite would lead to a large inward receptor current (French 1988).

This arrangement is comparable to the situation in the inner ear of vertebrates or the

lateral line organ of aquatic amphibians, whose apical ends are also immersed in a high

K^+ solution (Howard et al. 1988). Although the receptor currents of these insect neurons

6

have never been directly recorded, measurements of transepithelial potentials and ionic concentrations, as well as biochemical, morphological and histological data, suggest that the receptor current is mostly carried by potassium ions (French 1988).

Patch-clamp recordings have revealed mechanically-sensitive ion channels in several types of cells e.g. myoblasts (Guharay and Sachs 1984), endothelial cells (Lansman et al. 1987) and bacteria (Martinac et al. 1990). Crayfish stretch receptor neurons (Erxleben 1989) and cultured insect chordotonal organs (Stockbridge and French 1989) also have been shown to possess stretch-activated channels, but direct evidence about their role in mechanotransduction has not yet been obtained.

Encoding

When the receptor potential depolarizes the membrane above the threshold level, a train of action potentials with specific temporal characteristics is produced. Action potential encoding is seen in almost all mechanoreceptors of vertebrates and invertebrates. Where studied, it is found to be based on a similar combination of voltage-sensitive sodium and potassium currents to that originally described by Hodgkin and Huxley (1952a and b) in the squid axon and later described in almost all nerve cells (Hille 1992). They have also been described in detail for several mechanoreceptor cells (French and Torkkeli 1994).

7

1.3. Mechanisms of adaptation

With a maintained stimulus the responses of all receptors including mechanoreceptors decay in time. The adaptation properties of different mechanoreceptor types are variable: in Pacinian corpuscles, a skin mechanoreceptor of mammalia (Loewenstein and Mendelson 1965) and in spider slit sensilla (Seyfarth and French 1994) a prolonged stimulus only yields one or two action potentials, but in both the crayfish slowly- and rapidly- adapting abdominal stretch receptors, prolonged stimulation produces a train of action potentials, the frequency of which adapt at a different speed (Nakajima and Onodera 1969b).

Theoretically adaptation could occur at any or all stages of the transformation of the mechanical stimulus into a discharge of nerve impulses: **1.** transmission of mechanical deformation to the dendrite of the neuron, **2.** transduction of membrane deformation into electric current, **3.** electrotonic spread of the current from the dendrites to the soma and the axon, and modification of this current by passive membrane properties and voltage activated channels, **4.** current-induced depolarization of the electrically excitable membrane of the axon, leading to the generation of action potentials. Although time-dependent properties have been reported for some stretch-activated channels (French 1992; Hamill and McBride 1994), adaptation has not yet been shown at the transduction stage for any mechanoreceptor.

8

Dynamic modification of the signal can occur before or during the encoding process. The Pacinian corpuscle is often used as an example of a receptor cell whose receptor potential adapts, because removal of mechanical components reduced the adaptation (Mendelson and Loewenstein 1964). However, this treatment did not eliminate the rapid adaptation of the action potential discharge, indicating that at least part of the adaptation occurs at the stage of action potential encoding. The different adaptation speeds in the slowly and rapidly adapting stretch receptors of crayfish have been shown to be caused by separate ionic processes in the action potential encoding mechanism (Nakajima and Onodera 1969b).

Several mechanisms of adaptation during action potential encoding have been described: 1. Action potentials increase the intracellular Na^+-concentration and this can stimulate an **electrogenic Na^+-pump** that hyperpolarizes the membrane, causing an increase in the threshold for spike excitation (Nakajima and Takahashi 1966; Sokolove and Cooke 1971; Edman et al. 1983). This mechanism has been described, for example, in the slowly adapting crayfish stretch receptor (Nakajima and Takahashi 1966; Teorell 1971). The magnitude of the afterhyperpolarization that follows a spike burst (AHP) increases with the number of preceding action potentials and decays with an exponential time course (Sokolove and Cooke 1971). However, all mechanoreceptors do not have an AHP. For example, the rapidly adapting stretch receptor of crayfish actually depolarizes after the spike burst (Nakajima and Onodera 1969a and b). **2. A slow Na^+-inactivation** has been shown to raise the spike threshold and to lead to adaptation in the lobster

(Narahashi 1964) and frog axon (Vallbo 1964). It has never been clear whether this phenomenon is produced by the same Na^+-channels that generate the rapid upstroke of an action potential and have several components of inactivation, or by a separate group of Na^+-channels. **3.** A voltage-dependent Ca^{2+}-current produces a Ca^{2+} influx, for example, in frog muscle spindles in response to depolarization, and the increase in intracellular Ca^{2+}-concentration activates **a Ca^{2+}-activated K^+-current**, $I_{K(Ca)}$, which reduces the effectiveness of the depolarizing stimulus and increases the threshold for action potential generation (Nakajima and Onodera 1969a; Ito and Komatsu 1979; Ito et al. 1982; Lewis and Wilson 1982; Ottoson and Swerup 1985a and b). $I_{K(Ca)}$ has been shown to participate in the AHP of several different neurons (Hille 1992).

1.4. The cockroach tactile spine

The distal-most femoral tactile spine on the cockroach (*Periplaneta americana*) leg has been a subject of research for several decades. The first description of the response of this nerve ending to mechanical stimulation was given by Pumphrey (1936) and during the following decades the tactile spine provided a useful research subject for studying the impulse frequency modulation of a mechanoreceptor neuron (Pringle and Wilson 1952; Chapman and Smith 1963; French 1988; French 1992). Extracellular recording of action potentials in response to mechanical or electrical stimulation is simple in this preparation, and that has made it possible to use it routinely, even for student laboratories (Linden and Palka 1992).

10

The tactile spine itself is not innervated, but its movements stimulate a single sensillum that is located in the wall of the tactile spine at the junction with the articular membrane (Chapman 1965). The ultrastructure of the sensory ending has been studied by scanning and transmission electron microscopy (French and Sanders 1981) and the morphologies of complete neurons have been reconstructed by serial sectioning (French et al. 1993a). A diagrammatic illustration of a longitudinally sectioned tactile spine based on these studies is shown in Fig. 1.1. Inside the flexible socket, the spine can move in all directions, but the neuron has been shown to give the strongest responses to deflection of the spine towards the femur as well as axially into the socket (French 1980). The size and shape of the soma varies significantly between different preparations, but the morphology of the axon and dendrite are more consistent (French et al. 1993a). The dense glial wrapping of the neuron, especially around the somatic part, creates a barrier that interferes with the access of chemical agents to the cell and also makes it difficult to penetrate the neuron by intracellular glass microelectrodes.

French and Sanders (1981) suggested the use of the term "socket sensillum" for the tactile spine sensory apparatus, because it does not very clearly fall into any of the three groups of insect mechanosensilla described earlier. It most closely resembles the campanife sensilla, but it does not have the typical dome or bell shaped structure, since the terminal plug is relatively thick. This plug is apparently moved directly by the socket attachment as the spine is deflected rather than sensing strain of the cuticle, as is

11
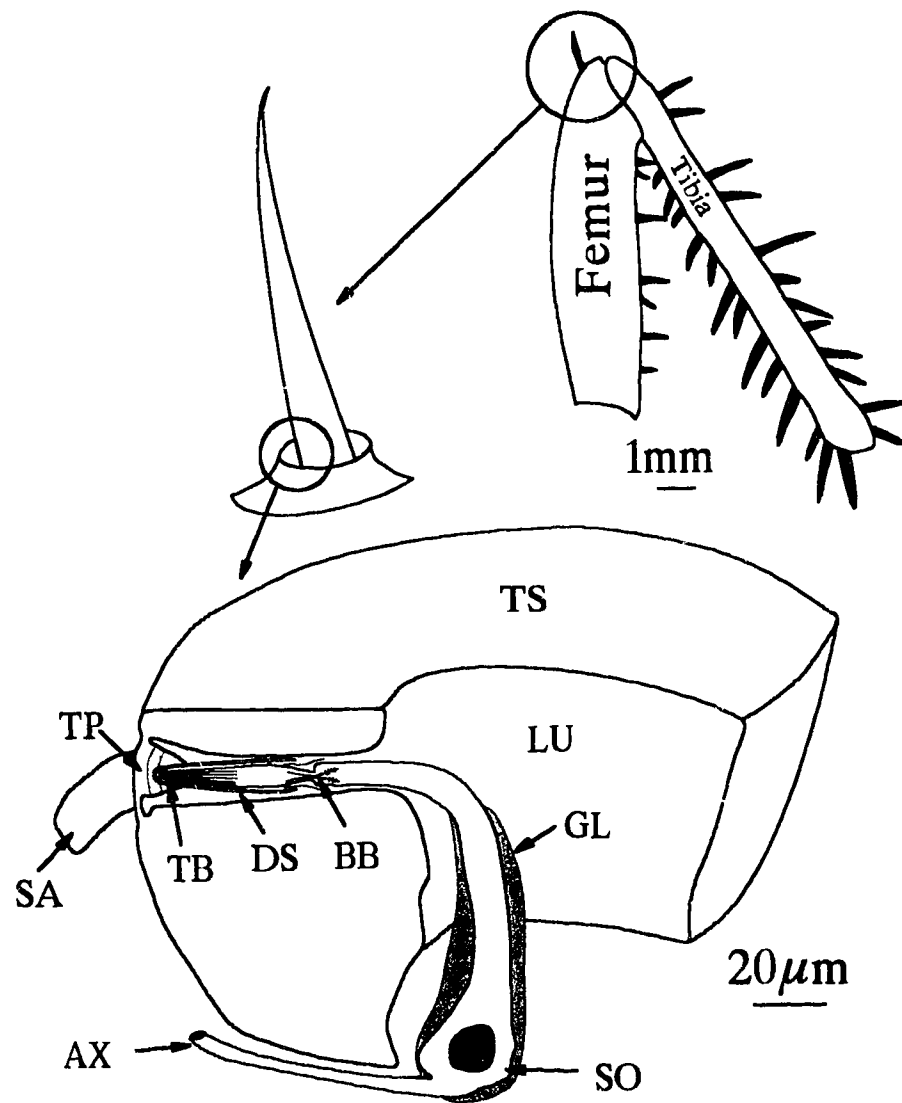
Figure 1.1. Femur and tibia of a metathoracic cockroach leg (*top right*). The tibia has more than 20 tactile spines, but only one long spine is located on the dorsal surface of the femur. The tactile spine lies in a flexible socket (*top left*) and the detailed diagram of the base of the spine (TS) (*lower*) shows that the sensory neuron inside the spine lumen (LU) is bipolar with a dendrite turning into the canal in the spine wall. The distal part of the ciliary basal body (BB) is surrounded by a dendritic sheath (DS). In the cytoplasm of the distal dendrite, the microtubules terminate in a tubular body (TB). The dendrite ends in the lamellar structure of the terminal plug (TP) that consists of several layers of cuticle. The trichogen and tormogen cells that surround the dendrite can not be seen at this magnification. The socket attachment (SA) is connected from the terminal plug to the adjacent socket wall. Especially the soma (SO), but also other parts of the neuron are surrounded by glial (GL) cells and the axon (AX) proceeds inside to the femur (Modified from French and Sanders 1983, French et al. 1993a).

12

the case in campaniform sensilla. Strain detection is unlikely to be significant, because of the thickness of the spine wall (Chapman 1965).

Pringle and Wilson (1952) examined the rapidly adapting behaviour of the tactile spine receptor, and found that the adapting response to a step deflection could be fitted by the sum of at least three exponential processes. Later it was shown by Chapman and Smith (1963), that a power law relationship also provided a good fit to the step response. Although the power law behaviour was subsequently observed in a wide range of receptors, including both insect Type I and Type II mechanosensilla, and photoreceptors of insects, as well as vertebrates (Thorson and Biederman-Thorson 1974) the physiological basis of this relationship has never been explained satisfactorily.

Rapid adaptation in the tactile spine receptor was shown to be produced by the action potential encoding mechanisms by French (1984a). He recorded extracellularly the decrementally conducted receptor potential in the receptor axon under subthreshold conditions and concluded that there was no phase difference between movement and receptor potential over a wide frequency range. The transduction of movement to receptor current produced a low-pass frequency response, instead of the high-pass frequency response seen in the action potential discharge, reflecting the decremental conduction of current along the axonal cable. This indicated that neither adaptation nor other dynamic modification of the signal occurred during coupling or transduction. This theory was later supported by the finding that direct electrical stimulation of the sensory

13

cell axon produced a dynamic response that was identical to the response given by mechanical stimulation (French 1984b). Following these discoveries, the focus of succeeding research into the adaptation properties of the tactile spine neuron in this laboratory has been directed at the action potential encoding mechanisms.

The analysis of the ionic currents contributing to encoding and adaptation in the tactile spine neuron has proved to be technically difficult. The results of the first intracellular recordings describing the properties of action potential discharge were published by Basarsky and French (1991). Before that, all the work was performed using extracellular recording techniques. A major problem in all of these experiments has been the strong barrier around the neuron, preventing the diffusion of chemicals to its extracellular space. This makes it difficult to use pharmacological agents to reveal the ion channel types contributing to rapid adaptation. Nevertheless, some important findings have been made. Extracellular experiments suggested that there are two main components of adaptation; the slow inactivation of sodium current and an electrogenic sodium-pump (French 1987; 1989a and b; Ramirez and French 1990; Basarsky and French 1991). In contrast, no clear evidence for the participation of potassium or calcium currents to adaptation was found (French 1984c; 1986a and b), even though calcium-activated potassium conductances have been shown to be one of the main components of adaptation in several other cell types (Hille 1992).

14

Extracellular recordings revealed an afterhyperpolarization following a burst of action potentials (French 1984c). The amplitude of this AHP increased with the number of action potentials in the burst and was eliminated by application of ouabain and blockers of calcium channels. Ouabain is a cardiac glycoside which inhibits the sodium pump (Glynn 1957, Hobbs 1982) and it was later shown to selectively block the slow component of threshold change underlying rapid adaptation (French 1989b). However, the identification of an electrogenic pump is difficult even under ideal conditions. Inhibition of the pump by ouabain or other cardiac glycosides leads to the accumulation of potassium ions in the extracellular space and results in the activation of potassium channels that, in turn, leads to significant depolarization of the membrane (Läuger 1991). In extracellular recordings the effect of ouabain on the resting potential can not be detected.

Cobalt and cadmium ions inhibit the entry of calcium into the cell (Adams 1982) and thus hinder the activation of any calcium-activated potassium conductance. Their effect on the AHP in the tactile spine neuron suggested the involvement of a calcium-activated potassium conductance in the adaptation. However, subsequent work failed to prove conclusively that cobalt or cadmium had the effect of prolonging the firing rate (French 1986a), that would be expected if a calcium-activated potassium conductance were an important part of adaptation. In fact, 15 mM cobalt decreased the firing rate, as did the same concentration of extracellular calcium, leading to the conclusion that these

15

ions were acting by the nonspecific divalent cation effect, rather than any mechanisms involving Ca^{2+}-channels (French 1986a).

Tetraethylammonium chloride (TEA) is a potassium channel blocker, that has been shown to affect many types of potassium currents (Hille 1992). Its only effect on the tactile spine neuron was to increase the duration of individual action potentials, without any effect on the adaptation (French 1984b and c) suggesting that the only current affected was the classical delayed rectifier, that is the main potassium current component producing the repolarization of an action potential. After conditioning hyperpolarizing current pulses, the threshold for action potentials decreased and the membrane time constant was elevated when 5 mM 4-aminopyridine (4-AP) was applied to the saline (French 1986b). This suggested the involvement of a potassium A-current in the threshold behavior.

Evidence for the participation of a slow inactivation of sodium current in the adaptation has been accumulated from several sets of experiments. The oxidizing agents chloramine-T and N-chlorosuccinimide, specific blockers of sodium channel inactivation, have been shown to remove the rapid adaptation (French 1987, Basarsky and French 1991) and especially its faster component (French 1989a). The same result was obtained with phentolamine, which has been shown to act on sodium channels in invertebrates and to inhibit spike generation and conduction in nerves and muscles (Ramirez and French 1990).

1.5. Outline of the thesis

In this thesis research I used both extra- and intracellular recording techniques in order to find out more about the mechanisms of rapid adaption in the femoral tactile spine neuron of cockroach. Before this study it has never been possible to apply voltage-clamp methods to any insect cuticular receptor. I used this method to reveal the individual currents contributing to action potential discharge and adaptation. The thesis is divided into two parts. The research projects whose results form the two chapters (2 and 3) of **PART I** were both completed using extracellular recording techniques and they gave valuable information about basic functions of the tactile spine neuron that were used in the following **PART II** (chapters **4, 5** and **6**), which presents the results of current- and voltage-clamp recordings.

Before I began this thesis work, I contributed to the measurement of the frequency response function of the tactile spine neuron, using intracellular recording techniques (Stockbridge et al. 1991). This work showed that the frequency response could be fitted by a pair of exponential filters. This result made the use of a power-law fit to describe the adaptation in tactile spine neuron questionable. Therefore, extracellular experiments using mechanical stimulation were repeated (Chapter 2) using significantly longer observation times than in the original experiments of Chapman and Smith (1963). The recordings were analyzed using a log binning method (Sigworth and Sine 1987), that is

more suitable for studying decay times with a wide temporal range. A sum of three exponential decays was found to give an accurate fit over the entire response duration.

For extra- or intracellular electrical stimulation the tactile spine is amputated and the electrode lowered into the spine lumen, where the neuron is located. Neither the microelectrode nor the neuron can be visualized during stimulation. Therefore, in Chapter 3 the threshold for electrical stimulation of the neuron was measured as a function of spatial position in the lumen in order to find out the location in the neuron where the action potentials are initiated. The spine was then fixed and serially sectioned for computer-aided reconstruction and the threshold measurements were aligned with reconstructions to produce maps of excitability around the neuron. This investigation showed that the lowest threshold was always close to the sensory dendrite or the soma, and it was obvious that the intracellular electrode could only impale these two parts of the cell. These results indicated that intracellular recordings are mostly done in the dendro-somatic part of the neuron and that the axonal part can only be reached when the electrode first enters the soma.

The results from intracellular experiments are described in the **PART II** of the thesis. The switching single-electrode current- and voltage-clamp techniques allowed full characterization of three different types of voltage-sensitive potassium outward currents, when the inward currents were first blocked with tetrodotoxin. It was not possible to get a good enough clamp to characterize the total inward current, because of the fast time

constant and incomplete space-clamp of the tactile spine neuron. The basic electrophysiological properties of the tactile spine neuron are described in Chapter 4. Chapter 5 presents the fast transient outward current (I_A), and a delayed rectifier type of potassium current (I_K) as well as a calcium-activated potassium current ($I_{K(Ca)}$) are characterized in Chapter 6. The function of I_K is shown to be solely in the repolarization of individual action potentials while I_A and $I_{K(Ca)}$ both decrease the action potential frequency during a maintained stimulation, indicating that they contribute to adaptation. In Chapter 7 I discuss these results and summarize the new findings.

PART I:

THE TIME COURSE OF ADAPTATION AND EXTRACELLULAR

EXCITABILITY OF THE TACTILE SPINE NEURON

20

2. THE TIME COURSE OF SENSORY ADAPTATION IN THE COCKROACH TACTILE SPINE NEURON[1]

2.1. Introduction

The adaptation behavior of the cockroach tactile spine neuron was originally examined by Pringle and Wilson (1952). They used a linear transfer function to analyze the action potential rates produced by both step functions and sinusoidal stimulation. They found that the adaptation of this receptor could not be fitted by a single time constant, but required the summation of at least three exponential decay processes. Their conclusions were based on a rather small range of stimulus frequencies and amplitudes, and were later criticized by Chapman and Smith (1963) who extended the analysis using similar theoretical and experimental approaches to Pringle and Wilson, but with a wider range of forcing frequencies.

Chapman and Smith (1963) showed that, when subjected to a ramp and hold stimulus the response of tactile spine neuron was not easily fitted by a small number of exponential decays, but was approximated by a power-law decay:

$$y = at^{-d} \tag{2.1}$$

where y = the action potential rate, a = a constant related to the sensitivity of the neuron, t = the time after the step, and d = a fractional exponent of time, a constant determining the rate of decay (Chapman and Smith 1963; French 1984b). The power-law has subsequently been used to describe adaptation in several other sensory receptors, including spider slit sensilla (Barth 1981; Bohnenberg 1981), the slowly adapting crayfish stretch receptor neuron (Brown and Stein 1966), insect multipolar receptors (Kuster and French 1983), primate touch receptors (Mountcastle et al. 1972), *Limulus* photoreceptor cells (Biederman-Thorson and Thorson 1971), and vestibular afferents in mammals (Tomko et al. 1981) and birds (Landolt and Correia 1980). The absolute values of the power coefficient d range from 0.2 to 0.7 in different organs (Barth 1981). In the cockroach tactile spine receptor, step responses gave values of 0.75 (Chapman and Smith 1963) and 0.82 (French et al. 1972). Frequency response function measurements showed that the exponent decreased significantly with increasing stimulus strength (French and Kuster 1981) and increased with temperature (French 1985).

A central problem with the power-law is its physical interpretation. The behavior seems to be linear in the sense that a sinusoidal input gives a sinusoidal output of the same frequency but different amplitude and phase. This has led to at least two suggestions of linear mechanisms that could be responsible for power-law behavior. The basic explanations that have been proposed are: 1. A combination of many exponential decays with varying time constants spread over the time course of the response (Chapman and Smith 1963; Thorson and Biederman-Thorson 1974). This theory requires many

different time constants when the behavior is observed over a wide frequency range (French 1984b). **2.** Distributed processes such as diffusion and transmission line systems (Moore 1960; Oldham and Spanier 1974), in which the exponent is $d = 0.5$, have been suggested for the tactile spine neuron (French and Sanders 1981). **3.** A nonlinear mechanical model has been proposed for the crayfish stretch receptor in which a nonlinear elastic component was connected to a linear viscous component (Brown and Stein 1966). The two latter explanations are concentrated upon the earliest stages of transduction. However, the basic processes causing sensory adaptation have not been completely explained in any mechanoreceptor. In the literature, power-law behavior has usually been explained without considering the nonlinear processes that occur during action potential encoding. However, adaptation has been demonstrated to take place during encoding in several different preparations (French and Torkkeli 1994) including the Pacinian corpuscle (Mendelson and Loewenstein 1964), slowly and rapidly adapting crayfish stretch receptors (Nakajima and Onodera 1969a and b), mammalian muscle spindles (Poppele and Chen 1972) and the cockroach tactile spine neuron (French 1984a and b; Basarsky and French 1991).

Intracellular electrical stimulation of the tactile spine neuron produced a frequency response function that could be fitted by a pair of simple exponential filters (Stockbridge et al. 1991). All the current- and voltage-clamp results shown in this thesis also demonstrate that the activation and decay of the ionic currents underlying adaptation follow exponential time courses, indicating that several parallel exponential processes

contribute to the rapidly adapting behavior. Therefore, mechanical step stimulation experiments were repeated to see if the step response really follows a power-law, or a combination of exponential decays.

An important problem in step response measurements is the time course of the adaptation. When a tactile spine is deflected by a step movement, action potentials appear within the first 10 ms following the step. Most occur during the first 2 s after the step, but they may still be produced at intervals of more than 10 s (Fig 2.2). This temporal range of at least $1:10^4$, together with the steep initial decay of the discharge makes it difficult to construct and fit linear histograms. An alternative procedure is to make a histogram with exponentially increasing bin widths versus time. Sigworth and Sine (1987) introduced a log binning method for analysis of ion channel dwell time distributions, in which the time axis, t, is transformed to a new variable $x = \ln(t)$. Under this transformation, an exponential distribution function has a constant shape:

$$\exp(x\text{-}\text{ß-}\exp(x\text{-}\text{ß}))\tag{2.2}$$

which is independent of the time constant, τ, with a maximum at $x = \text{ß} = \ln(\tau)$. Changes in τ shift the function along the abscissa, x. The theoretical basis for the construction of log histograms is explained in Appendix I.

2.2. Methods

Experimental preparation

A laboratory colony of cockroaches, *Periplaneta americana*, was kept at room temperature (22±2°C). Adult animals of either sex were used in the experiments. Metathoracic legs were amputated through the femur, close to the joint with the coxa. The experimental arrangement is shown in Fig. 2.1. The leg was fixed to a piece of cork board with two insect pins, which also served as extracellular electrodes. These pins were pushed through the mid-line of the femur, 1 - 2 mm apart and about half way along the length of the femur. The femur-tibia joint was at the edge of the board so that the large tactile spine in the femur near the joint with the tibia was hanging over the edge. The location of the spine at a right angle to the board was carefully chosen to allow the mechanical pusher to push the spine along its length. The femur was coated with petroleum jelly at the points of pin insertion in order to prevent desiccation, but the cut end of the femur was left uncovered to allow the main trachea in the femur to remain open.

Mechanical stimulation and recording

A servo-controlled loudspeaker (French and Kuster 1982) was used as a mechanical stimulator. The femoral tactile spine was connected to the loudspeaker by
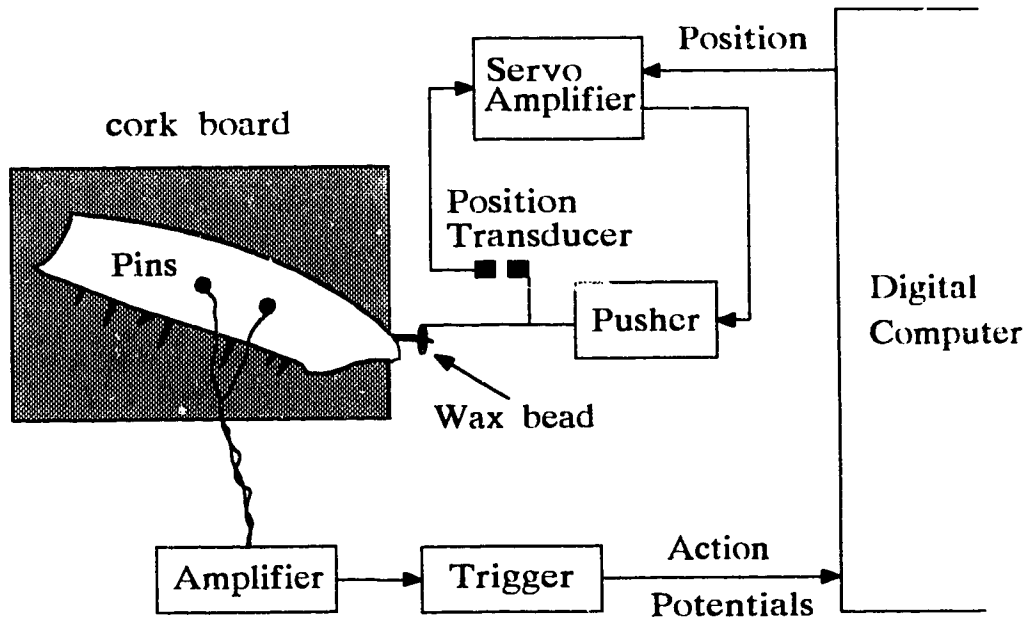
Figure 2.1. Experimental arrangement for stimulating and recording from a femoral tactile spine of the cockroach. The pusher consisted of a small audio loudspeaker driving a metal rod with a loop of silver wire at the end. The tactile spine was passed through this loop and fixed into position with a bead of wax. The pusher displaced the spine into its socket along its long axis. Action potentials were recorded extracellularly with insect pins as electrodes.

waxing it to a small loop of silver wire, connected to a metal rod fixed to the center of the loudspeaker. The wax was melted with a small soldering iron and the tactile spine was moved into the center of the wax bead while it was still molten. The wax was then allowed to cool for a few minutes before experiments were started. The loudspeaker was driven by a DC amplifier. The position of the rod was sensed by a position transducer consisting of an infrared phototransistor mounted on the rod and illuminated by a fixed infrared light emitting diode. The position transducer was used to complete a servo loop control of the loudspeaker position with electronic compensation for the speaker resonance. For the small distances (2 - 20 μm) used in these experiments this arrangement gave a good linearity of voltage versus position and good signal-to-noise ratio with minimum mechanical interference. The sensitivity of the transducer was calibrated at a number of output voltages by direct observation of position through a microscope with an ocular micrometer .

Action potentials in the afferent leg nerves were amplified by a differential amplifier (Grass P15), detected by a Schmitt trigger, and fed to a digital computer. Action potential firing and triggering were monitored continuously. Experiments were rejected if other action potentials reached the trigger threshold or if the action potentials from the tactile spine failed to reach the threshold at any time. All data processing was performed by custom-written software in the 'C' language. To construct log histograms, the action potentials produced by each step were initially collected into linear histograms with 1 ms wide bins. These histograms were 30 s wide and so they consisted of 30,000

27

bins. During the rest period between steps, the contents of the linear histogram were added to a log histogram, in which the bin widths increased exponentially with time after the step. The limits of this histogram were 1 ms to 100 s, and each decade was divided into 25 bins, so that the initial log histogram consisted of 125 bins. For fitting and plotting, the first decade of the histogram (1 ms to 10 ms) was ignored because the timing of these events was unreliable, due to conduction and triggering delays. The number of action potentials ignored in this manner was typically 1 - 3 per step. To illustrate the action potential record following a single step, the output of the extracellular amplifier was recorded on videotape using a 16-bit digitizer with 20 kHz sampling frequency. The tape recording was later sampled by a 12-bit analog-to-digital converter into a digital computer at 0.1 ms intervals and stored on a hard disk. Action potential data were then plotted using a linearly or logarithmically scaled time axis and a linear voltage axis.

Log histograms were fitted with rate functions that declined with the sums of several exponential components or a power-law. The log histogram bins contained action potential counts, rather than rates, to preserve the form of the Sigworth and Sine (1987) functions, which are distributions rather than rates (see Appendix I). The bins (units of action potentials) were fitted with the rate (units of action potentials/s) multiplied by the binwidth of the bin (units of s), using the Levenberg-Marquardt algorithm (Press et al. 1990). This algorithm provides a general method for fitting nonlinear functions of several variables to data by searching the multi-dimensional variable space for the minimum

28

squared error between the data and the fitted nonlinear model. The algorithm is widely used because of the efficiency and reliability with which it searches for the minimum. Linear histograms were obtained from log histograms by dividing the contents of each bin by its binwidth to give a similar appearance to conventional rate histograms, although the binwidths were still exponentially increasing. It should be noted that conventional linear histograms have the same form for either a rate or distribution ordinate because the bin width is constant throughout the histogram.

2.3. Results

Action potentials were counted into bins of exponentially increasing width and power-law (Fig. 2.2 and 2.3) or exponential (Fig 2.4) distributions were fitted to the products of the histogram bins and their bin widths. These histograms always had the form shown in Fig. 2.2, with a major peak at about 3 s, and one or more sub-peaks at shorter times, depending on the stimulus intensity. Under this transformation, a power-law function with exponent $1 > d > 0$ does not reach a maximum, but increases monotonically with the log time x. Power-law functions with $d > 1$ decrease monotonically with x. The power-law fit in Fig. 2.2 ($d = 0.7$) was obtained by restricting the fitting range to 0 - 1 s ($x < 0$). This exponent agrees well with the values obtained by Chapman and Smith (1963). Fig. 2.3 shows the same data transformed to a conventional linear histogram of action potential rate versus time. The same power-
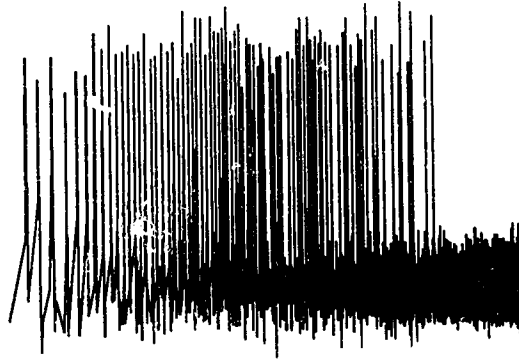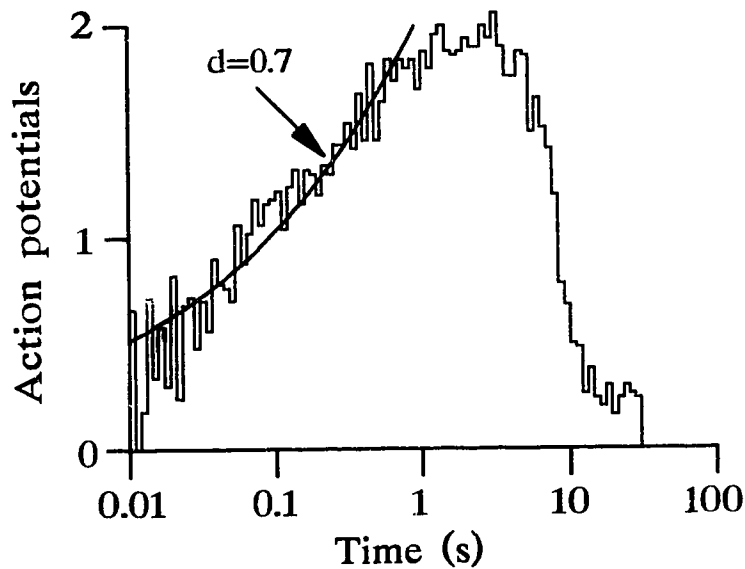
Figure 2.2. A histogram of action potentials from a cockroach tactile spine neuron following 8 μm step movements of the spine. The log binned histogram **B** was constructed from 50 steps of 30 s duration, with a 60 s pause before each step. The histogram has 25 bins per decade and the ordinate shows the mean number of action potentials per step. The best fitting power-law relationship for 1 s after the step ($d = 0.7$) is superimposed and it fails to fit the data at times beyond 1 s. An individual step response is shown above the histogram on the same log time axis **A**. The action potentials in this case were ~ 100 μV total height.
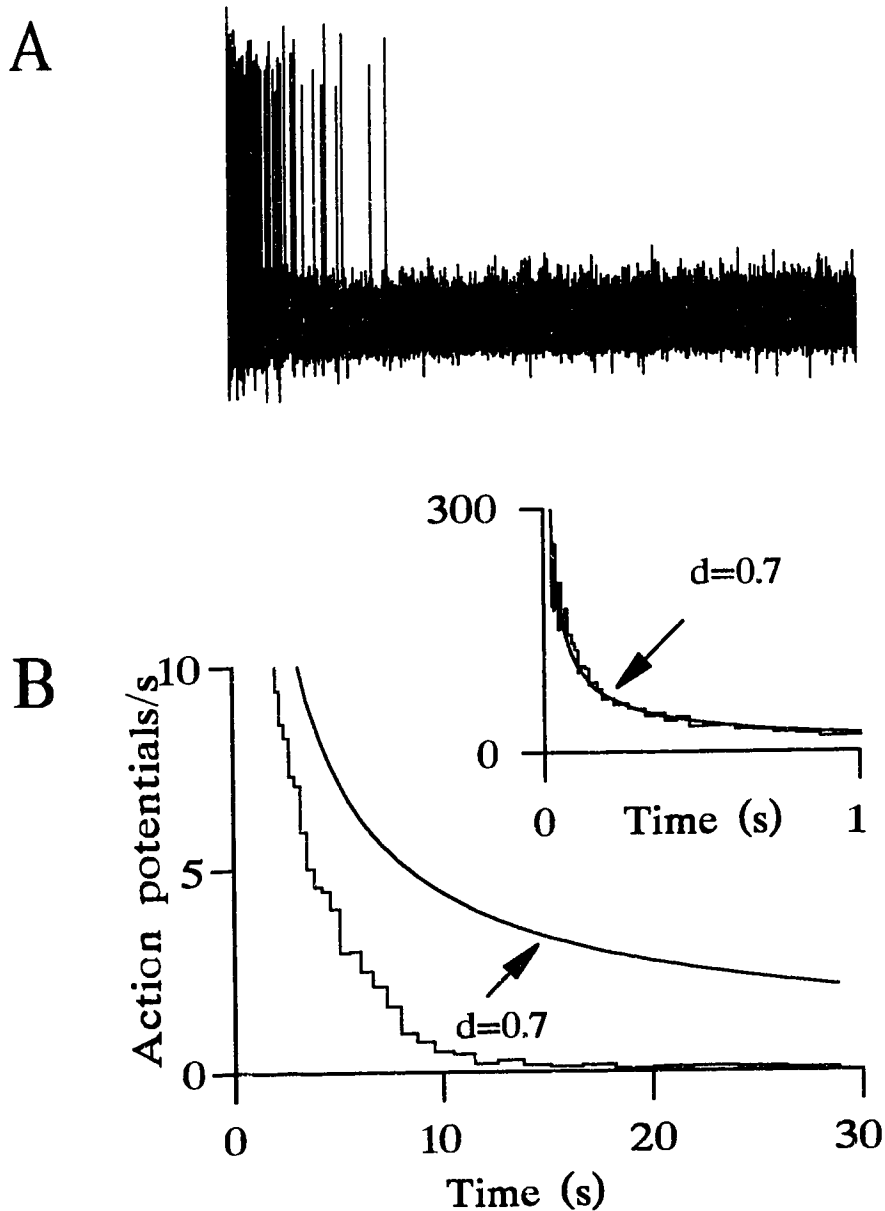
Figure 2.3. The same data as in Fig. 2.2 plotted on linear axes. The histogram bin heights were divided by their widths to give a plot of action potential rate versus time after the step. The power-law relationship also failed to fit the data at times beyond 1 s on linear axes, although it fitted the data before 1 s well (inset).

31

A

Action potentials

2

1

0

0.01 0.1 1 10 100

Time (s)

B

τ_1 τ_2 τ_3

Action potentials

2

1

0

0.01 0.1 1 10 100

Time (s)

C

Action potentials/s

10

5

0

0 10 20 30

Time (s)
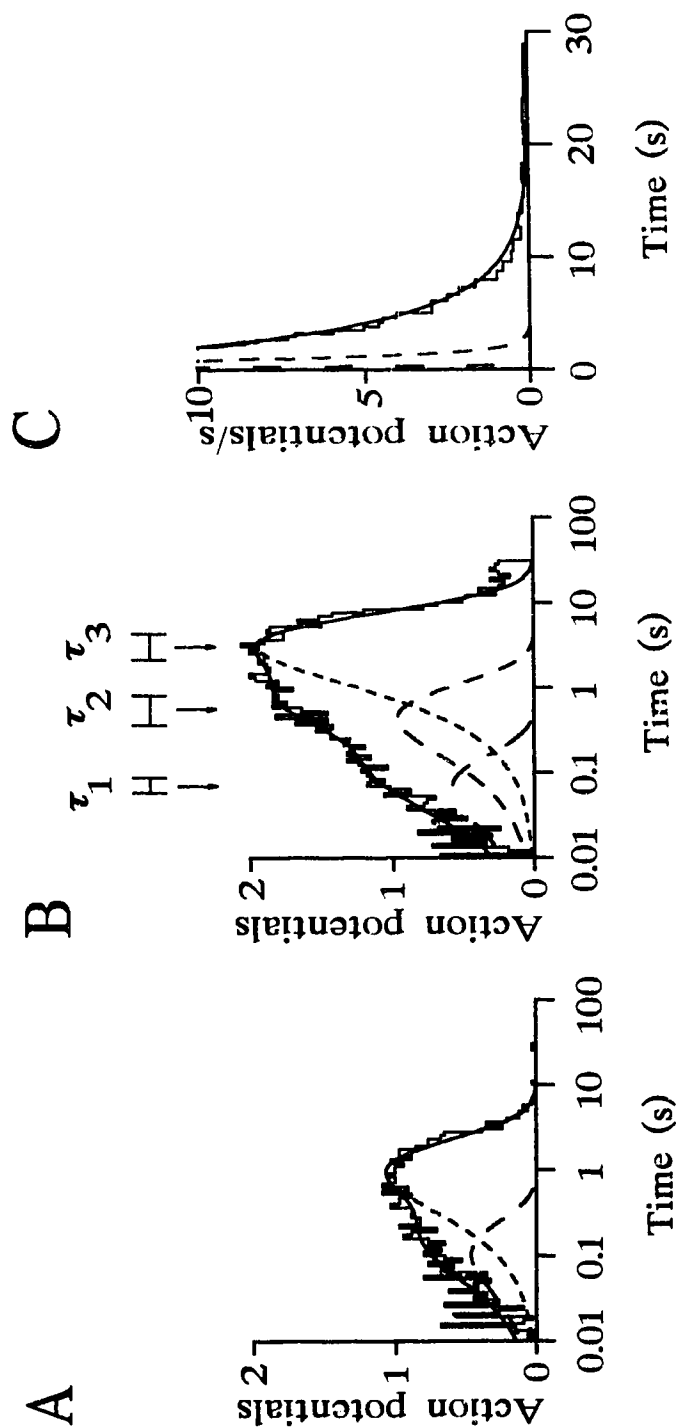
Figure 2.4. Histograms of step responses were well fitted by the sum of two or three exponential decays. The histogram from Fig. 2.2 is shown on both log **B** and linear **C** axes. together with best fitting triple exponential (solid lines) and its three separate time constants: $\tau_1 = 66$ ms, $\tau_2 = 450$ ms and $\tau_3 = 3,200$ ms (broken lines). On the linear plot, τ_3 lies entirely beneath the solid line on this time scale. The means and standard deviations of the three time constants from 14 experiments are shown above the log histogram. The data for the histogram in **A** was obtained from the same spine using a smaller (4 μm) step intensity. This data could be fitted with double exponential and gave time constants of $\tau_1 = 105$ ms and $\tau_2 = 972$ ms.

32

law fitted the linear data well at $t < 1$ s (Fig 2.3 inset) but did not fit the response over its full duration.

Unlike the power-law, sums of exponential decays fitted the log binned histograms well (Fig. 2.4). Fourteen different tactile spines were used with step amplitudes of 2-15 μm giving 31 - 178 action potentials per sweep. For smaller steps (e.g. 4 μm in Fig. 2.4A) the data could usually be fitted by a double exponential function:

$$y = a_1\exp(-t/\tau_1) + a_2\exp(-t/\tau_2) \qquad (2.3)$$

where t is time, a_n are amplitudes and τ_n time constants. When larger steps were used (e.g. 8 μm in Fig. 2.4B) for the same spine, a triple exponential function of the form

$$y = a_1\exp(-t/\tau_1) + a_2\exp(-t/\tau_2) + a_3\exp(-t/\tau_3) \qquad (2.4)$$

was required for a good visual fit to the histogram. The values of the three time constants were repeatable in different experiments with similar steps (Fig. 2.4B). Their mean values and standard deviations were $\tau_1 = 73\pm15$, $\tau_2 = 590\pm210$ ms, and $\tau_3 = 3,300\pm1,100$ ms (n = 14). The fitted functions accounted for at least 96% of the observed action potentials. The same triple exponentials also fitted linearly transformed histograms well, even at long intervals (Fig 2.4C).

33

2.4. Discussion

Although the power-law gave a reasonable fit to the first 1 - 2 seconds of the step responses, the log binning method showed that it failed when longer periods were explored. The study by Pringle and Wilson (1952) of adaptation in the tactile spine neuron was also based on a long (25 s) recording time and they proposed that the adaptation in this receptor could be fitted by three exponential terms. Previous investigations that supported the power-law theory (Chapman and Smith 1963; French et al. 1972) of the tactile spine have only examined periods up to 2.5 s. Other power-law fits to adaptation (Thorson and Biederman-Thorson 1974) have generally been restricted to temporal ranges of about $1:10^{2.5}$. Chapman and Smith (1963) based their power-law model on the form of the frequency response function, which showed a constant phase advance of $\sim 70°$ and a gain which increased as a power-law of frequency over the range 0.1 to 30 Hz. The longest time constant observed here was about 3.3 s, corresponding to a corner frequency of about 0.05 Hz, so that at least one more decade of frequency would be needed to detect it. Of course, sinusoidal experiments with cycle times of 100 s are technically demanding to perform.

The combination of short observation times, linear histograms and only two parameters, have maintained the widespread use of the power-law, but it probably represents an approximation to more complicated behavior, and the most likely explanation has always been the combination of several exponential relaxation processes

with different time constants (Thorson and Biederman-Thorson 1974). One factor that may be responsible for the differences between this study and the earlier power-law work is the improvements in technology that have occurred since the earlier measurements. It is technically demanding to apply an accurate step of current to such a small structure and it is even more difficult to provide a well-controlled mechanical step and to measure the step accurately.

The ability of triple exponential decay to fit the experimental data does not mean that the time constants must represent distinct physical processes. Evidence for connections between individual time constants and biological mechanisms can be obtained by experiments which specifically modify different processes, such as ion channel blockers. Future work will explore the ability of such modification to specifically change the amplitude of the three time constants.

In previous research conducted in this laboratory, two separate components have been shown to produce a labile threshold, which increases when the membrane is depolarized and decreases with moderate hyperpolarization (French 1989a). The time constants of both of these components decreased with depolarizing holding current. At rest, the faster time constant was about 70 ms, which agrees well with the first time constant obtained in the present experiments (τ_1 = 73 ms) and also with the results of the current stimulation study of French and Patrick (1994), which gave a time constant of 60 ms. Because of its selectivity to agents like chloramine-T (French 1987; Basarsky

and French 1991) and phentolamine (Ramirez and French 1990) this time constant has been linked to slow sodium channel inactivation. Longer time constants have also been reported for threshold shifts (about 1,000 ms) (French 1989a) and current stimulation (about 500 ms) (French and Patrick 1994), although their origin was not clear.

The fact that smaller intensity stimulation resulted in a good fit with two exponentials, suggests that all of the processes leading to adaptation do not turn on with moderate stimulation. These results also suggest that the time constant of each separate process decreases when the intensity of the stimulus increases. These factors make the separation of the processes complicated and may be the reason for the differences in the results obtained in the earlier investigations. The current- and voltage-clamp experiments in the later chapters of this thesis will describe some of the processes contributing to adaptation at the level of individual ionic currents. It would be worthwhile to examine the contributions of ionic currents to the time course of adaptation by repeating this work using intracellular electrical stimulation to reveal the time constants of adaptation, while the ionic currents are blocked using the same blockers as in the later chapters of this thesis.

3. LOCALIZATION OF EXCITABILITY IN THE TACTILE SPINE NEURON[2]

3.1. Introduction

In most neurons, the action potential initiation site is located in an axonal portion of the cell. For example, in myelinated axons it is at the first node of Ranvier. However, several exceptions to this rule have been found in vertebrate as well as invertebrate neurons. In insect cuticular mechanoreceptor neurons, sensory transduction is generally believed to occur in the apical segment of the dendrite, but the action potentials are probably generated in a more basal area of the dendrite that is electrically isolated from the tip by a high external resistance (Wolbarsht 1960) produced by the glial cells surrounding the dendrite.

An extracellular electrical stimulation technique for the cockroach tactile spine neuron has previously been developed in this laboratory to isolate the action potential encoding process from mechanotransduction. The spine is cut off above the neuron and a glass microelectrode is lowered through the lumen until it is near the neuron (Fig. 3.1). Negative electric current flowing into the electrode tip excites the neuron directly, and action potentials can be detected by independent extracellular electrodes in the femur (French 1984d).

During this kind of electrical stimulation of the tactile spine neuron, it is impossible to visualize the neuron or the electrode tip. Positioning the electrode at the most sensitive location adjacent to the neuron is accomplished by moving the micromanipulator in three dimensions while searching for the lowest electrical threshold (French 1984d). From the morphology of the tactile spine neuron that was known when this technique was developed, it was assumed that the lowest threshold occurred when the electrode was adjacent to the axo-somatic junction (French 1984d), implying that this is the region of normal action potential initiation. Subsequent morphological investigations using intracellular staining (Stockbridge and French 1991) and complete reconstruction from serial sections (French et al. 1993a) found that the neuronal soma often extends into the femur cavity and that the axo-somatic junction inaccessible to microelectrodes lowered through the lumen. Therefore, the region of the neuron having greatest sensitivity to extracellular electrical stimulation became uncertain.

The location of the action potential initiation site is of interest for understanding how the mechanoreceptor current flows into the neuron and how the voltage-activated channels are distributed on the neuron. Several studies of related insect mechanoreceptors, using mechanical and extracellular electrical stimulation, have suggested that action potentials can be initiated in the sensory dendrite (Erler and Thurm 1981; Guillet et al. 1980; Hamon et al. 1988). However, intracellular measurements in the tactile spine neuron gave a range of action potential amplitudes and durations, suggesting the existence of a passive somatic membrane and supporting the idea of axonal

38

initiation (Stockbridge and French 1991). Because it is generally believed that axons have fewer types of ionic conductances than somas or dendrites, it was also important to discover how the intracellular electrode impales the neuron and where in the neuron the intracellular recordings originate. In this study a computer-controlled 3-dimensional positioning system was used, combined with morphological reconstruction, to locate the position of lowest threshold during extracellular stimulation.

3.2. Methods

Experimental arrangement

The experimental arrangement is shown in Fig. 3.1. Adult cockroaches were taken from a laboratory colony. Metathoracic legs were amputated at the proximal end of the femur and mounted in a custom-made plexiglas chamber. Two fine insect pins passing through the femur about 3 mm from the spine were connected to an AC amplifier to observe action potentials in the afferent axon. The amplified action potentials were detected by a Schmitt trigger and the resulting electrical pulses were fed to a digital computer.

The tactile spine was cut off above the level of the neuron and covered by cockroach saline (124 mM NaCl, 10 mM KCl, 5 mM $CaCl_2$, 1 mM $MgCl_2$, 3 mM MOPS, 3.9 mM NaMOPS, 40 mM sucrose and the pH was 7.2; Chesler and Fourtner

1981). Fine forceps were used to push the air trachea against the spine wall opposite to the neuron, to minimize interference with the electrode. Glass microelectrodes were filled with 1 M NaCl and their resistance was about 10 MΩ. Negative current was driven through the electrodes by a voltage-to-current convertor. The current was measured by a virtual ground circuit connected to a reference electrode (Ag/AgCl) in a saline bath surrounding the tibia. The voltage-to-current convertor included single time constant compensation for electrode tip capacitance. The compensation was adjusted to give the best current response to a rectangular voltage command when the electrode was adjacent to the neuron. Response risetimes of < 100 μs were always obtained.

The threshold current to initiate an action potential was measured by a successive approximation procedure (French 1986b). An initial current pulse of 100 nA and 5 ms duration was passed through the electrode. If an action potential was detected by the Schmitt trigger, the current was reduced to 50 nA for the next pulse, otherwise it was increased to 150 nA. Following the next decision, the current was increased or decreased by 25 nA, and so on. This procedure was repeated 7 times at intervals of 1 s with the increase or decrease in current being halved each time, so that the final change was less than 1 nA. The pulse duration of 5 ms was about 5 times longer than the neuron's time constant (French 1986b), so that the current measured was assumed to be the neuron's rheobasic threshold current.

The stimulating microelectrode was mounted on a mechanical micromanipulator (Newport Instruments MX300R) whose three axes were driven by DC stepping motors and translators (Bodine Electric company 2410 Motors and THD-1801B Translators). The translators received TTL level logic signals from a digital interface connected to a digital computer. The motors could be stepped to 100 positions per rotation, and one rotation of the micromanipulator axes gave a movement of 50 μm. Therefore, the smallest available step corresponded to 0.5 μm at the electrode tip in each dimension. To reduce vibration, the motors were connected to the manipulator knobs via rubber shafts. Elasticity in the rubber, combined with friction in the micromanipulator, produced a hysteresis or backlash error during any movement reversal, but it was always <1 μm.

At the start of each experiment, the electrode was moved manually to a position of low threshold ($\sim$ 10 nA). The computer then moved the electrode automatically in steps of 5 μm and measured the threshold at each position. Movements were made in two planes. With Z corresponding to vertical movement down the lumen of the spine, the X-Z plane passed through the sensory dendrite of the neuron, while the Y-Z plane was at 90° to the X-Z plane (Figs. 3.1 and 3.2).
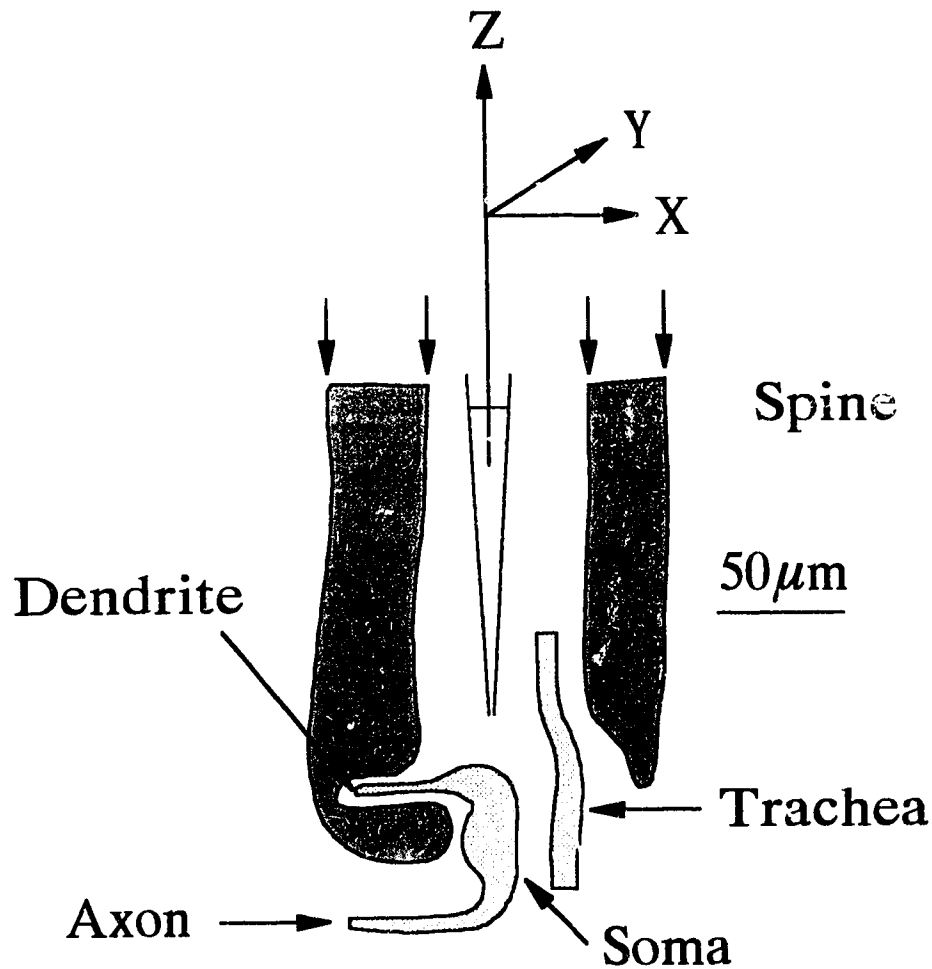
Figure 3.1. Experimental arrangement for mapping the extracellular threshold in the tactile spine neuron. The glass microelectrode was moved in 5 μm steps within the lumen of the tactile spine by a 3-dimensional computer-controlled micropositioning system. Electrical stimulation from the tip of the electrode caused action potentials in the neuron, that were detected by extracellular metal electrodes along the axon. The threshold for excitation was measured at each position of two orthogonal planes through a highly sensitive position that was obtained by manual searching. The 3-dimensional coordinates of points on the outside edge and center of the spine wall were used to align threshold maps with morphological reconstructions.

Two experimental problems were detected in initial experiments. First, the electrode often penetrated and killed the neuron, or if it touched solid parts inside the spine it was easily clogged or broken. The first indication of the electrode approaching a solid object was usually an increase in electrode resistance. Therefore, electrode resistance was measured before and after each step by passing a current pulse of 20 nA for 10 ms and measuring the resultant voltage change across the electrode. If electrode resistance changed by more than 10% it was assumed that the tip was approaching the wall, the neuron, or another solid component, and the electrode was withdrawn. Second, the viscosity of the lumen fluid was sometimes sufficient to bend the tip of the microelectrode during lateral movements. Therefore, the microelectrode was lowered vertically along its long axis with a threshold measurement every 5 μm until the tip touched something (electrode resistance increased), and then raised completely from the lumen before being moved sideways and lowered again.

After a set of threshold measurements, another computer program was used to measure reference points on the spine for alignment and shrinkage correction. Under a dissecting microscope, the tip of the electrode was positioned on the top, cut surface of the spine and the 3-dimensional coordinates of different points on the spine were recorded. The inner and outer diameter of the spine were measured (Fig. 3.1).

Tactile spines were fixed immediately after each experiment using half-strength

Karnovsky's fixative (Karnovsky 1965) pH 7.4 at 4 °C overnight, washed three times

in 0.1 M phosphate buffer saline (PBS), and post fixed in 1% osmium tetroxide in PBS

for 1 h at room temperature. After a further three washes in PBS, the tissues were

dehydrated in a graded series of acetone solutions. Tissues were infiltrated with Spurr's

embedding resin under vacuum for 2 h and cast in blocks that were hardened for 2 days

at 60 °C. Serial 1 μm thick sections were cut on a Reichert microtome with a diamond

knife and mounted on gelatin-coated glass slides. Sections were cut as perpendicular as

possible to the long axis of the spine. Sections were stained with a 1:1 mixture of 1%

methylene blue in 1% sodium borate and 1% azure blue in distilled water. Stained

sections were viewed under a compound microscope (usually at 600x magnification) and

traced with a drawing tube onto a digital graphics board (SummaSketch II). In order to

improve this process, the mouse attached to the graphics board was fitted with a green

light-emitting diode above the centre of the sensing coil. The diode illuminated the slit

of an electron microscope grid to produce a small and intense green light that could be

easily used to trace the different components of the section. Alignment of the sections

and reconstruction was carried out by custom software to give a 3-dimensional structure.

The smallest detectable movement of the cursor was ~0.05 μm or greater, interpolated

observations to 0.05 μm, and then smoothed the result to give a final sampled resolution

of 0.5 μm. However, the resolution of the optical system was approximately 0.5 - 1 μm,

using the Raleigh criterion. Figure 3.2 shows one traced sample section which was used for reconstruction of a complete tactile spine.

Fixation of tissues usually causes s: akage, and it was necessary to take this into account when aligning reconstructed spines with their threshold maps. The measured diameters of the top of the spine (Fig. 3.1) were used to scale the reconstructions (~20%) before they were aligned with their threshold maps. Test fixations of cockroach tissues showed a mean shrinkage of 18% (n = 3) for cuticle compared to 22% (n = 3) for nervous tissue, so the neuron was scaled up by an additional 4%. There was good agreement between the maximum excursions of the microelectrode, as measured by changes in electrode resistance, and the reconstructed surfaces of the neuron, lumen, and trachea, indicating that the shrinkage correction and alignment were in good agreement with the original tissues.

3.3. Results

Figure 3.3 shows a section through a reconstruction, combined with its threshold map, for the X-Z plane of a single tactile spine. Threshold values were represented on a scale of 0 - 200 nA with 10 divisions, using a random dot grey scale. In this case it is clearly seen that the site of maximum sensitivity was not at the axo-somatic region, but at the top of the soma, near to the dendrite. In this preparation, the axo-somatic region was not accessible by a microelectrode descending vertically through the lumen. This

45
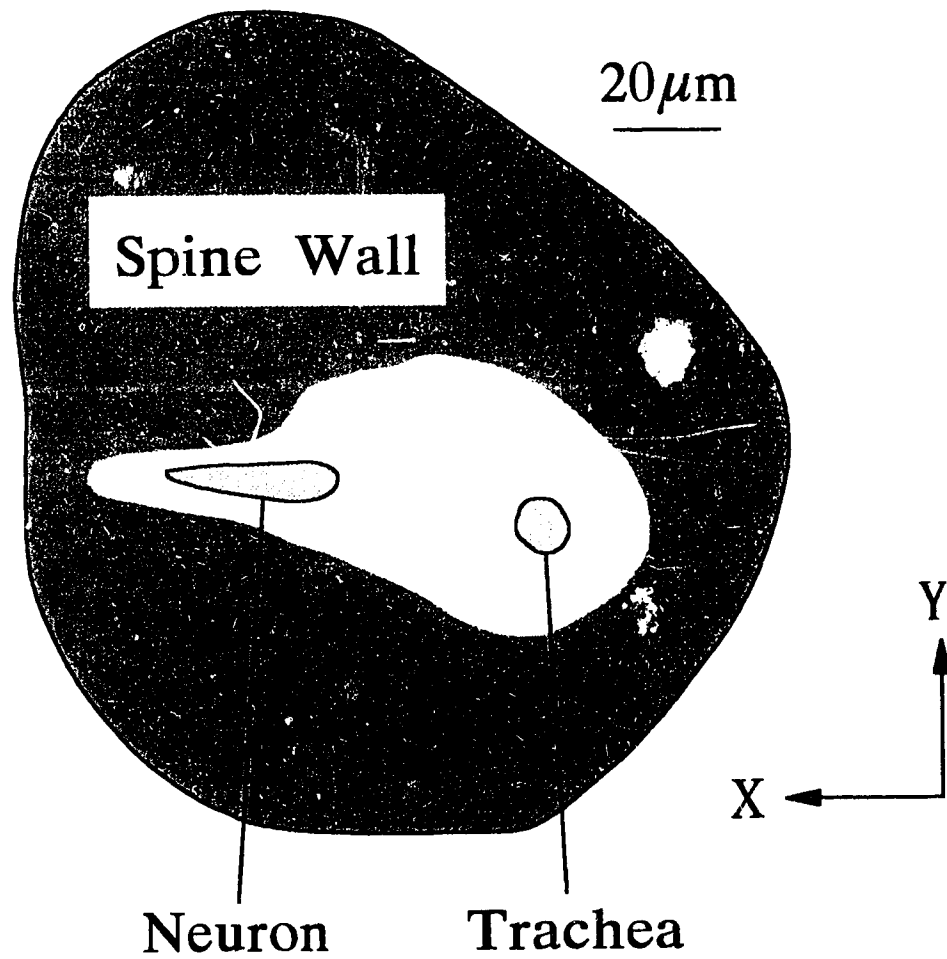
Figure 3.2. One of about 200 sections used to create a reconstruction. It shows the sensory dendrite of the neuron entering the canal that passes from the lumen to the outside wall.

46
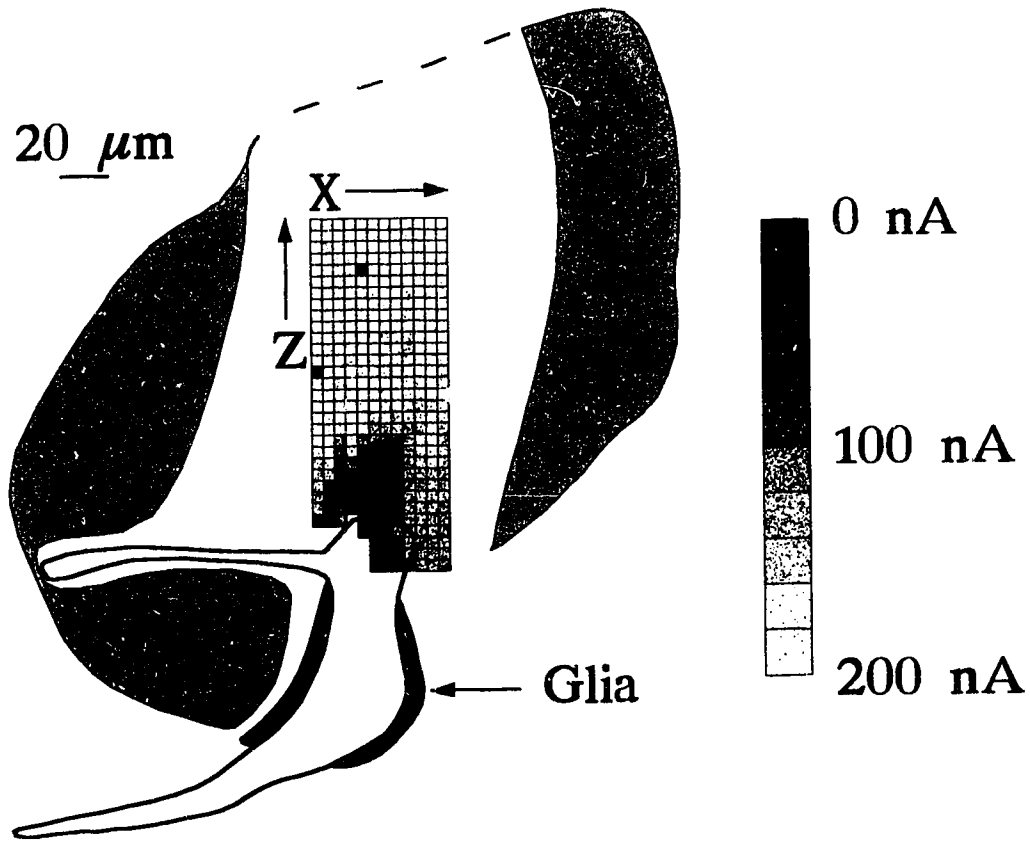
Figure 3.3. Map of electrical thresholds in the X-Z plane superimposed on a reconstruction of the tactile spine base. The random dot grey scale of threshold values is shown at right. This reconstruction also shows the wrapping of glial cells surrounding the soma of the sensory neuron. Uncontrolled action potentials from other neurons were sometimes detected by the Schmitt trigger, causing aberrantly low thresholds. Such randomly low thresholds can be seen at several positions on this map.
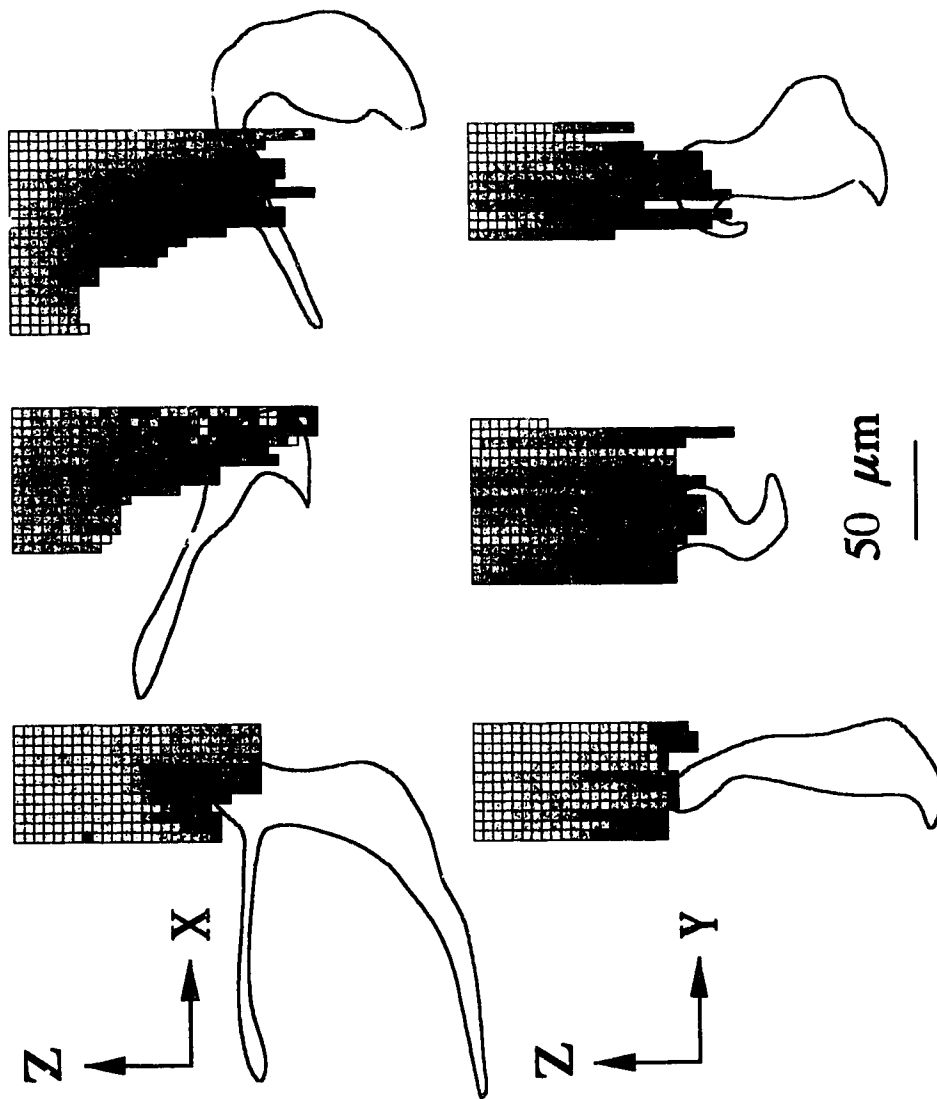
Figure 3.4. Maps of electrical thresholds for three different tactile spines, superimposed on the reconstructed neurons. X indicates the X-Z plane and Y indicates the Y-Z plane. The irregular shapes of the center and right X-Z maps correspond to the points at which the electrode touched the cuticular wall of the tactile spine.

48

figure also shows the glial wrappings that surround the tactile spine neuron (French et al. 1993a) and are believed to be responsible for the restricted chemical access to the neuron (Bernard et al. 1980). The fact that the map partly overlaps the reconstructed neuron suggests that the electrode tip either passed slightly to one side of the neuron, or deformed the neuron as it descended.

Seven different tactile spines were mapped in the X-Y and X-Z planes and then reconstructed. In every case the region of lowest threshold was close to the top of the soma and the sensory dendrite. The microelectrode was unable to reach the axo-somatic region in any experiment. Three examples of reconstructed neurons and maps are shown in Fig. 3.4. The shape of the inner surface of the lumen can be seen from the edges of the maps in several cases. The lowest thresholds measured in these experiments were typically 1 - 10 nA, similar to, or lower than, the values that have been reported previously from extracellular threshold measurements in the tactile spine neuron (French 1986b).

3.4. Discussion

These results showed that an extracellular electrode could not be lowered to a position close to the axon. This suggests that previous extracellular experiments also stimulated the dendro-somatic part of the neuron, and not the axon as proposed at that time (French 1984b and d). The axo-somatic junction may be electrically very sensitive,

but it is impossible to position a microelectrode close to it because of the shapes of the spine lumen and the sensory neuron. Electrical stimulation close to the dendrite is adequar to produce action potentials that propagate along the axon. However, it is still not known from these experiments if either the dendrite or the soma are excitable.

Several previous studies have suggested that the dendrites of arthropod bipolar mechanoreceptors are ctrically excitable. Stimulation and recording at the dendritic region of a locust noreceptor neuron gave evidence for two shapes of action potentials that interacted differently with antidromic stimulation, suggesting that the dendrite was excitable, but probably not the soma (Guillet et al. 1980). Similar experiments on cricket hair cells also suggested that both apical and basal dendritic regions were electrically excitable, but the regular site of impulse initiation was in the basal part of the dendrite (Erler and Thurm 1981). Dendritic potentials were measured in two types of cockroach cercal sensilla, bristles and filiform hairs, during mechanical and electrical stimulation, and during hypoxia (Hamon et al. 1988). In the bristle hair sensilla the action potentials appeared to start at the tip of the dendrite, but in the filiform hair sensilla much closer to the soma. Evidence for action potential initiation at the tip of the dendrite was also found in the long (120 μm) dendrite of a spider slit sensillum (Seyfarth et al. 1982). Intracellular recordings from crayfish tactile hair cells have also shown that spikes evoked by natural stimulation originate at a dendritic locus (Mellon and Kennedy 1964). In insect cuticular sensilla, intracellular recordings have not been done during mechanical stimulation to solve this problem.

Voltage measurements at dendrite tips are difficult to interpret because of the complex arrangements of electrical pathways surrounding them. Dendrite tips are usually isolated electrically, so that the exterior solution is not isopotential and normal cable conduction is unlikely. In contrast, the regions explored here are much more electrically accessible. The proximal dendrite and adjacent soma regions do have a glial wrapping, but they are not as thick as around the soma. The soma and the axon are located in the open lumen of the spine and the femoral cavity (French et al. 1993a) (Fig. 3.3) so that current densities around these structures should be relatively uniform.

An intracellular study of the tactile spine neuron found that action potential amplitude was inversely related to threshold, and that both varied widely when the neuron was penetrated via the spine lumen (Stockbridge and French 1991). Action potential width was also inversely related to the amplitude. This was interpreted to mean that recordings originated at variable distances from the action potential initiation site over a range of about 0 - 100 μm and were conducted to the electrode via a passive cable (the soma). The morphology of the tactile spine neuron (French et al. 1993a) suggests that these recordings were made from the dendrite and soma regions. The present work also confirms that the axon of the neuron can never be impaled directly via the amputated spine, although the electrode may pass through the soma to reach the axon. The range of distances across the soma from the dendrite to the axon is about 70 - 120 μm (French et al. 1993a) in agreement with the estimates based on electrical measurements.

Although the dendrite of the neuron may be electrically excitable, it seems equally probable that depolarization of the dendrite is conducted passively through the soma to an initiation site at the axo-somatic junction. The heavy glial wrappings (Fig. 3.3) always surround the soma but not the dendrite or axon (French et al. 1993a). These wrappings could provide electrical insulation to improve conduction through the soma. Further experiments will be required to discover if the passive transducer current is amplified by regenerative currents in the dendrite. The present data show that extracellular stimulation via the lumen probably excites the neuron through the dendrite or soma, rather than producing action potentials directly at the axo-somatic junction.

PART II:

THE IONIC BASIS OF THE ACTION POTENTIAL AND RAPID

ADAPTATION IN THE TACTILE SPINE NEURON

II.1. Introduction

The main purpose of this thesis research was to identify and analyze the ionic currents that contribute to action potential generation and rapid adaptation in the tactile spine neuron. This kind of analysis has not previously been performed on any other insect cuticular mechanoreceptors, because these cells are very difficult to impale with intracellular glass electrodes and conventional voltage-clamp methods are not suitable for such small cells.

Basarsky and French (1991) initiated intracellular recordings from the tactile spine neuron, and described its passive and active electrical properties. This was followed by the study of Stockbridge and French (1991) in which the cell's electrical activity and morphology were investigated using Lucifer yellow dye injection during intracellular recording. I performed my first intracellular recordings from the tactile spine neuron as a co-author of the Stockbridge et al. (1991) publication, which described the frequency response function of this neuron.

My first attempts to record the membrane currents with double-barrel microelectrodes were not successful, because of the damage to the neuron when it was impaled with these large electrodes, as well as the electrical coupling between the two barrels. An iterative voltage-clamp method developed in this laboratory offered a useful method for studying the currents when a very small voltage range was used, but it did

not allow current recordings with higher voltages. The discontinuous (switching) single electrode voltage-clamp (dSEVC) method proved to be the most effective method for this investigation. Even though the space-clamp of the neuron was not good enough to record the total inward current that produced the action potential, it was possible to analyze three different types of potassium outward currents. The methods section (II.2) will give a detailed description of the use of dSEVC with the specific requirements that are essential for the successful use of this technique and how they were accomplished in this work. The same methods were used in all chapters (4, 5 and 6) of this part of the thesis.

In Chapter 4 I describe the basic active and passive properties of the tactile spine neuron based on discontinuous current-clamp (dSECC) recordings and compare these results to earlier investigations from this neuron that were performed using the balanced bridge technique (Basarsky and French 1991). The characteristic action potential shape and firing pattern with step stimulation will be described.

The outward potassium currents are analyzed in Chapters 5 (I_A) and 6 (I_K and $I_{K(Ca)}$). Previous extracellular investigations of outward potassium currents (French 1984c; 1986a and b) did not give any clear evidence about their contributions to adaptation, even though they have been shown to have significant roles in the adaptation behavior of several other neurons (Hille 1992). However, it will be shown in these chapters that $I_{K(Ca)}$ and I_A do indeed have important functions in the adaptation of the tactile spine neuron, while I_K only seems to be involved in the repolarization of individual action potentials.

55

Some differences between the results shown in this thesis and previous research probably arise from an improved dissection method that allowed better diffusion of the chemicals into the neuron, especially when combined with longer chemical application times.

II.2. Methods

Experimental arrangement

Metathoracic legs from animals of either sex were amputated at the proximal end of the femur and mounted in a Plexiglass chamber. Insect pins passing through the femur near nerve 5 made it possible to observe the action potential activity in the neuron continuously during dissection and impalement. The femoral tactile spine was cut off above the level of the sensory neuron. A piece of cuticle (~5 mm^2) was removed from the femur close to the spine to improve the diffusion of the chemical agents into the neuron, and covered with cockroach saline (124 mM NaCl, 10 mM KCl, 5 mM CaCl$_2$, 1 mM MgCl$_2$. 3 mM MOPS. 3.9 mM NaMOPS and 40 mM sucrose and the pH was 7.2 (Chesler and Fourtner 1981)). The entire experimental arrangement was mounted on a gas driven vibration isolation table (Technical Manufacturing, Micro-g) and all experiments were performed at room temperature.

For current-passing and voltage-recording the discontinuous (switching) single-electrode voltage-clamp (dSEVC) time sharing technique was used. This arrangement requires very low capacitance electrodes to allow the fast hanges between the two modes. Borosilicate glass microelectrodes (outer diameter 1 mm and inner diameter 0.5 mm) were pulled with horizontal pullers (Sutter Instrument Co, CA). Two pullers were used: model P-87, in which a 2.5 mm platinum $\therefore$ filament was used for heating, or model P-200 that used a laser. The electrodes were filled with 3 M KCl and their resistances in the cell were 40 - 80 MΩ. For current-clamp recordings, electrodes having resistances of up to 150 MΩ were used. The stray pipette capacitance was mostly between the pipette and the bath solution, and this capacitance could be reduced by coating the electrode shanks with sylgard or sealing wax. In initial experiments, sealing wax diluted with chloroform turned out to be more suitable, because heating the sylgard to cure it, usually clogged the very sharp electrodes. Coating thickens the pipette wall and also prevents the bath solution from creeping up the pipette. Also, the saline level in the bath was kept as low as possible to further reduce the capacitance, while making sure that the cell did not dry out during the experiments.

To penetrate the sensory neuron, the electrode was advanced down the lumen of the spine by a micromanipulator (Newport Instruments) (Fig. II.1), that could be moved in three planes. The position of the electrode near the neuron could be observed as an

increased action potential frequency in the extracellular recording while high frequency oscillation was applied to the microelectrode in the "buzz" mode of the amplifier. Penetration was usually accomplished with a rapid movement of the manipulator, either simultaneously with buzzing or with delicate tapping of the air-table. The position of the electrode tip inside the neuron could not be seen, but the most probable place of penetration was shown in Chapter 3 to be the basal dendrite or the soma. From the original penetration position the electrode could usually be pushed down inside the neuron by about 10 - 50 μm so that the tip of the electrode was deep inside the soma or possibly even in the axon. Before voltage-clamp recordings, the impaled cell was allowed to stabilize for at least 15 min.

Before voltage-clamp of the outward currents (Chapters 5 and 6), the inward currents were blocked by 10 μM TTX. Blockade of sodium channels prevented the conduction of current into the axon and allowed optimal space-clamp of the small somata. In other insect receptor cells with similar shapes and sizes to the tactile spine neuron, it has been shown that the input resistance of the axon is higher than that of the soma, and that recordings made from the soma are not significantly affected by the electrical properties of the axon (van Hateren 1986).

The current- and voltage-clamp measurements were performed using the dSEVC method (Wilson and Goldner 1975; Finkel and Redman 1984) with a NPI SEC-10L amplifier, which allows good capacitance compensation of high resistance electrodes

A

CCS   S1   voltage recording
0 volts

G_T

current
passing

I_O

voltage   current
clamp   clamp

$V_e + V_m$ +1   A1   SH V_{ms} A2   S2

V_c V_I

V_m

B

current
passing   voltage
recording

S1

$V_e + V_m$

sample   sample

V_c

V_{ms}

V_{ave}
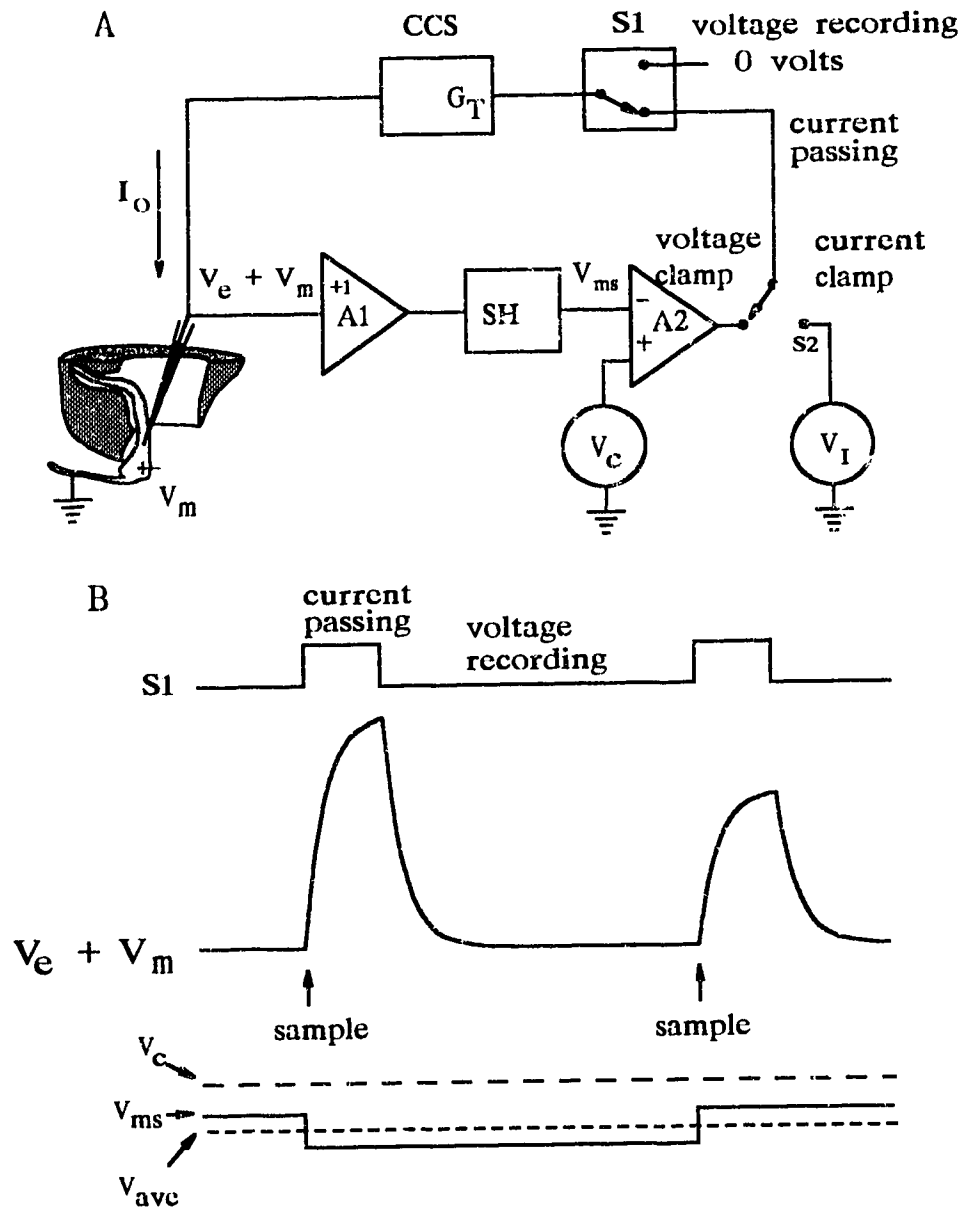
Figure II.1. A block A and timing B diagrams describing the principles of operation of the switching single-electrode current- and voltage-clamp. The switch S1 is closed during the current-passing and grounded during the voltage-recording period. Microelectrode voltage (V_e) charges exponentially during the current-passing period and discharges exponentially during the voltage-recording period. The sum of membrane potential (V_m) and V_e is sampled at the times indicated by arrows. The output (V_{ms}) of the sample-and hold device (SH) only changes at the time of each sample. Comparing V_{ms} and command voltage (V_c) in amplifier A2 determines the magnitude and sign of the next current pulse. V_{ave} is the average value of V_{ms} (Modified from Finkel and Redman 1984).

59

(Polder and Swandulla 1990). Some of the initial current-clamp experiments were done with an Axoclamp-2A amplifier. Fig. II.1 shows a block diagram and the timing of the switching single-electrode clamp: The voltage ($V_m + V_e$) is recorded using a single microelectrode and buffered by a high-speed amplifier (A1). V_m is the deviation of the membrane potential from the resting potential and V_e is the voltage developed on the microelectrode resistance and capacitance by the current I_0. At the beginning of the timing diagram V_e is near zero. The sample-and-hold device (SH1) samples $V_e + V_m$ at the time indicated by the arrow in II.1.B, and the sampled voltage (V_{ms}) is held for the complete cycle. The sampled voltage is compared with the command voltage (V_e) by the differential amplifier (A2). The output of this amplifier becomes the input of a controlled-current source (CCS) if the switch S1 is in the current passing position. The current that CCS injects to the microelectrode is directly proportional to the input voltage, regardless of microelectrode resistance. The gain of CCS is G_T. When S1 switches to the voltage-recording position and the input of CCS becomes 0 volts, that causes the output current to be zero, $V_e + V_m$ decays passively towards V_m. Before a new voltage sample is taken and the cycle repeated, sufficient time (up to 10 electrode time constants) must be allowed for V_e to decay to within a fraction of a millivolt from zero. When switch S2 is in the current-clamp position the input of CCS during the current-passing periods is a current command voltage V_1. The resulting current causes a shift in the membrane potential. If the microelectrode voltage decays near zero during the interval between current pulses, V_{ave} (the average value of V_{ms}) is a reliable measure of the membrane potential (Finkel and Redman 1984).

60

Weckström et al. (1992) described the following conditions for obtaining reliable results during a switching single-electrode voltage-clamp:

$$f_e > 3f_{sw}, f_{sw} > 2f_s > 2f_f > f_m$$

(II.1)

where: f_e is the upper cut-off frequency of the intracellular electrode in the cell (the time constant recorded for the electrodes used in this work was 1 - 2 μs, thus $f_e = 80 - 160$ kHz),

f_{sw} is the switching frequency of the single-electrode clamp (in these experiments 20 - 53 kHz was possible and 25 - 35 kHz was used),

f_s is the sampling frequency of the data collection system (100 - 2000 μs was used, giving $f_s = 500$ Hz - 10 kHz),

f_f is the upper cut-off frequency of the low-pass filter used for current recording (3.3 kHz in these recordings), and

f_m is the upper cut-off frequency of the membrane. (The membrane time constant of the tactile spine neuron is ~1 ms (French 1986b), so that $f_m = 160$ Hz)

The head-stage output showing the actual recorded voltage, which consists of the electrode voltage and the cell voltage ($V_m + V_e$), was observed during the experiments and the switching frequency was adjusted to the optimal value (25 - 35 kHz) allowed by
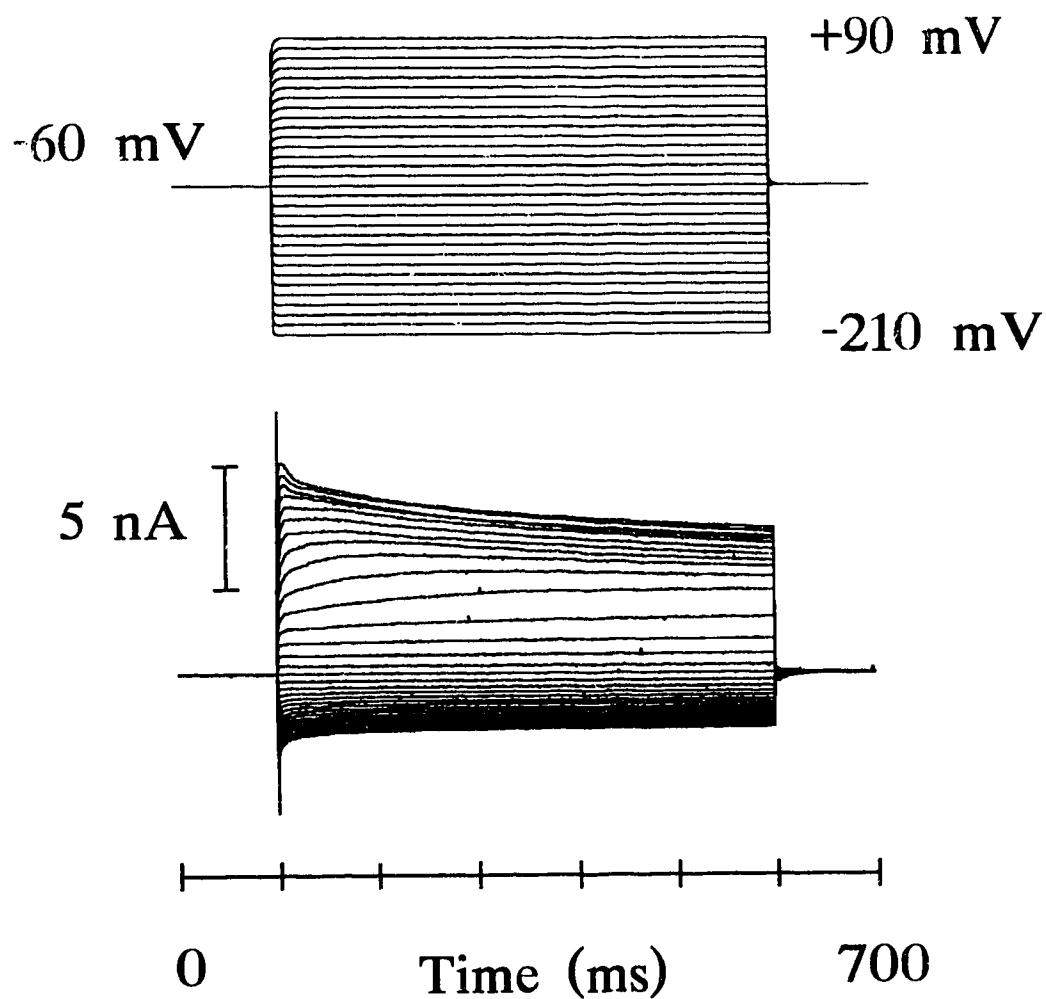
Figure II.2. When the inward currents were blocked with 10 μM TTX the outward currents could be recorded over a large scale of voltages. The actual voltage records from the amplifier are shown above, and the current recordings below. Five averages were used for each recording. In this cell the clamp was stable even at voltages of 150 mV above and below the holding potential. Passive currents were not subtracted from these recordings.

the electrode time constant (1 - 2 μs when optimally compensated). Thus, these recording conditions satisfied the criteria for a reliable single-electrode clamp. A duty cycle of 1/8 (current-passing/voltage-recording) was used in all experiments. The actual membrane voltage was recorded and is shown in the voltage protocol of Fig. II.2.

The software used in the voltage-clamp (and current-clamp) experiments was custom written in this laboratory. The software provided voltage or current commands via a 12-bit digital to analog convertor. Electrode current and membrane potential were recorded via a 12-bit analog to digital convertor. Membrane potential was low-pass filtered at 33.3 kHz by the voltage-clamp amplifier. When necessary, the capacitive and leakage currents were subtracted from recordings by taking the difference between the responses to symmetric negative and positive voltage pulses.

In some of the current-clamp experiments, the step stimulation was done with a Grass SD9 stimulator or a Hewlett- Packard 3310A function generator depending on the desired pulse length and frequency. The stimulus and response were stored using a digital tape recorder and later transferred to a digital computer.

Chemicals

Pharmacological agents used to block membrane currents were dissolved in cockroach saline and freshly prepared for each experiment, or kept frozen at the same or higher

concentrations. In order to keep the cell's osmolarity unchanged when 5 mM 4-aminopyridine (4-AP, Sigma) was added, an equal molarity of KCl was removed from the saline. When 50 mM tetraethylammonium chloride (TEA, Kodak) was used, both the NaCl and KCl concentrations were adjusted. When 5 mM $CoCl_2$ or 5 mM $CdCl_2$ were used, the $CaCl_2$ was removed from the saline. 124 mM $NaCl_2$ was replaced totally with same molarity of choline chloride to block the sodium currents. 10 μM tetrodotoxin (TTX, Sigma), 5 and 10 μM apamin (Sigma), 10 and 30 μM charybdotoxin (CTX, Research Biochemicals International) were simply added to the normal saline.

The diffusion times from the bath to the neuron to produce their effects varied considerably between different chemicals and preparations. For example, the blockade of action potentials with TTX took 20 - 130 min. For this reason, very stable and long lasting recordings of up to 6 hours were needed to complete voltage-clamp analysis of the outward currents.

4. THE BASIC ELECTROPHYSIOLOGICAL PROPERTIES OF THE TACTILE SPINE NEURON

4.1. Introduction

The basic electrophysiological properties of the tactile spine neuron, using intracellular stimulation and recording techniques, were described by Basarsky and French (1991) and Stockbridge and French (1991). Their calculations of the passive membrane parameters were based on morphological data obtained from the electron microscopical work of French and Sanders (1981). However, new information about the general structure of the spine neuron and its surrounding tissues as well as their significant variability, has been obtained more recently (French et al. 1993a) from serial sectioning combined with computer-aided reconstruction of the base of the spine. Therefore, the specific membrane resistivity for the known range of the cell sizes, as well as the mean surface area of the neuron, were re-examined in this chapter.

It was shown in Chapter 3, that the impalement of the tactile spine neuron by a microelectrode lowered down through the amputated spine, could only happen in the dendro-somatic part of the neuron, rather than the axon. However, it was often possible to push the electrode deeper in the cell after the initial impalement, probably even into the axon. Therefore, typical voltage responses from current stimulation of each cell were

recorded before further experiments, in order to discover any differences between the action potential waveforms or firing patterns in different parts of the cell.

4.2. Results

Basic electrophysiological properties

A total of 84 intracellular recordings from the tactile spine neuron were selected for this analysis. Recordings were considered successful when the baseline potential shifted by 60 mV or more in the hyperpolarizing direction, accompanied by action potentials of 50 to 120 mV. The mean values of resting potential, membrane input resistance, action potential. $\Gamma^{\star}$ and threshold current are given in table 4.1. The resting membrane potential was obtained directly from the amplifier, about 15 min after the penetration if the recording stabilized during this waiting period. The result was verified at the end of each experiment as the electrode was withdrawn from the cell, sometimes leading to corrections of the resting potential value by up to ± 15 mV, but mostly the error was only few millivolts. The cell's input resistance was defined from the linear part of the current-voltage curve at hyperpolarizing potentials during voltage-clamp recordings. Action potential amplitude was measured from the oscilloscope screen when small suprathreshold depolarizing pulses were given in the discontinuous current-clamp mode (dSECC). The threshold for spike initiation was also recorded using dSECC. The mean

voltage threshold was 7.9 mV according to the mean membrane resistance and the threshold current

TABLE 4.1. Summary of the electrophysiological properties of the tactile spine neuron.

	Resting potential (mV)	Input resistance (MΩ)	Action potential amplitude (mV)	Threshold current (pA)
Mean	-64.9	52.ɔ	77.0	150
Standard Deviation	±8.0	±23.5	±14.6	±140
Number of experiments	84	54	82	55

French et al. (1993a) showed that the shape and size of the soma of the tactile spine neuron varies considerably between different animals. The smallest somata were nearly spherical in shape and the largest ones almost cylindrical. The volumes of the small cells were ~ 12,000 μm^3 (French et al. 1993a) and thus, the surface area of a spherical cell was ~ 2534 μm^2. In contrast, cylindrical cells were typically ~ 100 μm long and had a volume of ~ 30,000 μm^3 and a surface area of ~ 6761 μm^2. Using the mean value of 52.3 MΩ for membrane resistance (Table 4.1) gives a specific membrane resistivity for a spherical cell of 1323 Ωcm^2, and the same calculation for a cylindrical cell gives a specific membrane resistivity of 3536 Ωcm^2. The estimated value of the membrane time constant of the tactile spine neuron is 1.5 ms (Stockbridge and French 1991). Using the mean membrane resistance value obtained in the current work, the membrane capacitance
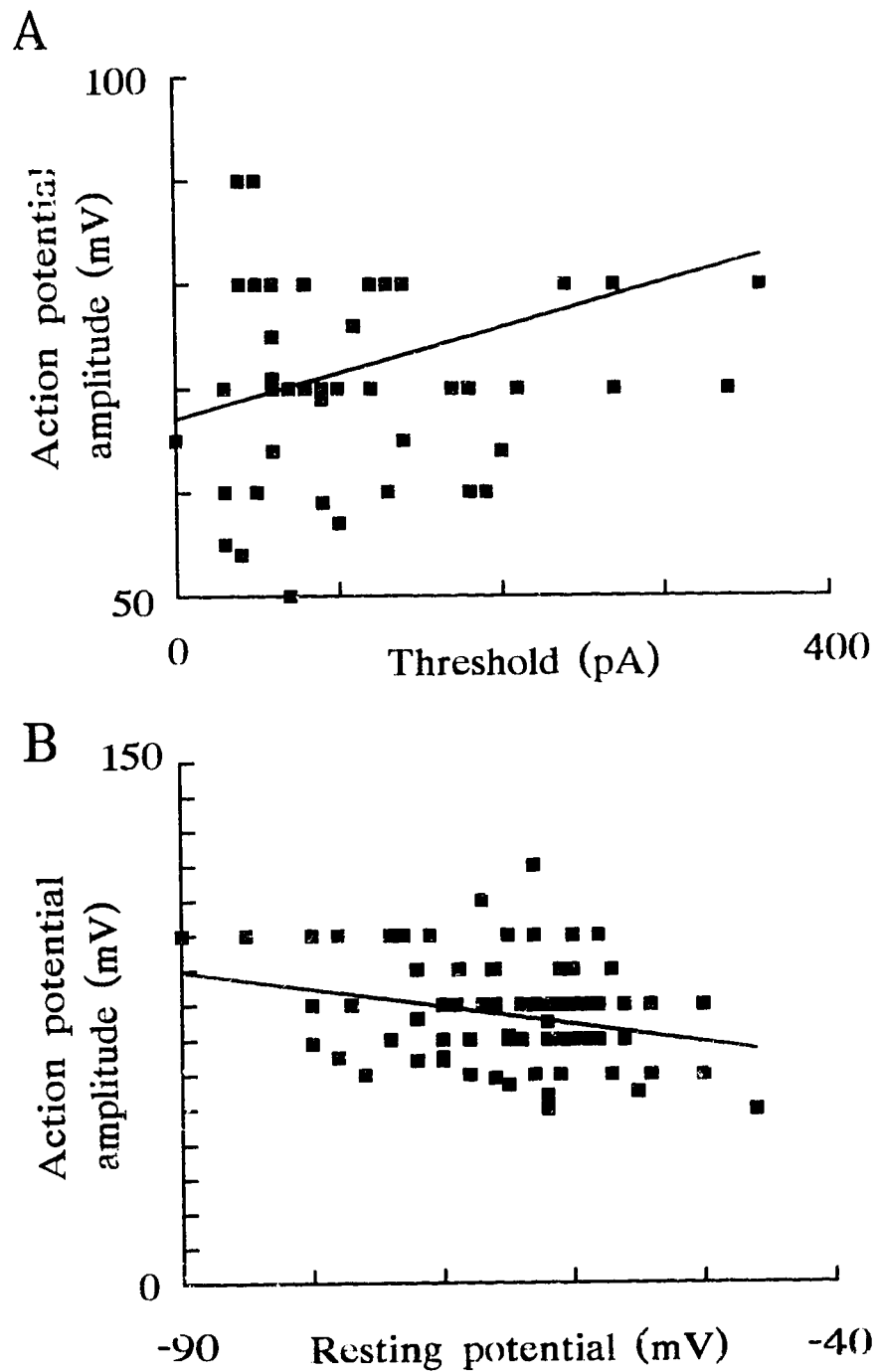
FIGURE 4.1. **A** Action potential amplitude correlated significantly with the threshold current ($r = 0.304$, d.f. = 49, p < 0.05). **B** A similar correlation was found when action potential amplitude was compared to resting membrane potential ($r = -0.275$, d.f. = 80, p < 0.05).
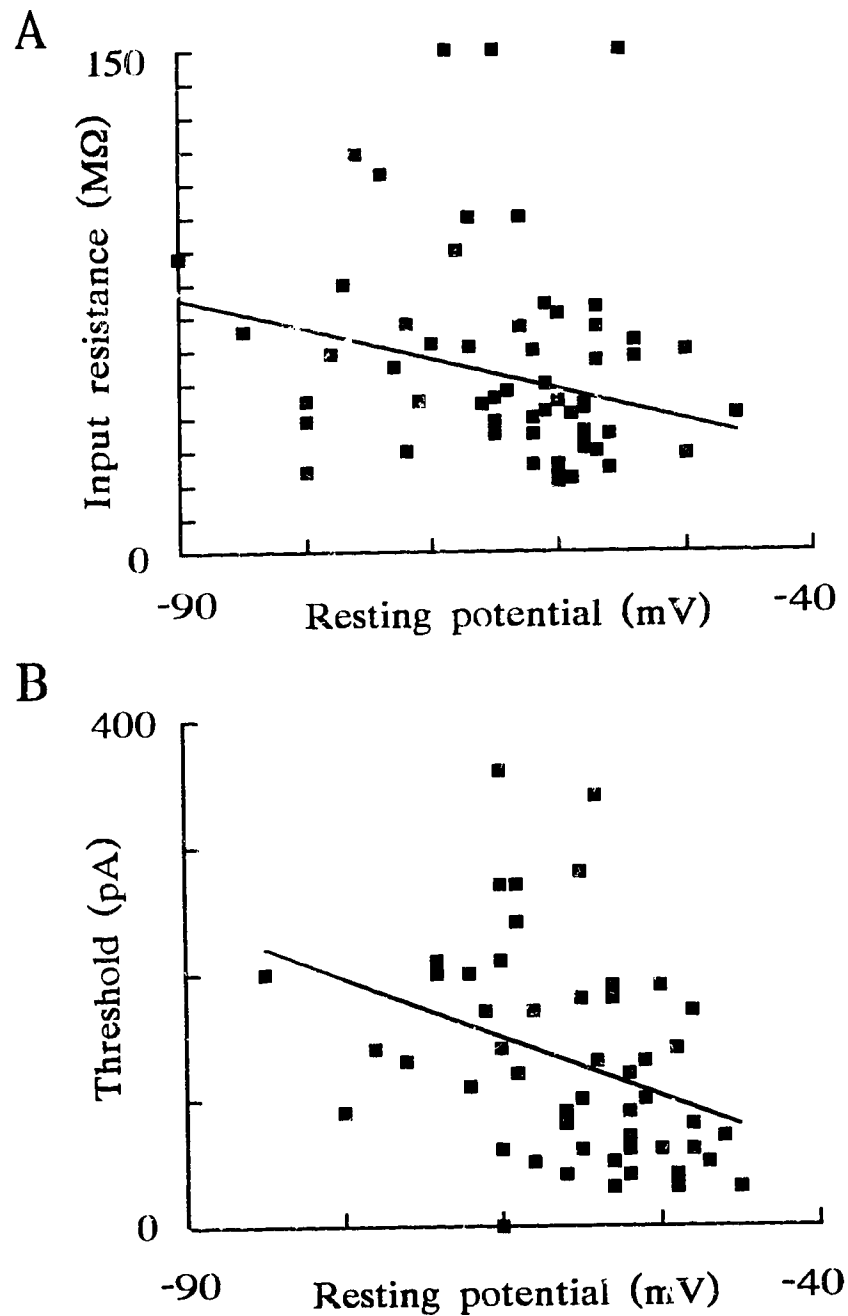
FIGURE 4.2. A The input resistance of the neuron was higher when the resting potential was more negative ($r = -0.351$, d.f. $= 52$, $p < 0.05$) and **B** the threshold current was smaller when the resting potential was more depolarized ($r = -0.340$, d.f. $= 51$, $p < 0.05$).

value becomes 28.0 pF, from which the surface area of the cell can be calculated to be 2870 μm^2 assuming the specific membrane capacitance to be 1 $\mu F/cm^2$.

Higher action potential amplitudes were recorded when the threshold current was larger (Fig. 4.1A), and more negative resting potentials also produced bigger action potentials (Fig. 4.1B). With more positive resting potentials the input resistance (Fig. 4.2A) and the threshold current (Fig. 4.2B) were lower than with more negative resting potentials. However, these correlations were statistically significant only at the level of p < 0.05.

Voltage responses

Typical responses of the tactile spine   .ron to hyperpolarizing and depolarizing step current stimulations in dSECC are shown in Fig. 4.3. There was only a small difference in the sizes of action potentials during a burst, the first spike being always the highest. After each action potential, whose duration from the half amplitude rise to half amplitude fall was about 1 ms, the cell repolarized rapidly and a new action potential was generated after a new depolarization crossed the threshold. After the end of a hyperpolarizing current pulse, which removed the sodium inactivation, anodal break action potentials were often generated. Fig. 4.4 shows the voltage response of the neuron with different amplitudes of depolarizing stimulation. With a moderate maintained stimulation, i , this case 50 and 70 nA, the firing frequency decayed to silence before the termination of

20 mV

50 ms

-70 mV

250 pA

-750 pA
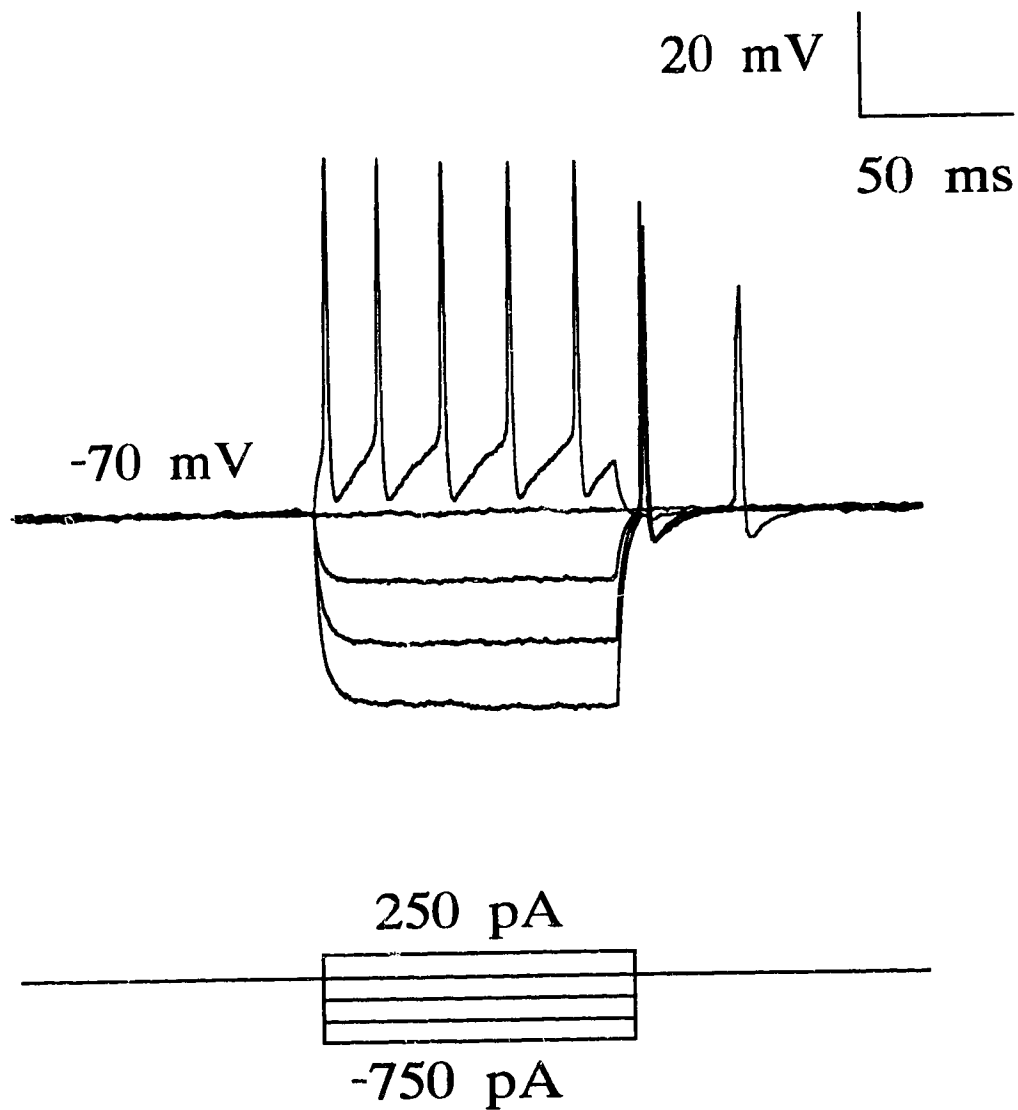
FIGURE 4.3. A typical current-clamp recording from a tactile spine neuron when 100 ms hyperpolarizing and depolarizing current steps were used for stimulation. A 250 pA current pulse produced a burst of action potentials that did not decay before the end of the pulse. When hyperpolarizing steps were terminated, anodal break action potentials were generated. The res' ng potential of this cell was -70 mV.
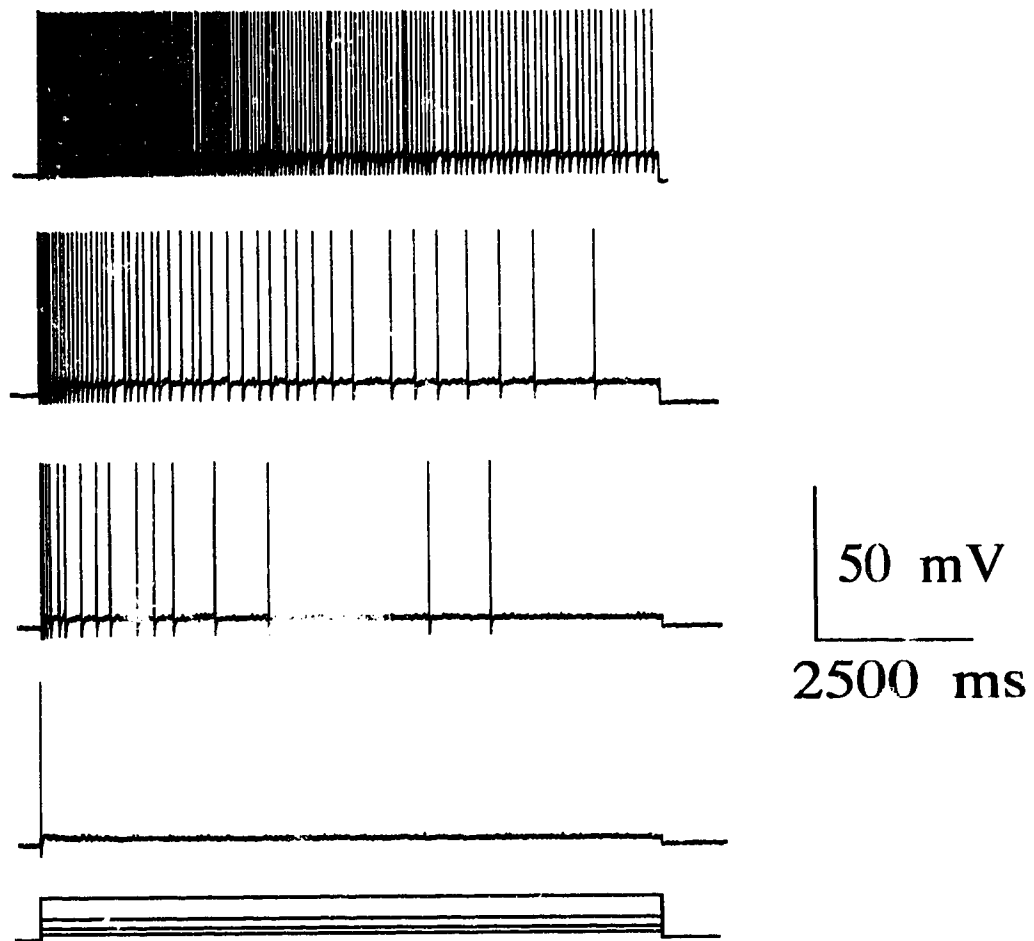
FIGURE 4.4. Four voltage responses to different amplitude depolarizing current pulses showing the decay of action potential frequency during a maintained stimulus. The resting potential of this cell was -72 mV. Current stimuli of 50, 70, 100 and 200 pA were used.

72

A

10 mV

200 ms

500 pA

B

1 mV

100 ms
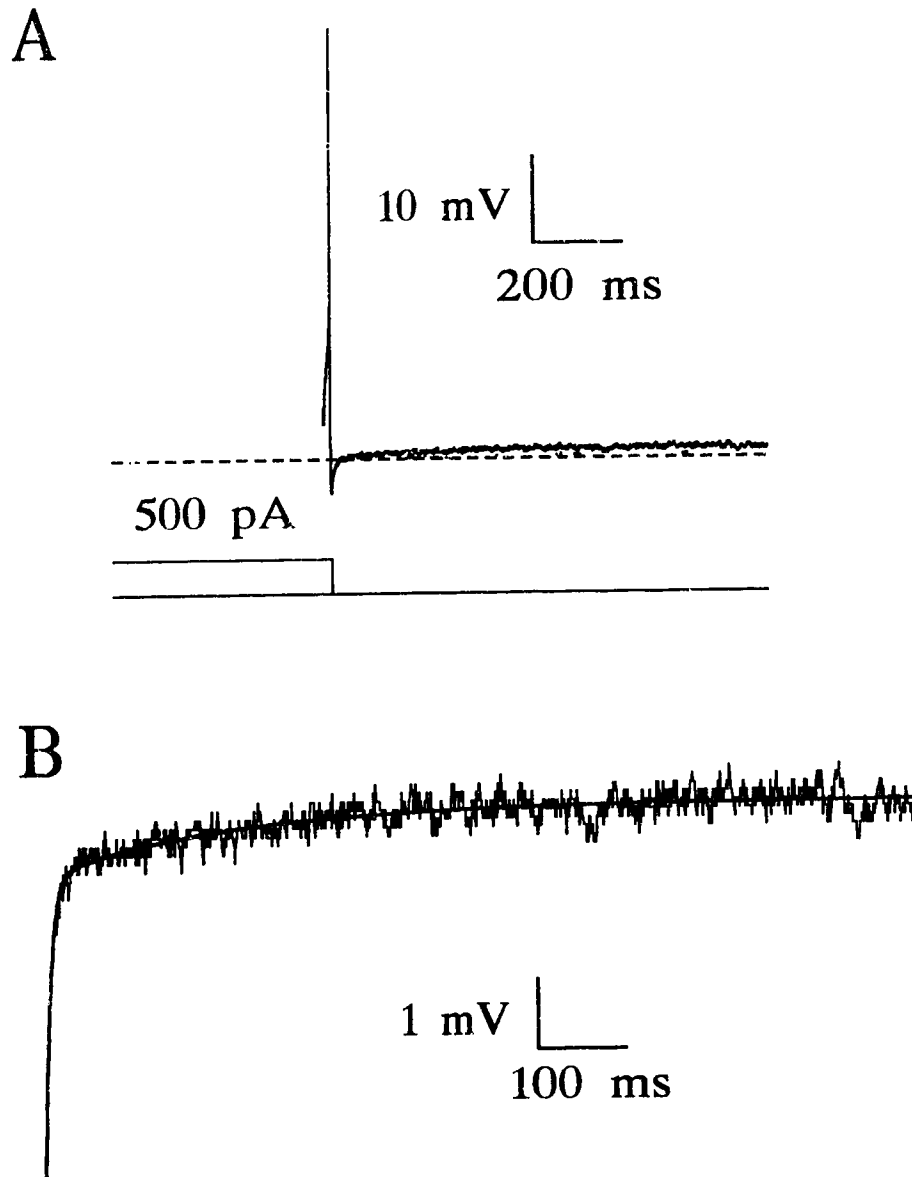
FIGURE 4.5. After a burst of action potentials a small and fast afterhyperpolarization, in this case 4 mV, was detected. An even smaller depolarization followed this AHP. The last action potential and the following afterpotential from a burst are shown in A. A 500 pA stimulus of 500 ms duration generated 33 action potentials. The dotted line represents the zero voltage level. B The same afterpotential as in A, but on different time and voltage scales. The smooth line is a double exponential fit to the afterpotential and it gave time constants of 7 ms and 207 ms.
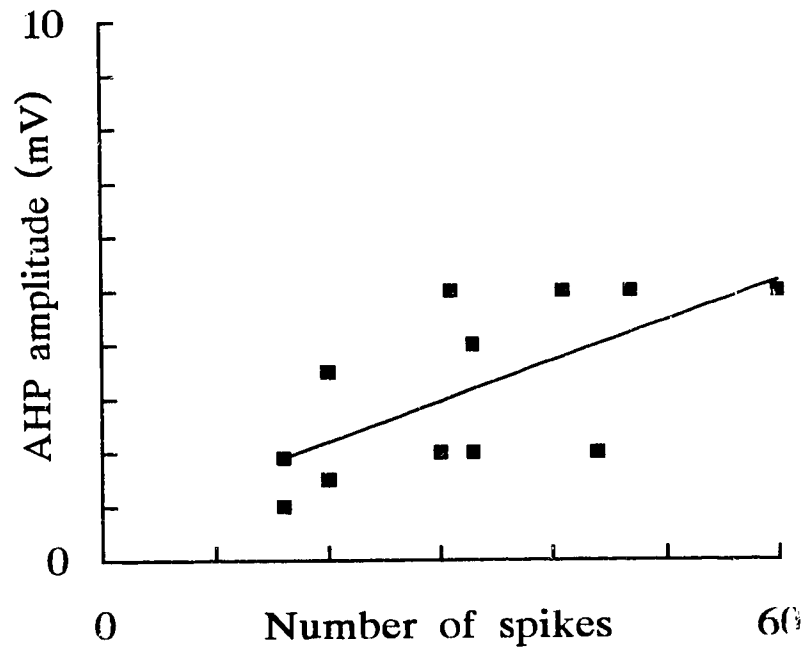
FIGURE 4.6. The amplitude of the AHP increased significantly with the number of action potentials in the preceding burst ($r = 0.645$, d.f. $= 10$, $p < 0.05$). Recordings were made from four different cells with three different stimulus amplitudes (250, 500 and 750 pA) of 500 ms duration.
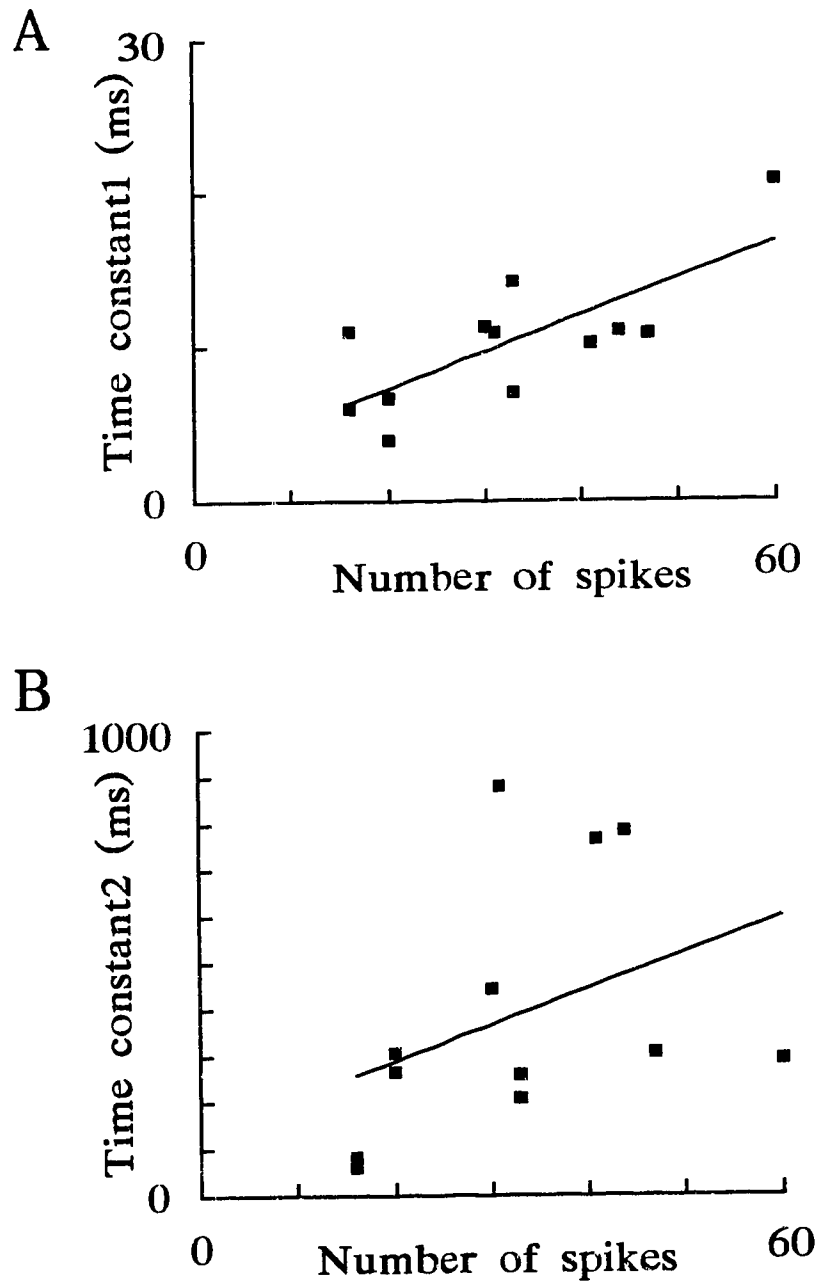
FIGURE 4.7. Both of the time constants of the decay of the afterpotential were slower with increasing numbers of action potentials in the burst. The correlation of the faster time constant **A** was statistically signifiant ($r = 0.729$, d.f. $= 10$, $p < 0.05$), but the slower time constant **B** was not ($r = 0.384$, d.f. $= 10$). The same cells as in the experiments in Fig. 4.6 were used for determining the time constants with double exponential fit.

stimulus. When more depolarizing stimulation was used, in the cell of Fig. 4.4 100 and 200 pA, the decay of action potential frequency was still detectable, but significantly slower than with lower current amplitudes. The waveforms of the individu.. action potentials as well as the firing pattern in response to maintained stimulus were similar in all stable recordings and did not indicate any difference in the pos: n of the electrode inside the cell.

After a burst of action potentials a small but clear afterhyperpolarization was observed (Fig. 4.5). This AHP did not always decline directly back to zero level, but often a depolarizing afterpotential was detected. The amplitude of the AHP increased with the number of action potentials in the preceding burst (Fig. 4.6) the maximum amplitude being 5 mV after a 750 mV current pulse of 500 ms duration. The decay of this afterpotential could be fitted with two exponentials as shown in Fig. 4.5B. The faster time constant of the decay varied between 4 and 21 ms (Fig. 4.7A) depending on the number of action potentials in the preceding burst. The slower time constant was not as clearly dependent on the number of action potentials in the burst (Fig 4.7B) and it varied between 60 and 900 ms. Both afterpotentials were absent when the action potentials were blocked with 10 μM tetrodotoxin, or sodium ions in the saline were replaced with choline.

4.3. Discussion

The mean values of the action potential amplitudes (77 mV) and resting potentials (-64.9 mV) were in the same range, but bigger than those recorded earlier by Basarsky and French (1991). These numbers are typical for nerve cells. The mean membrane resistance was about 15 MΩ lower than in the previous work. However, its standard deviation was rather high, probably indicating the range of the cell sizes, that were reported previously (French et al. 1993a). The mean threshold current was less than half of that obtained earlier by Basarsky and French (1991). Most of these differences may result from improved recording methods and the selection of more stable cells for recordings.

The specific membrane resistivity calculated for a small spherical cell was 1,323 Ωcm^2 and for a large cylindrical cell 3,536 Ωcm^2. Basarsky and French obtained the value of 1,812 Ωcm^2 for specific membrane resistivity when the diameter of the cell was assumed to be 30 μm and its input resistance 64 MΩ. The specific membrane resistivity in different cell types varies from 1,000 to 50,000 Ωcm^2 (Kuffler et al. 1984) depending on the ion channel density of the cell in question. The results obtained from tactile spine neuron in this and other studies (Basarsky and French 1991) indicate a high ion channel density typical of an excitable cell. The calculated surface area from the morphological data of French et al. (1993a) of the tactile spine neuron varied between 2534 and 6761 μm^2. When the surface area was calculated using the electrophysiological

77

parameters obtain... rere and in Stockbridge and French (1991) a value of 2870 μm² was obtained. These results indicate that the intracellular recordings were made mostly from smaller cells, even though the initial assumption was that it is not possible to impale the smaller cells without damaging them.

Stockbridge and French (1991) showed that the action potential amplitude was inversely correlated with the threshold in the tactile spine neuron. In the current work this kind of correlation was not found (Fig. 4.1A). In fact, there was a small, just above the statistical significance level, correlation in the opposite direction, indicating that the action potential amplitude was smaller when the threshold was lower. However, in the earlier work significantly smaller action pote... ials were used (down to 20 mV) for recordings than in this thesis.

The small differences in the resting potentials and action potential amplitudes (Fig. 4.1B) as well as resting potentials and input resistances (Fig. 4.2A) indicate that the cell sealed well after penetration and that the regions of the cell being recorded from are electrically similar.

A small reduction in the size of the action potentials following the first one in the burst was often observed. However, this difference was only a few millivolts compared to e.g. the spider slit sensilla (Seyfarth and French 1994), whose action potential amplitude always decreases strongly during the burst, and where some of the neurons can

78

only fire one action potential during a maintained stimulation. The constant spike size observed in this work indicates a very fast recovery of sodium channels from inactivation after an action potential that may be associated with rapidly activating and inactivating current(s), or possible an electrogenic pump that hyperpolarizes the cell after each spike and releases the sodium inactivation. The fact that the generation of action potentials could be totally prevented by the application of 10 μM TTX in the saline, or by replacing the external Na$^+$ completely with choline, suggests that the action potentials are solely produced by a sodium current as in many other neurons. The action potential size and shape as well as the firing pattern were similar in all recordings. In comparison, in the slowly adapting stretch receptor neuron of the lobster, the spikes in the dendrite and soma are significantly wider than in the axon (Grampp 1966). Small spikes were sometimes recorded in the present experiments soon after the initial penetration, but these cells usually died very soon afterwards. or in some cases normal size spikes could be recorded when the electrode was pushed deeper into the cell. It is possible that at least some of these small action potentials originated from another part of the cell than the normal size spikes, but they may just as well be an indication of incomplete penetration.

In some amphibian (Barrett and Barrett 1982) and mammalian (Blight and Someya 1985) myelinated axons the action potential decay has two separate phases; a fast repolarization followed by a very slow repolarization without a fast hyperpolarization as observed here. This depolarizing afterpotential has been suggested to be caused by charging of the axolemmal capacitance by current passing through the myelin sheath

during the action potential (Barrett and Barrett 1982) or by the leakage pathway under the myelin sheath (Blight and Someya 1985). In the case of tactile spine neuron, the strong glial cell wrapping, that has been suggested to function as a primitive myelin sheath, does not seem to have this kind of an effect.

Even though the tactile spine neuron has been classified as a rapidly adapting receptor, because of its ability to adapt in a few seconds to a maintained stimulus, strong electrical intracellular stimulation could produce a burst of action potentials that lasted tens of seconds. In Chapter 2 mechanical stimulation was also shown to produce long lasting bursts of action potentials. However, the tactile spine neuron always adapts eventually to a constant stimulus and thus is clearly a phasic receptor.

The afterpote⌐'   ⌐vs a burst of action potentials had two phases, the initial

fast hyperpr'   v a few milliseconds and then the membrane slowly, over

hundre'   ;ri'ed slightly before returning to the base level (Fig.

4.5). I   were dependent on the number of preceding action

potentia,   ₋₁ the spiking was blocked with TTX. In guinea pig vagal

motoneurons ₋₁₋ ₁ast AHP has been shown to be produced by voltage-gated K^+-channels, that activate during the spike and then close soon afterwards (Yarom et al. 1985). In frog spinal motoneurons the slower phase was shown to be produced by calcium-activated potassium channels, that were sensitive to apamin or the Ca^{2+}-channel blockers, Co^{2+} or Mn^{2+} (Barrett and Barrett 1976). In the slowly adapting crayfish stretch receptor, the

80

afterhyperpolarization was suggested to be caused by an electrogenic Na^+-pump (Nakajima and Takahashi 1966; Teorell 1971). Attempts to block the Na^+-pump with ouabain in this work failed to prove its involvement in the generation of the afterpotential. Ouabain induced a spontaneous firing followed by a prominent depolarization of the resting potential, and in both of these conditions the investigation of the small afterpotential became impossible. A similar kind of spontaneous firing also followed the application of blockers of I_A (Chapter 5) and $I_{K(Ca)}$ (Chapter 6) and their involvement in the generation of afterpotentials remained unclear. Tetraethylammonium chloride (TEA) prevented the repolarization after the upstroke of individual action potentials and also the AHP after a burst (Chapter 6), but TEA is a rather unselective blocker of different types of potassium channels (Hille 1992). Because of the dependence of the afterpotential on the preceding action potentials, it was not possible to study it directly in voltage-clamp when excitability was blocked by TTX. There are several possible explanations for the generation of the afterdepolarization: Inactivation of an outward potassium current after the end of depolarizing pulse may be strong enough to cause a depolarization. During the stimulus, intracellular Ca^{2+}-stores may be depleted and an inward Ca^{2+}-flux needed to refill the storage.

The site of action potential initiation in the tactile spine neuron still remains unclear after this work. Full size action potentials could be recorded in almost all experiments. The following chapters will provide information about the differences in the ionic current flow in the voltage-clamp recordings, which suggest differences in the recording positions

of the electrode inside the cell. The ionic mechanisms that shape the action potentials and

regulate the firing frequency will also be described.

5. A TRANSIENT OUTWARD CURRENT IN THE TACTILE SPINE NEURON[1]

5.1. Introduction

The time- and voltage-dependent properties of an excitable cell are largely determined by the distribution and relative numbers of ion channels that can be activated by changes in membrane voltage. Potassium channels form the most diverse family of different types of voltage-sensitive ion channels (Latorre et al. 1984; Rudy 1988). For example, the determination of resting membrane potential, the shape of the action potential, adaptation of firing frequency, pacemaking activity in cardiac muscle cells, and the integration of synaptic inputs are functions of various voltage-sensitive potassium channels (Thompson and Aldrich 1980; Adams and Galvan 1986; Rudy 1988; Kolb 1990). Several potassium currents, including the delayed rectifier type K^+-current (I_K), the calcium-dependent K^+-current ($I_{K(Ca)}$), the inward rectifier K^+-current and the transient A-type K^+-current (I_A), can be discriminated by their voltage sensitivities, kinetics of activation and inactivation, and pharmacological modulation (Thompson and Aldrich 1980; Rudy 1988). Single-channel recordings have revealed that several different channel types can contribute to each of these components and the identification of several genes, especially in

Drosophila, has lead to the view that there is a large variety of subtypes of K^+-channels (Tempel et al. 1987).

In this chapter I will describe the transient outward current in the tactile spine neuron. I_A was first found in molluscan neurons by Hagiwara et al. (1961) and later described more completely by Connor and Stevens (1971). This current has characteristics that distinguish it from other K^+-currents. I_A operates in the subthreshold region for action potential generation, activating transiently with small depolarization after a hyperpolarization (Rudy 1988; Norris et al. 1992), and it can usually be separated pharmacologically from other K^+-currents. In some cells I_A is more sensitive to inhibition by 4-aminopyridine (4-AP) than tetraethylammonium chloride (TEA), which selectively blocks I_K (Thompson 1977; Rudy 1988). Several different alleles of the *Shaker* gene in *Drosophila*, which vary in their activation and inactivation properties, have been identified as encoders of various A-channel types (Tempel et al. 1987).

In the tactile spine neuron I_A has very fast activation and inactivation kinetics, and it has an important function in the rapid adaptation of the neuron.

5.2. Results

Voltage-clamp

When the TTX-treated neuron was depolarized from rest, a voltage-dependent outward current was observed (Fig. 5.1A). When the membrane was first hyperpolarized and then depolarized, an additional transient component of outward current appeared in about half of the preparations studied (Fig. 5.1B). Passive currents were not subtracted from the recordings in Fig. 5.1.

After subtraction of passive currents, the maximum amplitude of the transient outward current was ~2.5 nA and the steady-state leakage current was ~3 nA at the maximum voltage. The transient part of the outward current could be separated from the total outward current by subtracting the currents with and without a hyperpolarizing prepulse (Fig. 5.2A). Application of 4-AP removed the transient outward current, but did not affect the steady state outward current (Fig. 5.2B). A small non-inactivating outward current could be observed after both subtractions. This current may be caused by a small error in the subtraction protocol or it may be part of a calcium-sensitive potassium current, which will be described in the Chapter 6. However, because of its significantly slower time constants of activation and inactivation it did not affect the kinetic analysis of the transient current. Application of 50 mM TEA in the saline reduced the steady state
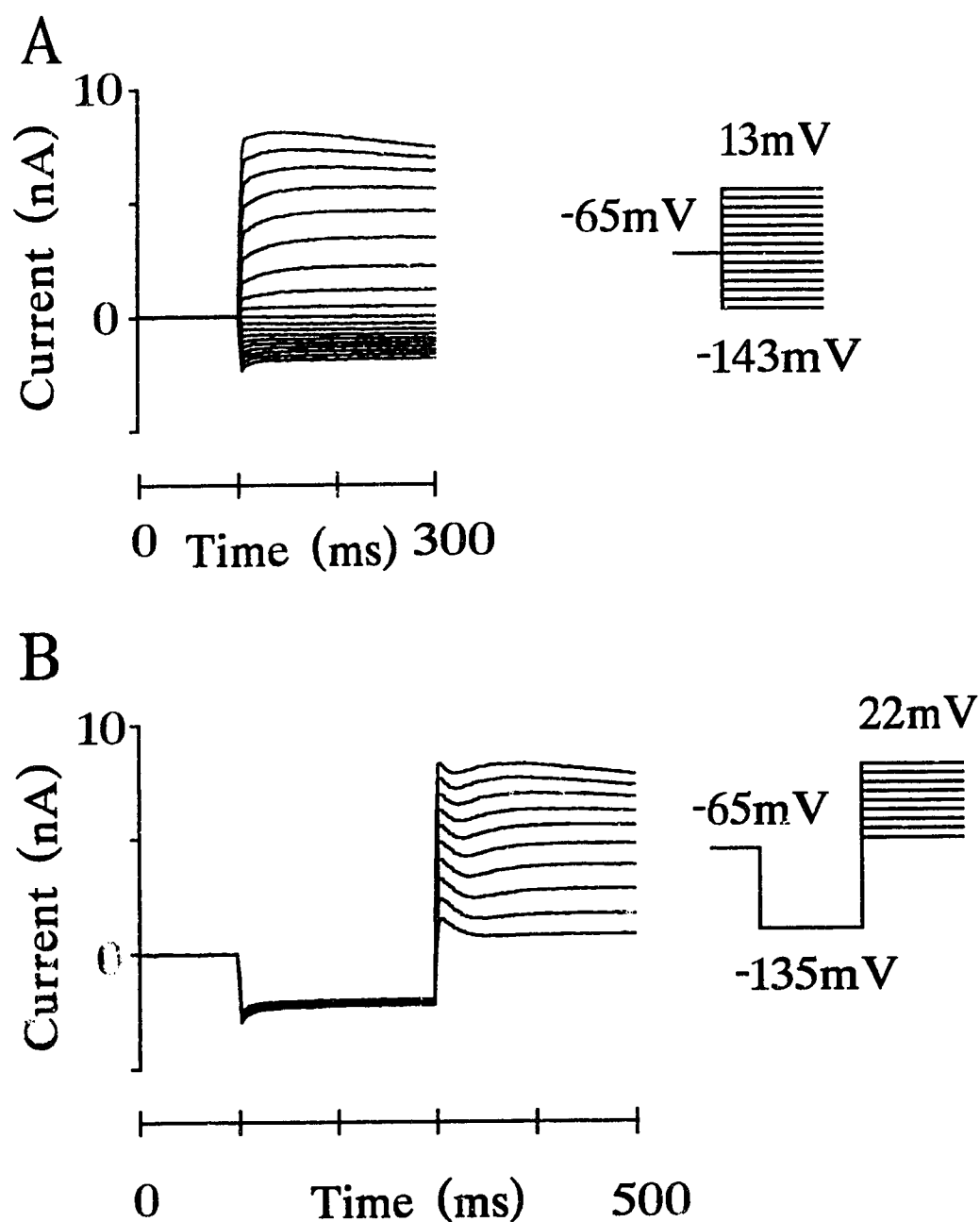
Figure 5.1. Outward currents were recorded after the inward currents were blocked with 10 μM TTX. The stimulus protocols, that were used to elicit the transient outward currents are shown inset in **A** and **B**. The outward currents evoked without conditioning prepulse are shown in **A** and **B** shows the currents that were produced after a conditioning hyperpolarizing pulse. Passive currents were not subtracted.

86
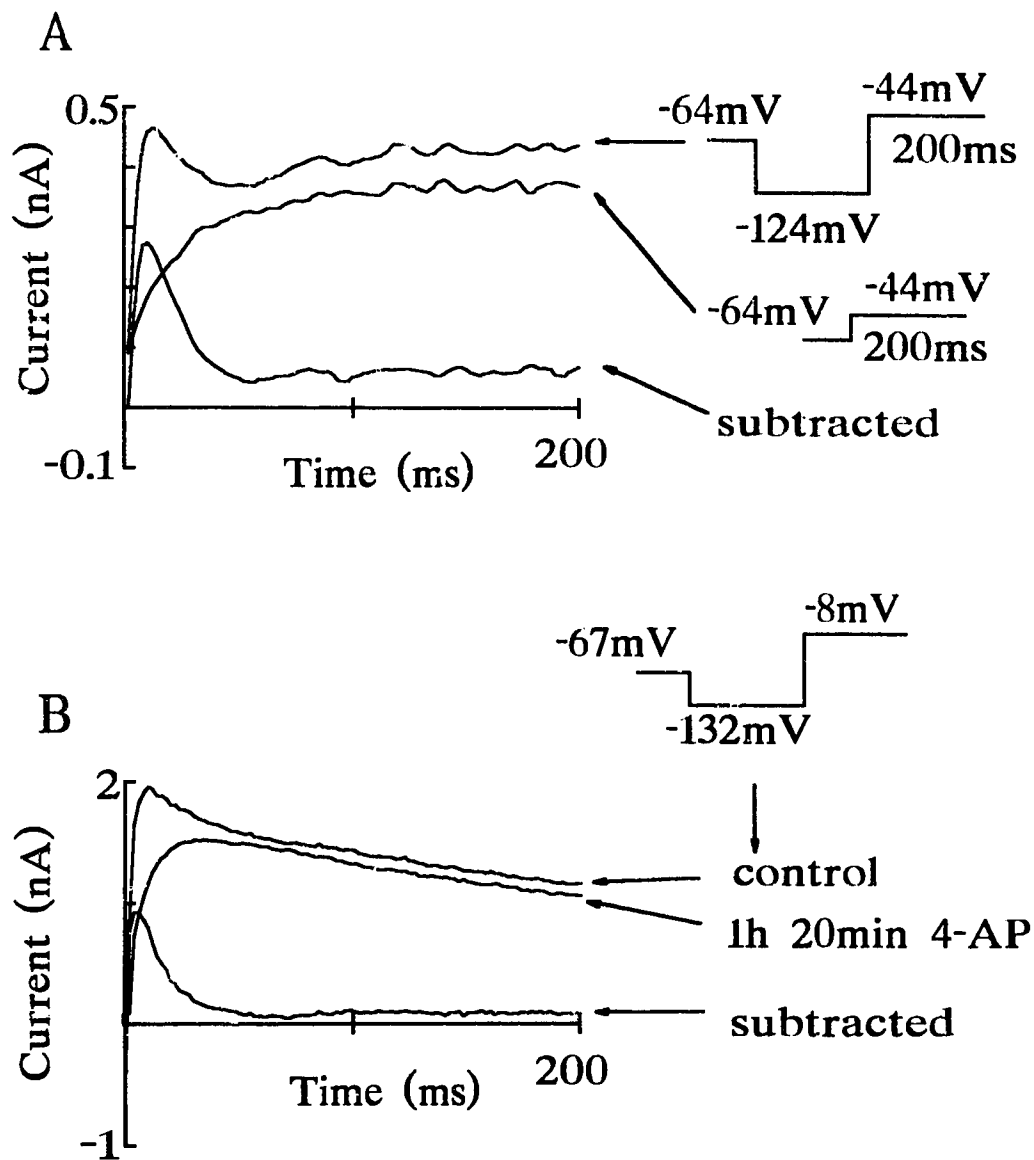
Figure 5.2. When the current produced by a voltage step without a negative prepulse was subtracted from that produced with a hyperpolarizing prepulse, A it revealed a rapidly activating and inactivating outward current. 5 mM 4-AP removed this transient outward current B, but did not affect the delayed outward current. Passive currents have been subtracted.

outward current by about 50%, but did not have any effect on the transient outward current (data is shown in Chapter 6).

The delayed outward current had at least two separate components and one of them activated in the same time scale as the transient current (Chapter 6). This made it impossible to estimate the reversal potential of the transient current from the tail currents, because they were contaminated with the tail currents of the other outward currents. However, Figure 5.4 shows that the transient current probably reversed below -75 mV, that is near the reversal potential for potassium ions under these conditions.

Kinetics of the transient outward current

The time dependence of the transient outward current was well-fitted by the function:

$$I = I_\infty [1 - e^{(-t/\tau_1)}]^m e^{(-t/\tau_2)}$$

(5.1)

where I_∞ is the current level expected in the absence of inactivation, τ_1 and τ_2 are the time constants of activation and inactivation, respectively and m is an integer exponent (Hodgkin and Huxley 1952b; Connor and Stevens 1971). The experimental data were well-fitted using $m = 4$ in equation (5.1) as shown in Fig. 5.3. The activation time constant, τ_1, was voltage dependent, with its minimum below 0.5 ms. The inactivation time constant, τ_2, was 10 - 20 ms and not strongly voltage dependent. The time-to-peak

value of the current with command voltages above 0 mV was about 10 ms (data not shown).

The voltage dependencies of activation and inactivation of the transient outward current were studied by measuring the peak current during double voltage pulse protocols. The experimental activation data were fitted by a Boltzmann distribution of the form (Andersen and Hablitz 1992; Baker et al. 1993):

$$g/g_{max} = \frac{1}{1 + e^{-(V-V_{50})/s}} \tag{5.2}$$

where g is conductance, V is membrane potential, V_{50} is the membrane potential at half maximal activation, and s is the slope factor. Conductance was calculated from:

$$g = I/(V - E_{rev}) \tag{5.3}$$

where I is the current and E_{rev} is its reversal potential. Fitting was performed by the Levenberg-Marquardt general nonlinear fitting algorithm (Press et al. 1990). Since E_{rev} was unknown, it was treated as a fitting parameter, along with g_{max}, V_{50}, and s. From five sets of activation data, the mean values of the fitted parameters were: $V_{50} = -56.5 \pm 3.7$ mV, $s = 6.4 \pm 2.2$ mV, $g_{max} = 24 \pm 21$ nS, and $E_{rev} = -94.5 \pm 9.7$ mV.

89
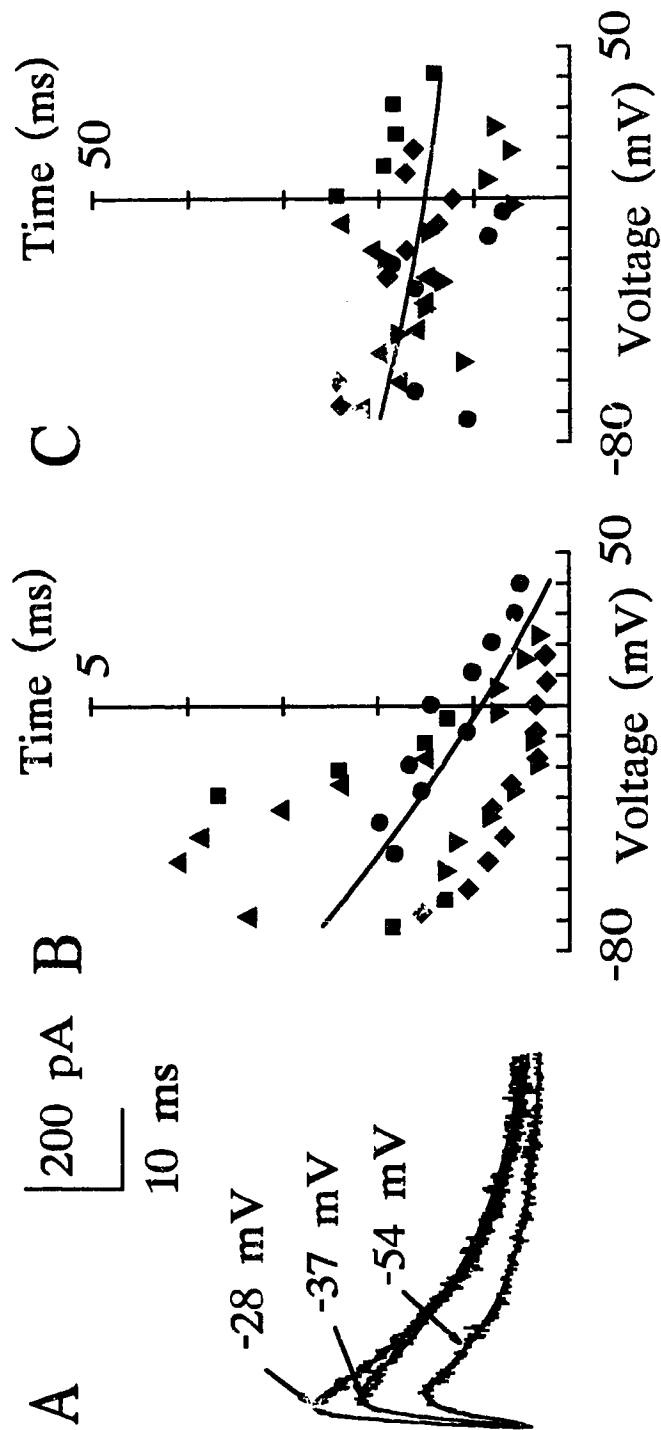
Figure 5.1. The transient outward current could be fitted by the Hodgkin-Huxley relationship (Eq. 5.2) with an exponent of $m = 4$. A shows the currents produced by steps to three different voltages from -62 mV, together with the fitted values of Eq. (5.2) (thicker lines). The time constants of activation **B** and inactivation **C** from Eq. (5.2) are shown as functions of voltage. Data points in **B** and **C** are from five different cells and the continuous lines were drawn by eye.

90
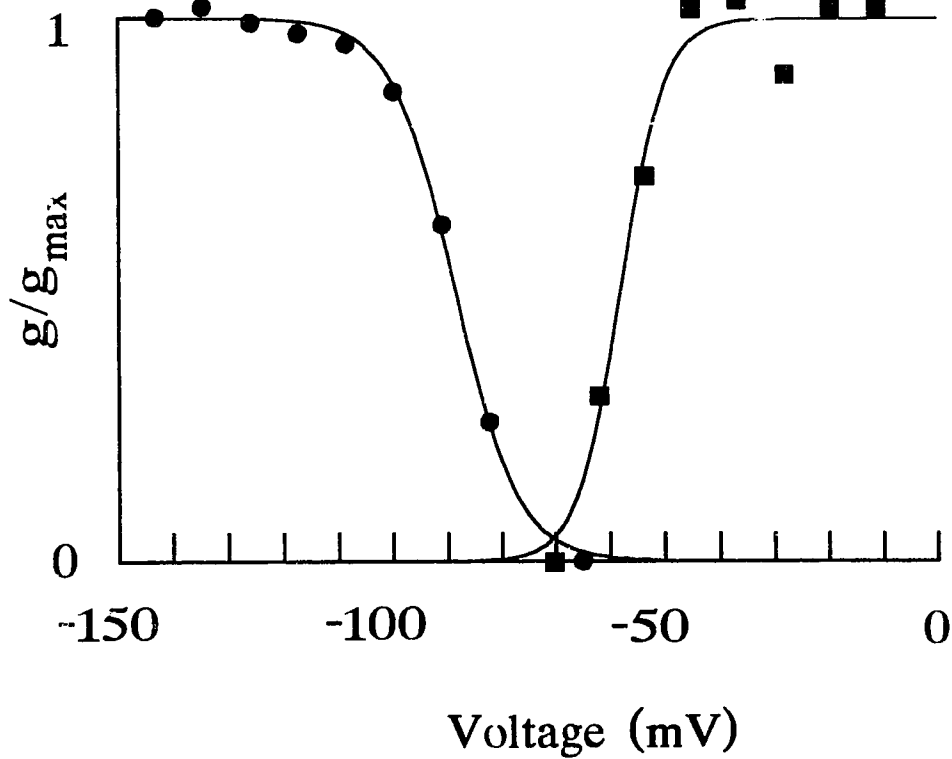
Figure 5.4. Voltage dependence of activation and inactivation of the peak transient outward current. For the activation data (squares), the cell was held at -70 mV, then hyperpolarized to -130 mV for 200 ms, and finally depolarized to different voltages. For the inactivation data (circles), the cell was hyperpolarized to different levels and then depolarized to -50 mV, where the peak activation was recorded. Continuous lines show fitted Boltzmann distributions to the normalized conductance. Current was converted to conductance during the fitting procedure, using the reversal potential and peak conductance as fitting parameters. For the two experiments shown here, the fitted parameters were: (Activation) $V_{50} = -57.9$ mV, $s = 4.1$ mV, $g_{max} = 12$ nS, $E_{rev} = -90.5$ mV; (Inactivation) $V_{50} = -88.6$ mV, $s = 5.75$, $g_{max} = 23$ nS.

A similar procedure was used for inactivation, using the reversal potential of -94.5 mV. From three experiments the fitted parameters were: V_{50} = -86.7±1.7 mV, s = 7.5±1.3 mV, and g_{max} = 18 nS. Examples of fitted conductance relationships for activation and inactivation experiments are shown in Fig. 5.4.

The equivalent gating charges for activation and inactivation were calculated from:

(5.4)

$$s = kT/ze$$

where k is the Boltzmann constant, T is absolute temperature, e is the elementary charge, and z is the valency of the equivalent gating charge. With s = 6.4 mV and kT/e = 25.26 mV (Hille 1992), the gating charge for activation was 3.9. For inactivation, when s = 7.5 mV, the gating charge was 3.4.

The time course of recovery from inactivation of the peak transient outward current was studied using a two pulse protocol, where the duration of the hyperpolarizing prepulse was varied (Fig. 5.5). The data points were fitted using a single exponential function with a time constant of 15.9 ms. The curve reached a plateau at a pulse duration of 50 ms.
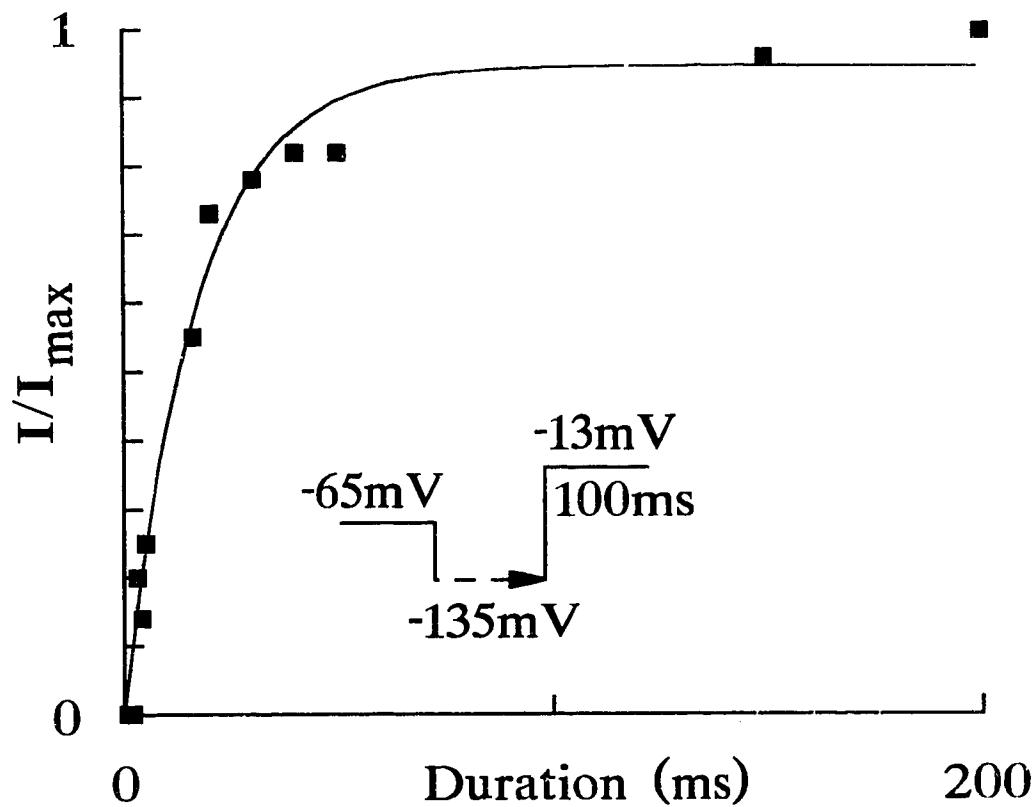
Figure 5.5. Recording of the time course of recovery from inactivation of the peak transient outward current. In these experiments the duration of the hyperpolarizing prepulse was varied (inset). The experimental points were fitted by a single exponential function with a time constant of 15.9 ms (continuous line). The peak current was normalized relative to its maximum value.

93

Current-clamp

A typical example of a current-clamp recording, before and after application of 5mM 4-AP, and also after washing with saline is shown in Fig. 5.6. In the control situation the cell adapted completely after about 2500 ms of the constant stimulus. The threshold for action potential initiation was 210 pA in this cell and 30 min after application of 4-AP it decreased to 50 pA. After 4-AP application, the same constant stimulus produced a significantly higher action potential frequency (Fig. 5.6). In this typical experiment, the duration of a single spike was 1.3 ms (half amplitude rise to half amplitude fall) before and after the 4-AP application. Its amplitude also remained quite constant, decreasing from 69 mV to 67 mV after 4-AP treatment, indicating that the transient outward current does not contribute to action potential repolarization. The effect of 4-AP was augmented by membrane hyperpolarization and reduced by depolarization. After a 30 min wash, the threshold for action potential production increased to 140 pA and the action potential frequency with a constant 500 pA stimulus declined to near the control situation. 4-AP never caused any depolarization in the tactile spine neuron; instead a slight hyperpolarization was sometimes seen, as in the experiment of Fig. 5.6.
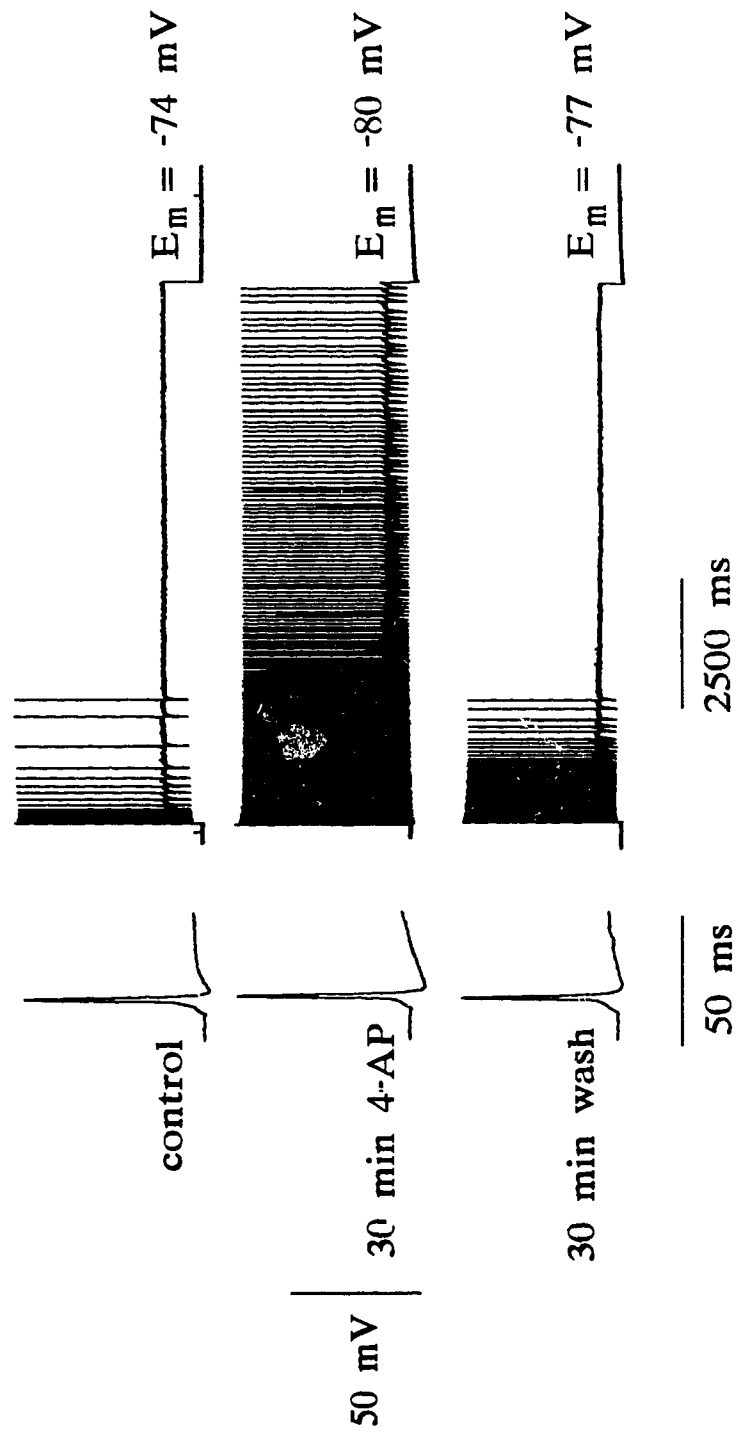
Figure 5.6. A current stimulus of 500 pA for 10 s elicited a burst of action potentials that adapted completely in about 2500 ms. Application of 4-AP for 30 min reduced the adaptation by decreasing the threshold for action potentials. 4-AP did not affect the amplitude or duration of the individual spikes, and its effect was reversible.

95

5.3. Discussion

Characterization of I_A

This is the first description of I_A in an insect mechanosensory neuron and also the first voltage-clamp study in this type of neuron. The activation and inactivation kinetics of I_A in the tactile spine neuron, and especially the voltage range where the current operates, are different from most of the other nerve cells where it has been studied (Rudy 1988). The activation threshold of I_A in the tactile spine neuron is about -75 mV and it reaches a maximum at -30 mV. The half maximal activation is achieved at -56.5 mV and half maximal inactivation at -86.7 mV. The time constants of activation and inactivation are about 0.2 ms and 15 ms respectively at the highest recording voltages (Fig. 5.3), and the maximum current is reached in about 10 ms. The activation and inactivation curves (Fig. 5.4) both have typical I_A sigmoidal shapes. The equivalent gating charge for activation was estimated to be 3.9, which is a typical value for potassium currents. The gating charge for inactivation was 3.4, which is somewhat lower than reported previously (Hille 1992).

Functions of I_A

A-currents with similar activation rates to the tactile spine neuron have been described before in pigeon semicircular hair cells (Lang and Correia 1989), guinea-pig type II vestibular hair cells (Rennie and Ashmore 1991), crab axons (Connor 1975;

Quinta-Ferreira et al. 1982), and crab coxal receptor neurons (Mirolli 1981). However, their activation thresholds were higher than in the tactile spine neuron (from -65 to -45 mV). Threshold values for I_A similar to those seen here have been reported in some insect neurons. For example, the threshold of I_A in blowfly monopolar neurons is -70 to -80 mV (Hardie and Weckström 1990). In all these cells the threshold for activation was near the resting potential, so that I_A could contribute to the membrane conductance during small depolarizations from rest.

The blocking action of 4-AP in the tactile spine neuron was clearly voltage-dependent as found earlier in several other preparations (Thompson 1982; Dubois and Rouzaire-Dubois 1991). The block was relieved by depolarization but restored by hyperpolarization indicating that 4-AP acts upon open channels. 5 mM 4-AP induced a very fast block compared to some other chemicals that we have used on this preparation (TTX and TEA), and 4-AP specifically removed the transient outward current without affecting the steady-state outward current. The dependence of the block on 4-AP concentrations varies greatly among different neural preparations. However, the dependence of the 4-AP effect on the voltage history makes it difficult to compare these results (Ulbricht and Wagner 1976). The results with tactile spine neuron are even more difficult to relate to other neurons because of the significant barrier around the neuron (Bernard et al. 1980) that causes a variable diffusion rate from the bath to the neuron. However, the effect of 4-AP in these experiments was specific in removing the transient outward current without

affecting the steady-state outward current. Correspondingly, TEA did not affect I_A, but removed half of the steady-state outward current.

The time constant of recovery from inactivation of A-current in the tactile spine neuron was 15.9 ms (Fig. 5.5) in agreement with other results, such as 17.3 ms in rat neocortical neurons (Andersen and Hablitz 1992). Hyperpolarization for a few milliseconds was enough to remove part of the inactivation and full activation was possible with a 50 ms prepulse.

In previous extracellular studies of the tactile spine neuron (French 1986b), 4-AP reduced the threshold and increased the membrane time constant slightly with hyperpolarization. Here we found that even 5 - 10 mV hyperpolarization for less than 5 ms was enough to remove the inactivation of I_A, and allow small depolarizations to activate the current. Thus, I_A in the tactile spine neuron can have an important function at normal physiological potentials. The current-clamp experiments showed that removing I_A with 4-AP increased the action potential frequency by decreasing the threshold for spikes. This indicates that I_A regulates the action potential frequency as in other preparations (Rogawski 1985; Rudy 1988).

In the tactile spine neuron I_A did not affect spike repolarization, as reported for example in frog myelinated nerve fibres (Dubois 1982). The afterhyperpolarization in the tactile spine neuron could not have been produced by I_A, as in some other neurons (Storm

1987: Ruppersberg et al. 1991). The amplitude of the small AHP in the tactile spine neuron actually increased when the I_A was blocked by 4-AP and the spike frequency increased (Fig. 5.6).

The threshold for action potential initiation in the tactile spine neuron is labile, increasing with depolarization and decreasing with hyperpolarization (French 1986b). This process has two time constants of 20 - 70 ms and 200 - 1000 ms depending on the recording techniques used (French 1986b; French 1989a; French and Patrick 1994 Stockbridge et al. 1991). The faster time constant has been linked to slow inactivation of sodium channels, because it can be removed with pharmacological agents that affect sodium channel inactivation (French 1987; French 1989a; Ramirez and French 1990 and Basarsky and French 1991). Although I_A raises the threshold of the neuron, it is too fast to be associated with either of the two above mentioned time constants of adaptation. Instead, its activation following a step depolarization will contribute another, faster component of adaptation at the start of the step response. In addition, I_A will be partially activated at the end of each action potential and will increase the interspike interval. Blockade of I_A should therefore increase the firing frequency throughout an adapting burst, as seen in Fig. 5.6.

In conclusion, the cockroach tactile spine neuron has an A-current with a narrow voltage operating range. It activates and inactivates at low voltages and with time constants that are among the fastest ever reported. This current lengthens the interspike

interval by opp)sing membrane depolarization and increases the threshold for action potentials, but does not participate in the repolarization of individual spikes. It is specifically blocked by 4-AP and is insensitive to TEA. I_A cont. butes to short term adaptation by decreasing the spike frequency during a constant depolarizing stimulus with a fast time constant that has not been described previously.

6. SLOWLY INACTIVATING OUTWARD CURRENTS IN THE TACTILE

SPINE NEURON

6.1. Introduction

Delayed rectifier potassium current (I_K)

Hodgkin and Huxley (1952a) first described the delayed rectifier type of K^+-current (I_K) in the squid axon. They showed, that I_K activates with a delay upon membrane depolarization, rising more slowly than the sodium current and forming the main component of action potential repolarization, and then slowly inactivates. Similarly functioning currents were later found in the frog node of Ranvier (Frankenhaeuser and Huxley 1964) and numerous other vertebrate and invertebrate nerve cells (Rudy 1988; Kolb 1990).

Because no selective pharmacological agonist has been found for delayed rectifier K^+-channels, their separation from other slowly inactivating potassium channels is often difficult. I_K can be blocked by quaternary ammonium ions, for example tetraethylammonium (TEA), that may act from extra- or intracellular- or both sides of the membrane depending on the neuron (Armstrong 1971; Stanfield 1983). Cesium ions (Wagoner and Oxford 1987), 4-AP and dendrotoxins (Hille 1992) have also been shown to block delayed K^+-channels, but all of these chemicals also block several other

potassium channel types, and therefore cannot be used as exclusive agents in the classification of K^+-channels.

Rudy (1988) described the criteria for classifying a K^+-current as a delayed rectifier as follows: **1.** The overall kinetic behavior and voltage dependence of the current should be similar to that described by Hodgkin and Huxley (1952a) for I_K (i.e. delayed activation after a depolarizing step, slow inactivation from hundreds of milliseconds to several seconds and sigmoidal dependence on voltage). **2.** I_K should be clearly distinct from the transient outward current, with slower inactivation kinetics and without the need for membrane hyperpolarization before activation. **3.** I_K should not be activated by a rise in the internal Ca^{2+} concentration, as are various calcium sensitive K^+-currents ($I_{K(Ca)}$).

Calcium-activated potassium currents $(I_{K(Ca)})$

Several types of potassium channels have been described that increase their permeability to potassium ions in response to increases in intracellular calcium concentration (McManus 1991). The rise in intracellular calcium concentration that follows the upstroke of an action potential, leads to an efflux of potassium ions through Ca^{2+}-activated K^+-channels, which hyperpolarizes the membrane. Therefore, $I_{K(Ca)}$ is always a repolarizing current and it regulates action potential frequency and duration in neurons and other excitable cells (McManus 1991).

Ca^{2+}-activated K^+-channels can be divided to two main categories based on differences in single-channel conductance, voltage dependence and sensitivity to blockers. The distinct contributions of these channel types to the overall cellular K^+-current is variable in different cell types (Kolb 1990). The large-conductance Ca^{2+}-activated K^+-channels (BK-channels) have been found in most cell types studied with the patch-clamp technique (Kolb 1990). The unitary conductance of these channels varies from 150 to 300 pS depending on the cell type. The sensitivity of BK-channels to Ca^{2+} increases with membrane depolarization. Nanomolar concentrations of the highly basic protein charybdotoxin (CTX), which is derived from the venom of the Israeli scorpion *Leirus quinquestriatus*, block these channels from the extracellular side (Miller et al. 1985). Low concentrations (0.1 - 1 mM) of TEA also block some of the BK-channels (Rudy 1988; Kolb 1990), but they cannot be blocked by apamin, a peptide from bee venom, which blocks the small conductance Ca^{2+}-sensitive K^+-channels.

BK-channels have been shown to induce the repolarization of the action potential and contribute to the regulation of firing frequency in several excitable cells, for example bullfrog sympathetic ganglia (Adams et al. 1982; MacDermott and Weight 1982) and snail neurons (Crest and Gola 1993). The BK-channels open during the early depolarization of an action potential, causing fast repolarization of the membrane potential, and then rapidly turn off. This terminates Ca^{2+} entry and the membrane returns to resting level (Pallotta et al. 1981; Romey and Lazdunski 1984).

The unitary conductance of the small conductance Ca^{2+}-activated K^+-channels (SK-channels) is only 10 - 14 pS (Blatz and Magleby 1986). They have not been shown to be dependent on voltage, and they are responsible for a slow afterhyperpolarization following action potentials in bullfrog sympathetic neurons, rat skeletal muscle and rat sympathetic neurons (Rudy 1988) and they are therefore often called AHP-channels (Pennefather et al. 1985). SK-channels can not be blocked by externally applied TEA (Pennefather et al. 1985; Blatz and Magleby 1986) or CTX, as can the BK-channel. Nanomolar concentrations of apamin, blocked the AHP-channels in rat skeletal muscle cells (Romey and Lazdunski 1984; Blatz and Magleby 1986), in bullfrog sympathetic neurons and in cat spinal motoneurons (Zhang and Krnjevic 1987).

The classification of K^+_{Ca}-channels into BK and SK groups has been challenged by description of several intermediate conductances (Crest and Gola 1993). Intermediate-conductance Ca^{2+}-activated K^+-channels (IK) do not fit into either of these two basic groups, and they probably include several types of channels that differ in their voltage- and calcium sensitivities as well as single-channel conductances (McManus 1991). Their unitary conductance is 50 - 150 pS and they are typically blocked by apamin but not by CTX or external TEA (McManus 1991). However, they often share pharmacological similarities with some BK- and SK-channels in the same tissue, for example, in rat brain synaptosomes they can be blocked by CTX and in rat brain by submillimolar TEA (Reinhart et al. 1989).

The fast AHP, that is produced by BK-channels in hippocampal neurons, regulates the early action potential frequency while the long-lasting AHP, that originates from the action of SK-channels, is responsible for long-term adaptation (Lancaster and Adams 1986; Madison and Nicoll 1986). When the fast AHP is blocked by TEA, the duration of action potentials, as well as their initial frequency, is increased (Lancaster and Adams 1986; Storm 1987). When the long-lasting AHP is blocked, the spike duration does not ch ge, but the adaptation is prevented (Lancaster and Adams 1986; Madison and Nicoll 1982; Rudy 1988).

Extracellular recordings from the tactile spine neuron failed to show any involvement of a delayed rectifier type K^+-current in the adaptation behavior (French 1986b), but TEA was shown to increase the duration of the action potentials (French 1984c). Convincing evidence has not previously been gained for the existence of any Ca^{2+}-activated K^+-conductance in the spine neuron (French 1986). However, voltage-clamp experiments revealed a prominent outward current that activated rapidly after depolarization and did not totally deactivate during a maintained stimulus of up to 1 s. This current was clearly voltage-dependent and reversed near the equilibrium potential for potassium ions. The purpose of this chapter is to identify the components of the total outward current, to describe their kinetic behaviours and their functions in spike repolarization and frequency modulation of the tactile spine neuron.

6.2. Results

The current-clamp experiments described in this work are based on recordings from 16 different tactile spine neurons and the voltage-clamp data was obtained from 15 neurons. The complete series of current-clamp recordings, when blocking agents were used, lasted three to four hours (control recording, blocking action and rinsing). For voltage-clamp recordings, an additional one to two hours was consumed in waiting for the TTX to block the inward currents. Only recordings that remained stable during this total period, with no changes in the electrode resistance, were used for analysis.

The total voltage-sensitive outward current

The membrane currents were recorded while stepping the potential to different levels from a holding potential that was close to rest. Fig. 6.1 shows two series of current recordings from two different cells when positive and negative steps were used and the leakage currents were subtracted. In nine recordings the current reached a clear peak and decayed to a smaller steady-state value with two time constants as in the experiment shown in Fig. 6.1A and B. In the other six recordings the steady-state and peak values of the current were nearly identical, and the current decayed very slowly with only one time constant or in some cells it did not decay at all during the observation period of 500 ms (Fig. 6.1C and D). The leakage currents were subtracted from these and other figures of original recordings using the following equation:
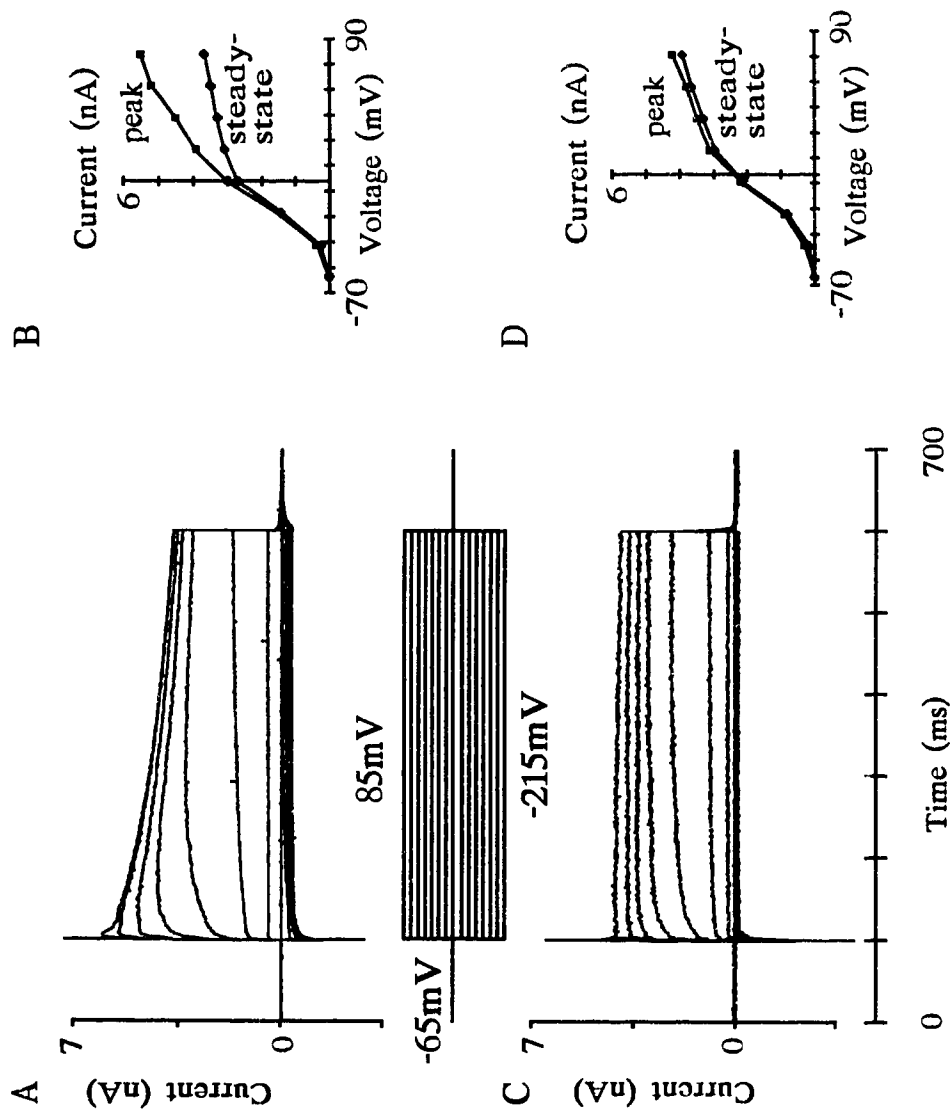
Figure 6.1. Outward currents produced with positive and negative voltage steps from holding potentials of -65 mV to the voltages indicated between the current recordings (**A** and **C**). The current-voltage graphs (**B** and **D**) show the peak currents at about 5 ms and the steady-state currents at 500 ms. The leakage currents were subtracted as explained in the text.

107

$$I_{leak} = I_{obs} - (V_m - V_H)/R_m \qquad (6.1)$$

where, I_{leak} = the leakage current, I_{obs} = the observed current, V_m = membrane voltage, V_H = holding voltage and R_m = membrane resistance obtained from the linear part of the current-voltage curve at negative potentials.

Tail currents

Tail currents (= instantaneous currents) are relaxation currents which persist for a period of time after the end of command voltage step. Immediately after the step, the magnitude of the tail current should reflect the number of ion channels that were open at the end of the command. Therefore, tail current reversal potentials can be used to determine the reversal potential of currents generated by a standard voltage step. Fig. 6.2 shows an example of tail currents of the total outward current in the tactile spine neuron. The voltage was stepped from the holding potential of -65 mV to a test pulse of -5 mV for 500 ms to activate the outward current, followed by repolarization to different potential values. The amplitude of the tail current without leakage subtraction was measured 1 to 3 ms and 200 ms after the repolarization. The steady-state current at 200 ms was assumed to consist mainly of the leakage current at potentials from 20 mV above to 60 mV below the holding potential. The peak and steady-state current values were plotted against the repolarization potential (Fig. 6.2). The reversal potential was defined as the intersection of these two curves (Ritchie 1987). The average reversal
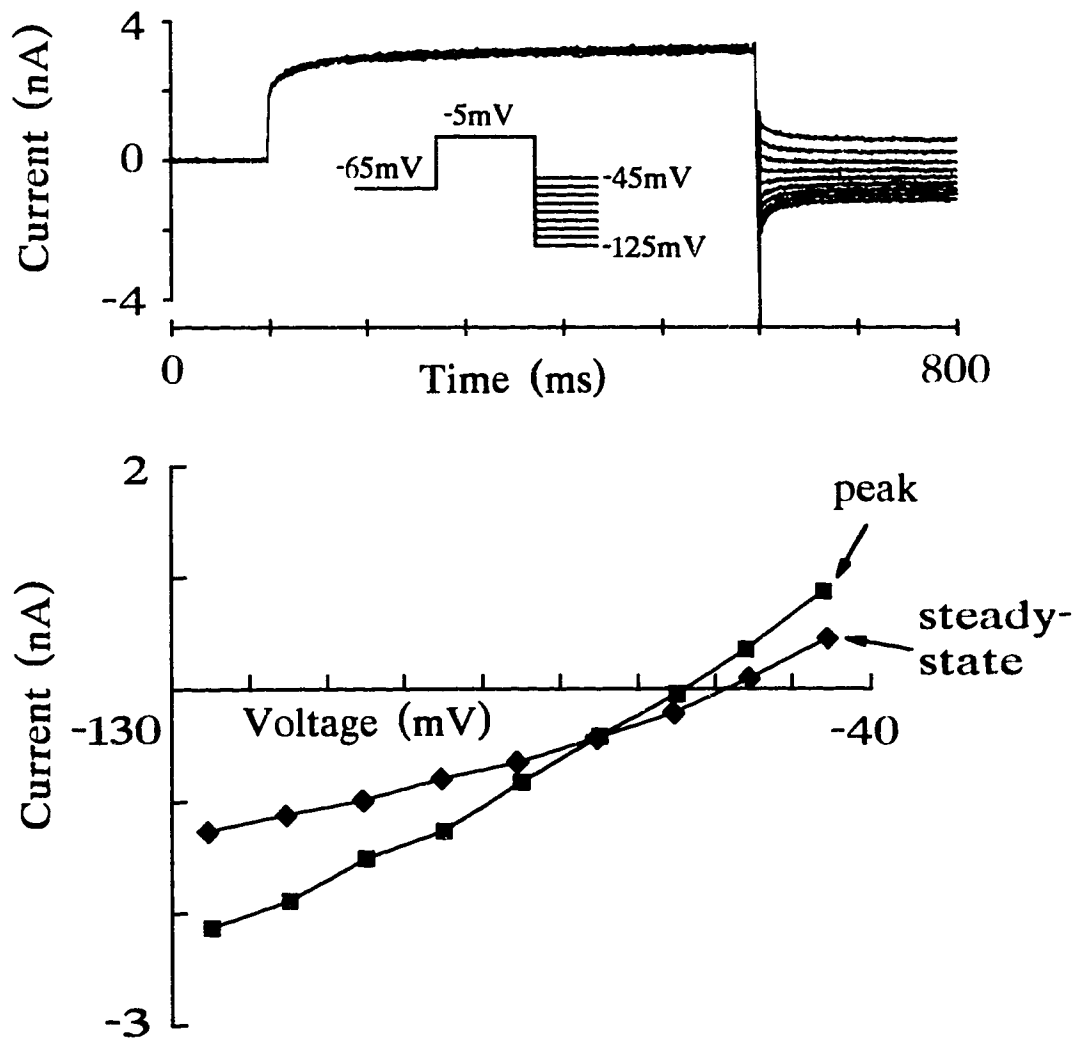
Figure 6.2. Tail currents elicited with steps to different values after a constant step from holding potentials of -65 mV to -5 mV are shown above. The peak values of the tail currents at 2.5 ms and at the steady-state (200 ms) are plotted against voltage (below). Reversal potential was taken to be the voltage at which the two current-voltage curves intersect (see text). In this example the reversal potential was -75 mV.

potential of 15 tactile spine neurons was -81.9±17.9 mV (mean and standard deviation).

Activation and inactivation of the total outward current

The time constants for the total outward current were determined using the exponential power equation (5.1, page 87) if only one inactivation time constant was needed to fit the decay of the current. If the current decayed with two time constants equation (6.2) was used to fit the experimental data.

$$I = I_{\infty}[1 - e^{(-t/\tau_1)}]^m([\alpha e^{(-t/\tau_2)}] + [(1 - \alpha)e^{(-t/\tau_3)}]) \tag{6.2}$$

where I_{∞} is the current level expected in the absence of inactivation, τ_1 is the time constant of activation and τ_2 and τ_3 are the two time constants of inactivation, m is an integer exponent and α is the relative amplitude of the two inactivation components (Hodgkin and Huxley 1952b). Fig. 6.3 shows that the experimental data was well fitted using $m = 1$ in equation (5.1) or (6.2).

Figs. 6.4 and 6.5 show the time constants of activation and inactivation if one or two exponentials were needed to describe the decay. The activation time constants were somewhat dependent on voltage (Figs. 6.4A and 6.5A) varying from less than one
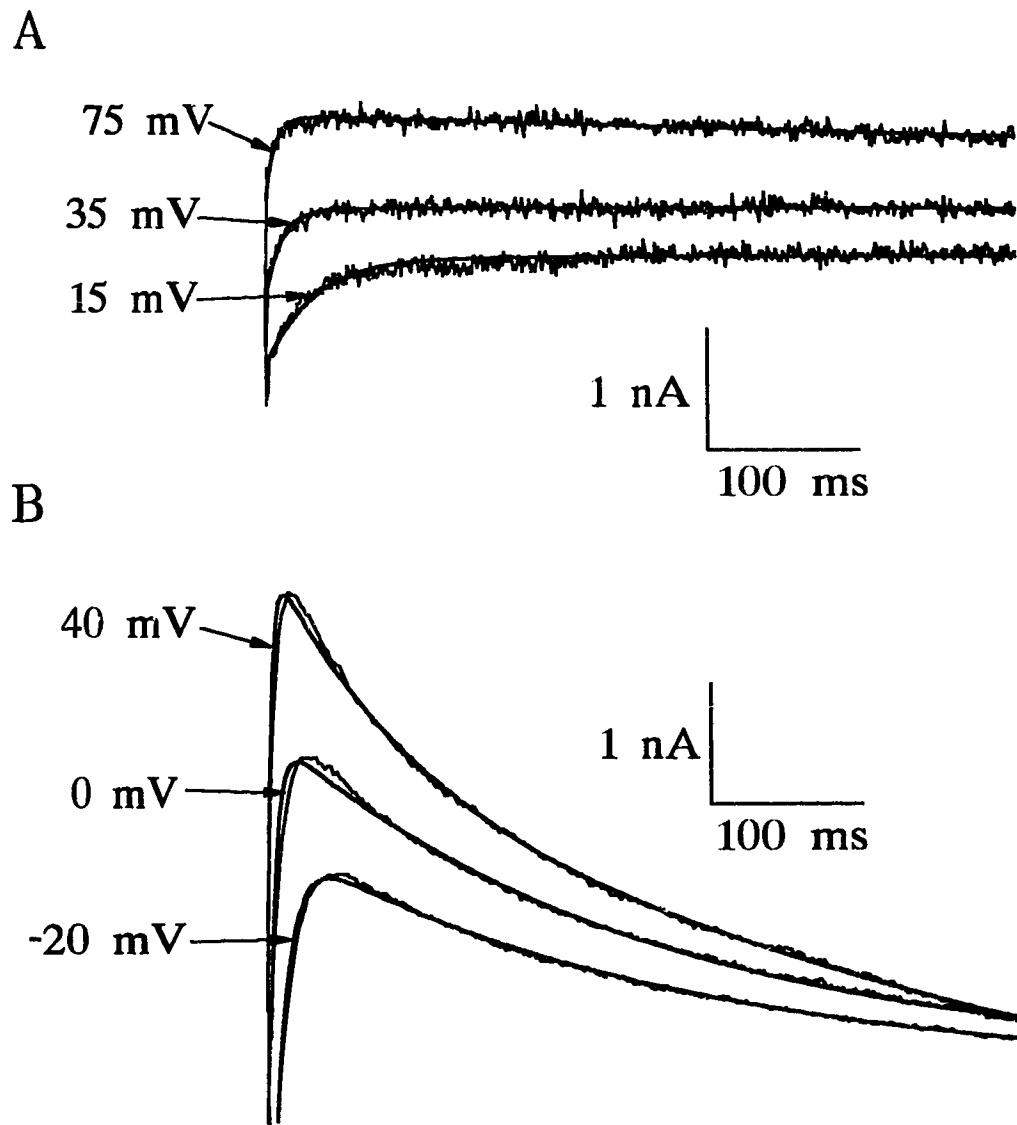
Figure 6.3. The current produced by steps to three different voltages from holding potentials of -65 mV and -60 mV in two different neurons are shown in **A** and **B** respectively. The thicker line in **A** is the Hodgkin-Huxley type fit with one exponential decay (Eq. 5.1) and **B** a similar fit but with two exponential decays (Eq. 6.2).
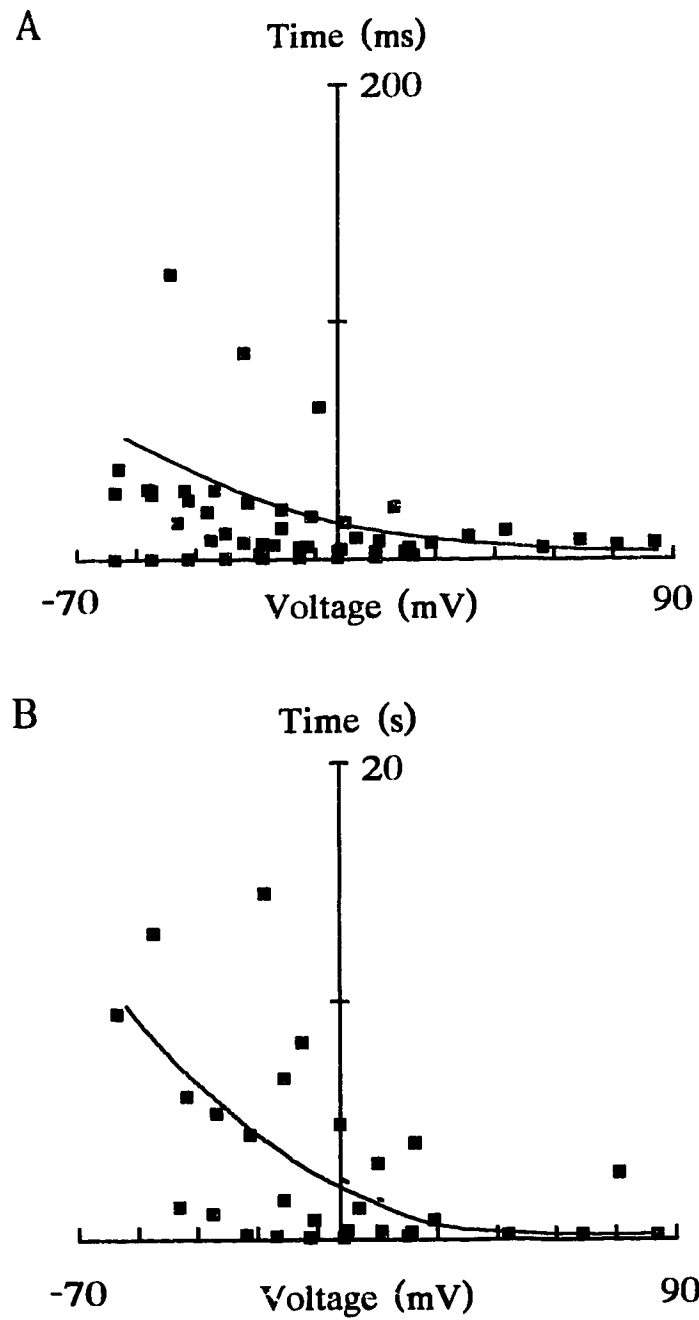
Figure 6.4. The activation **A** and inactivation **B** time constants obtained when one exponential decay was needed to fit the experimental data (Fig. 6.3A, Eq. 5.1). The data points are from recordings of six different cells, and the continuous lines were drawn by eye.
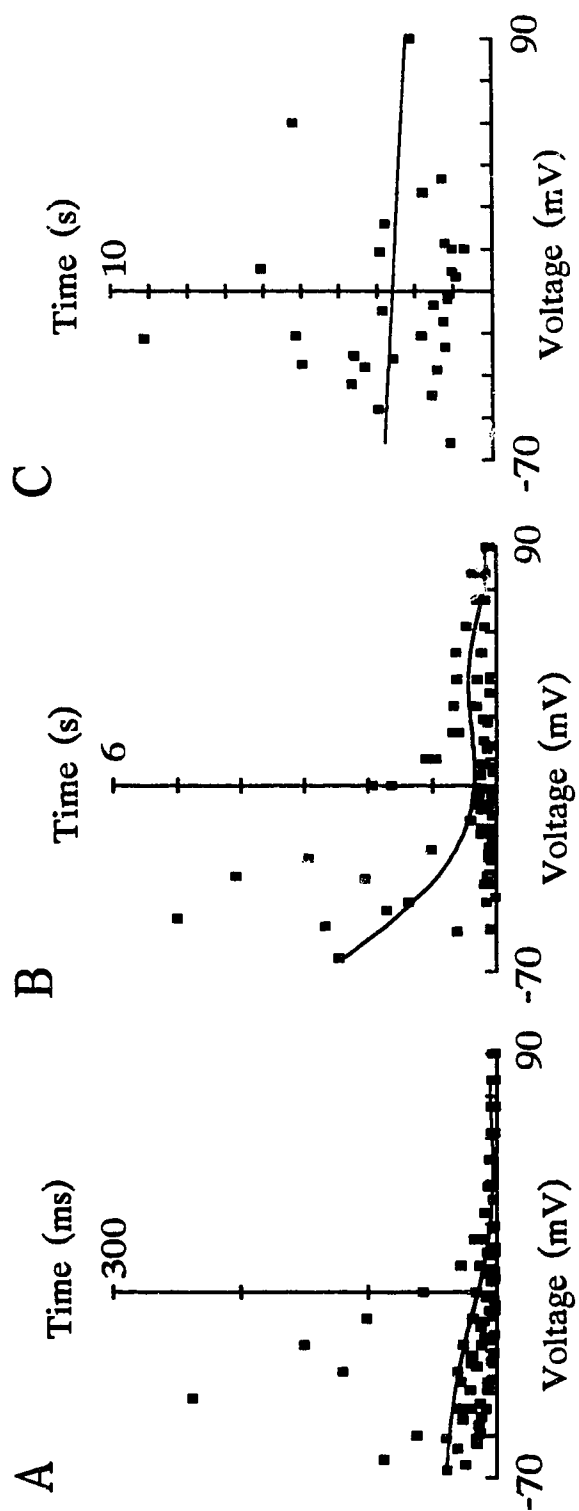
Figure 6.5. The activation time constants **A** and fast **B** and slow **C** inactivation time constants from recordings of nine different cells where the experimental data was fitted using two exponential decays (Fig 6.3B, Eq. 6.2). The continuous lines were drawn by eye.

113

millisecond at more positive voltages to up to few hundred milliseconds with moderate depolarization. The total outward current activated at about the same rate if there was one time constant of inactivation or two. The voltage dependence of inactivation time constants in the first group of cells varied from about 100 ms up to more than 10 seconds (Fig. 6.4B). If the experimental data could be fitted with two exponential decays, only the first time constant of decay was dependent on voltage, varying from about 50 ms to several seconds. The second time constant was more consistent at different membrane voltages, with the average value being 2.5 s. The electrophysiological properties from the recordings of cells with the different current profiles in the voltage-clamp experiments are summarized in Table 6.1.

The only statistically significant difference between the two different groups was found between the action potential amplitudes ($p = 0.0122$), when tested with a single sided T-test. There was no clear difference in the membrane resistance, or the threshold for action potential initiation, as would be expected if the electrodes were at very different locations inside the cell.

Table 6.1. Electrophysiological properties of cells with two different types of current responses. Type I indicates cells whose response was fitted using one exponential decay and Type II means the cells whose response were best fitted with two exponential relaxation time constants. The values are given as means ± standard deviations.

	Type I	Type II	Total
Resting potential (mV)	-64.7 ±6.4	-64.3 ±5.4	-64.5 ±5.6
Reversal potential (mV)	-81.0 ±13.6	-82.4 ±21.0	-81.9 ±17.9
Input resistance (MΩ)	46.8 ±13.2	38.6 ±12.7	41.9 ±13.0
Action potential amplitude (mV)	65.0 ±10.5	75.6 ±5.3	71.3 ±9.2
Threshold current (pA)	130 ±60	211 ±120	177 ±100
Number of experiments	6	9	15

Pharmacology

Experiments with known blockers of potassium currents never produced a complete block of the outward current; a portion of the current always remained after such treatment. The most prominent effect was obtained when the extracellular calcium ions were replaced with equal concentrations of Co^{2+} or Cd^{2+} (Fig. 6.6), which block
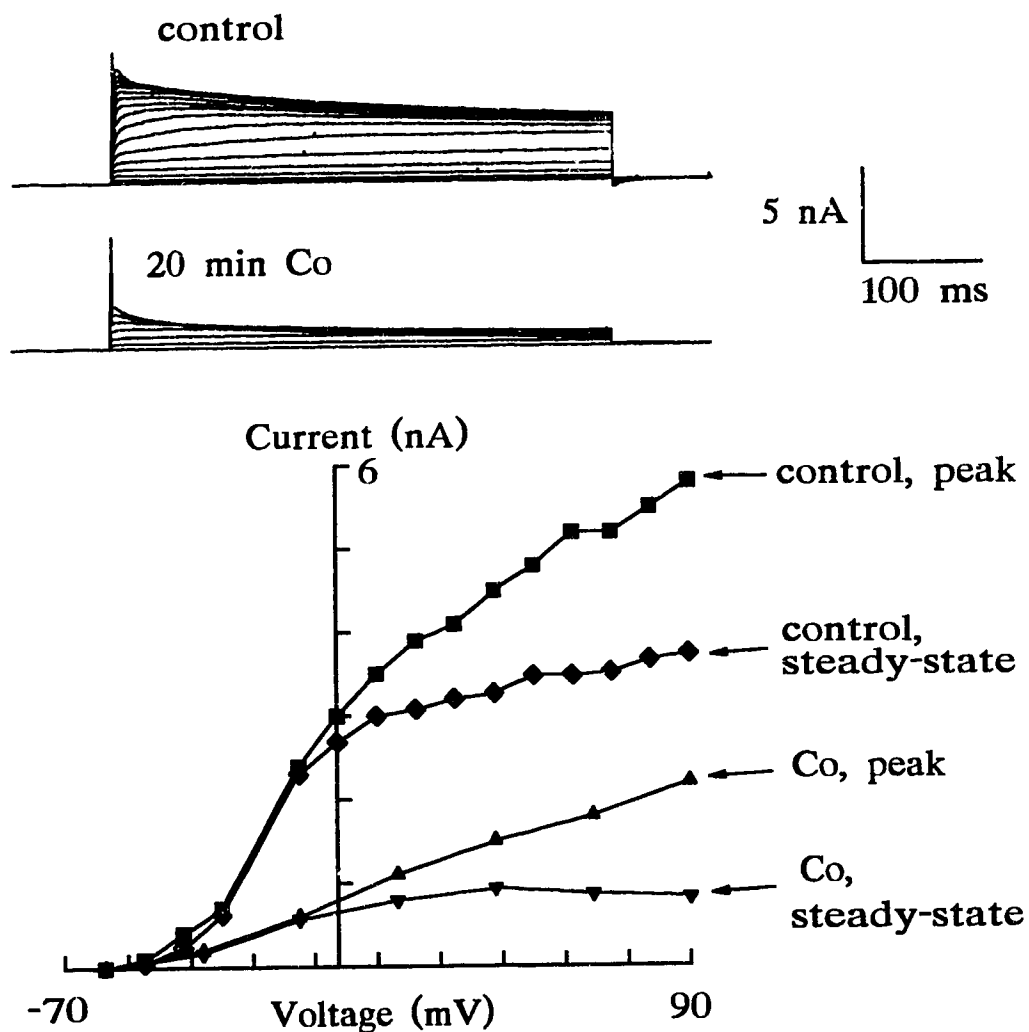
Figure 6.6. A typical example of the effect of Co^{2+}-ions on the outward currents. Upper part shows leakage subtracted current recordings in normal saline and 20 min after replacement of extracellular Ca^{2+} with the same concentration of Co^{2+}. After this treatment about one third of the voltage-sensitive current still remained. The current-voltage curves of the peak and steady-state outward currents in control and Co^{2+}-saline are shown below.

116

control

5 nA

100 ms

1h TEA

Current (nA)

5

control, peak

control,
steady-state

TEA, peak

TEA,
steady-state

-70

60
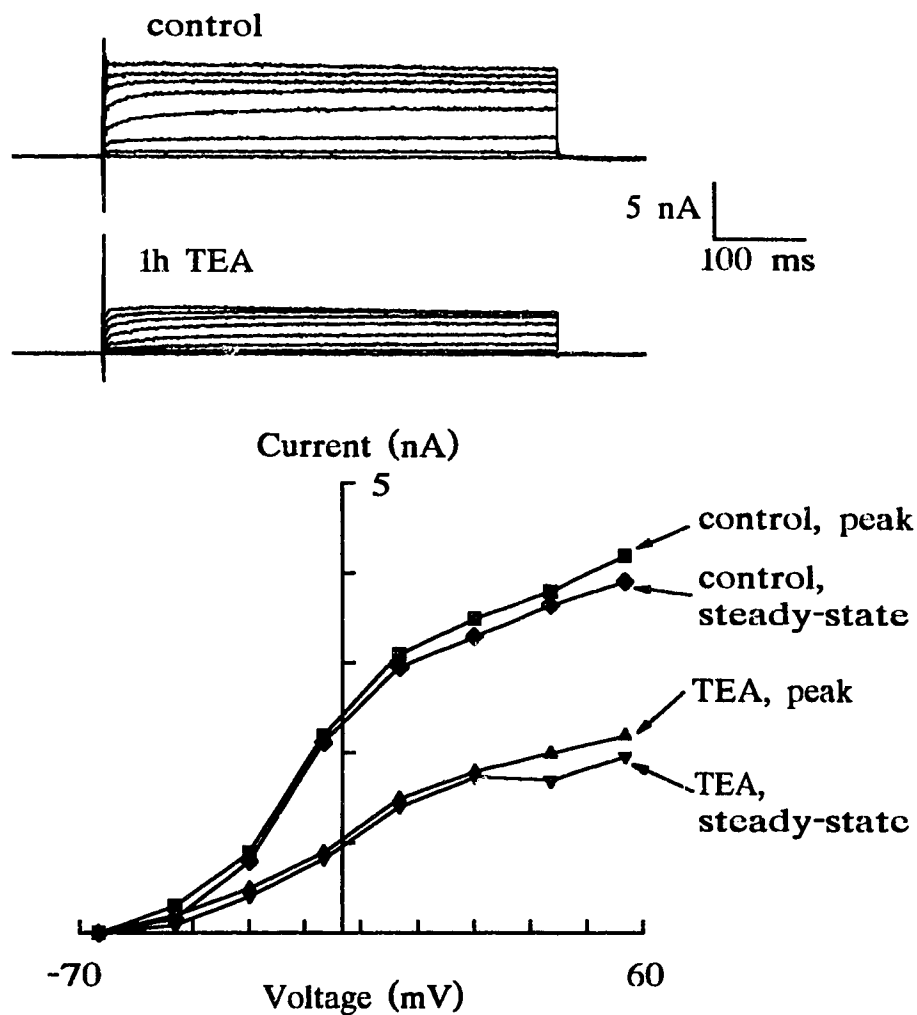
Voltage (mV)

Figure 6.7. A typical example of the effect of 50 mM TEA on the voltage sensitive outward currents. The leakage subtracted original current recordings are shown above in normal cockroach saline and 1 hour after application of 50 mM TEA iʰ ᵗhe saline. TEA reduced the current to half of its original amplitude as shown in the current-voltage relationship curve (below) of the peak and steady-state outward currents before ᴀnd after TEA treatment.

117

Ca^{2+}-channels and thus inhibit the $I_{K(Ca)}$. The voltage-sensitive outward current was reduced to about one third of its original amplitude in the recording shown in Fig. 6.6. A similar reduction of the current was observed in three different experiments. The blocking action of Co^{2+} was stronger than Cd^{2+}. Longer application times, up to 1 h 30 min, did not produce any more block. This result indicates that the largest part of the voltage-sensitive outward current is also sensitive to intracellular Ca^{2+}-concentration. The toxins that are known to block $I_{K(Ca)}$, CTX and apamin, were not used in the voltage-clamp experiments, because apamin did not have any effect on the voltage response in the normal saline, as will be shown in the results of current-clamp experiments, and the blocking effect of CTX was very slow. CTX has also been shown to block other voltage-sensitive K^+-currents (Hille 1992).

A typical example of the effect of 50 mM TEA on the outward currents is shown in Fig. 6.7. In four different experiments the maximal block with TEA was about half of the total voltage-sensitive outward current. TEA has been known to block almost all types of K^+-currents and its effect on the tactile spine neuron apparently overlaps with the blockers of Ca^{2+}-channels. 4-aminopyridine, which was shown to block I_A in Chapter 5. did not have any significant effect on the persistent outward current, and TEA did not block I_A.

In order to find out if TEA or Co^{2+} blocks different parts of the outward current, the time constants of activation and inactivation of the current in normal saline

118
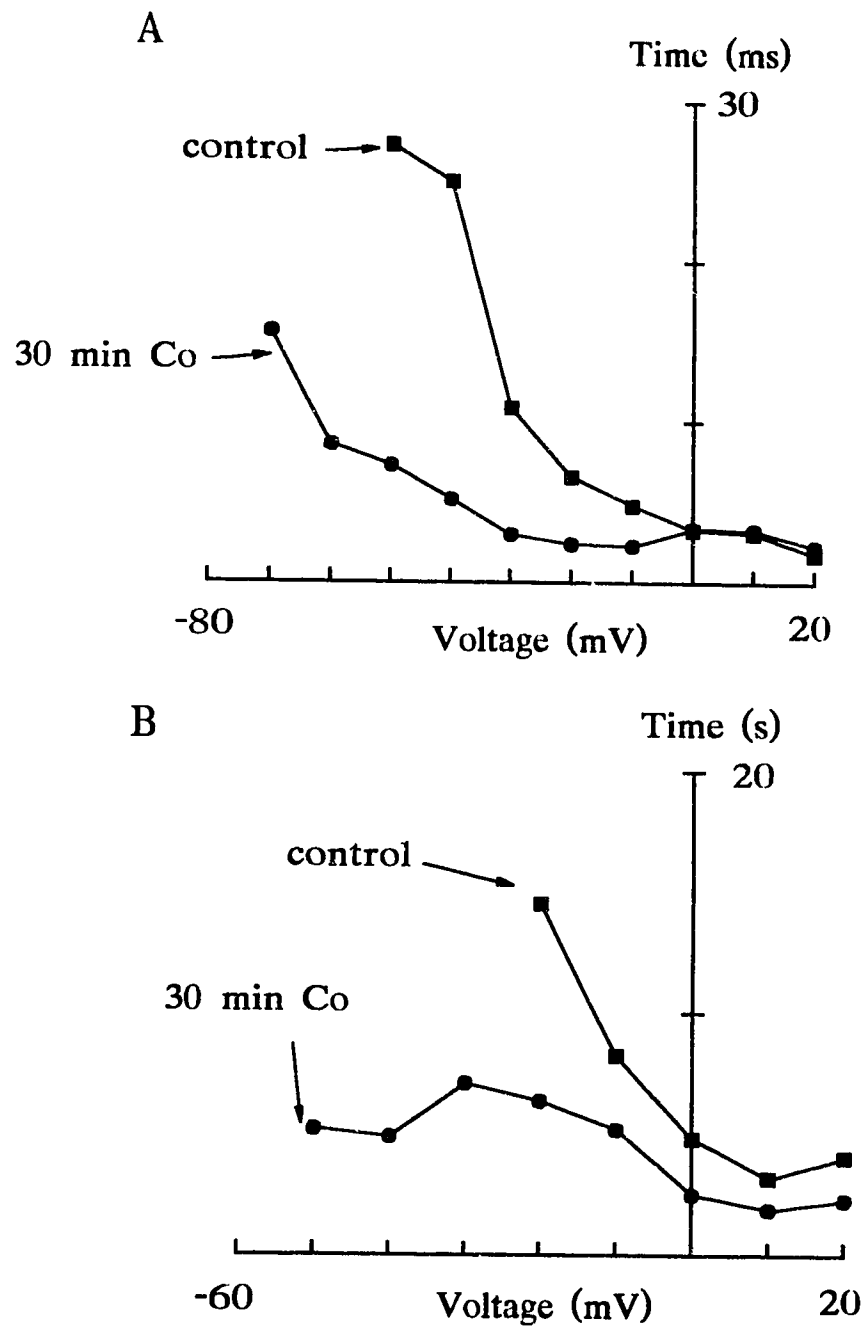
Figure 6.8. The effect of Co^{2+} on the time constants of activation **A** and inactivation **B** The part of the outward current that was resistant to the Ca^{2+}-channel blocker showed faster activation and inactivation kinetics, especially at lower voltages.

119
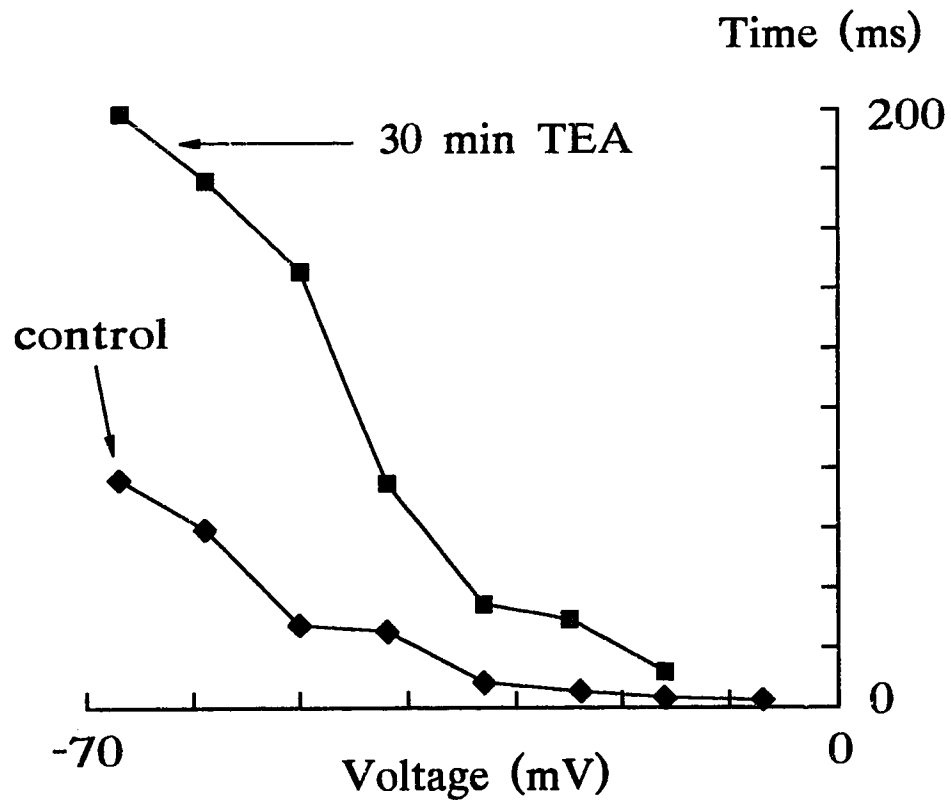
Figure 6.9. At moderate depolarizations the time constant of activation became slower after the cell was treated with 50 mM TEA.

120

were compared to the time constants of the persistent currents. Exponential power function (Eq. 5.1) was used to find the time constants as explained earlier, using an exponent of 1 in all experiments. Fig. 6.8 shows the time constants of one experiment with Co^{2+} in the saline. At moderate depolarizations the activation time constants were significantly slower in normal saline than after the application of Co^{2+} (Fig. 6.8A), ranging from 15 to 100 ms near rest to less than 1 ms at potentials above 0 mV. At higher depolarizations no differences between the control and Co^{2+}-persistent current were found. In the recording shown in Fig. 6.8B only one decay time constant was needed to fit the control current response, and after Co^{2+}-treatment it was somewhat faster than in the control solution. If two time constants of inactivation were observed in control saline, only one, which was faster than either of them, remained after Co^{2+} treatment. The inactivation time constants were not strongly dependent on voltages, ranging from 150 ms to 5 s. In one experiment where Cd^{2+} was used as a blocking agent, there were no significant changes in the time constants, but in this case larger part of the outward current also remained after the treatment. TEA had an opposite effect on the activation time constants as shown in Fig. 6.9. The activation time constant of TEA-persistent current varied from 30 to 200 ms near rest to less than 1 ms at potentials above 0 mV. No inactivation was observed until high depolarizations, and even then the time constant of inactivation was very slow, often more than 10 s.

The reversal potentials for the Co^{2+}- and TEA-insensitive parts of the currents were determined as described earlier for the total outward current and shown in Figs. 6.10. and 6.11. The mean reversal potential for the TEA-insensitive part of the outward current was -86.8±7.9 mV (n = 4) and for the Co^{2+}-resistant current it was -91.7±18.9 mV (n = 3).

Activation of the TEA- and Co^{2+}-insensitive outward currents

The usual method for defining the activation curve of an outward current is to use a double-pulse protocol, where the membrane is first stepped to various potential levels to activate the conductance and at the end of each step the potential is brought to a constant level where the current is recorded instantaneously (Frankenhaeuser 1963). Attempts to perform such an analysis of tail currents from the outward currents of the tactile spine neuron were not successful because of the very small amplitude and rapid decay of the tail currents. However, Figs. 6.10 and 6.11 show that the outward currents that were resistant to Co^{2+} or TEA were both linearly dependent on the membrane potential, (i.e. the peak tail current vs. voltage curves were linear). This means that the range of membrane potentials over which the conductances are activated can be derived directly from the current-voltage curves, such as in Figs. 6.6. and 6.7.
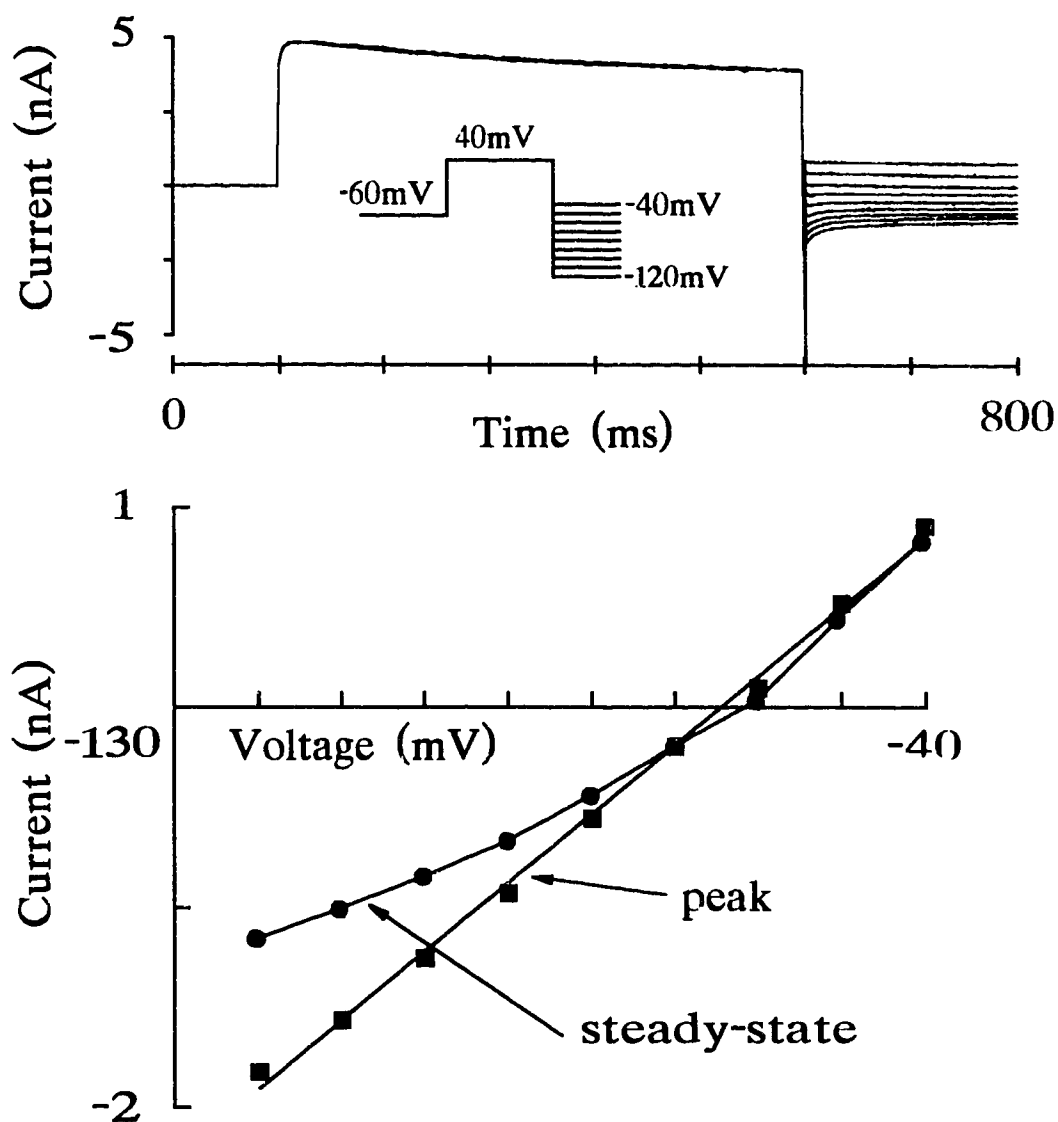
Figure 6.10. The reversal potential for the Co^{2+}-insensitive part of the outward current was determined using the same method as described earlier for the total outward current (Fig. 6.2). The peak and steady-state values of the tail currents (above) were plotted against the voltage (below) and the reversal potential was defined as the intersection of these two curves, in this case the reversal potential was -70 mV.
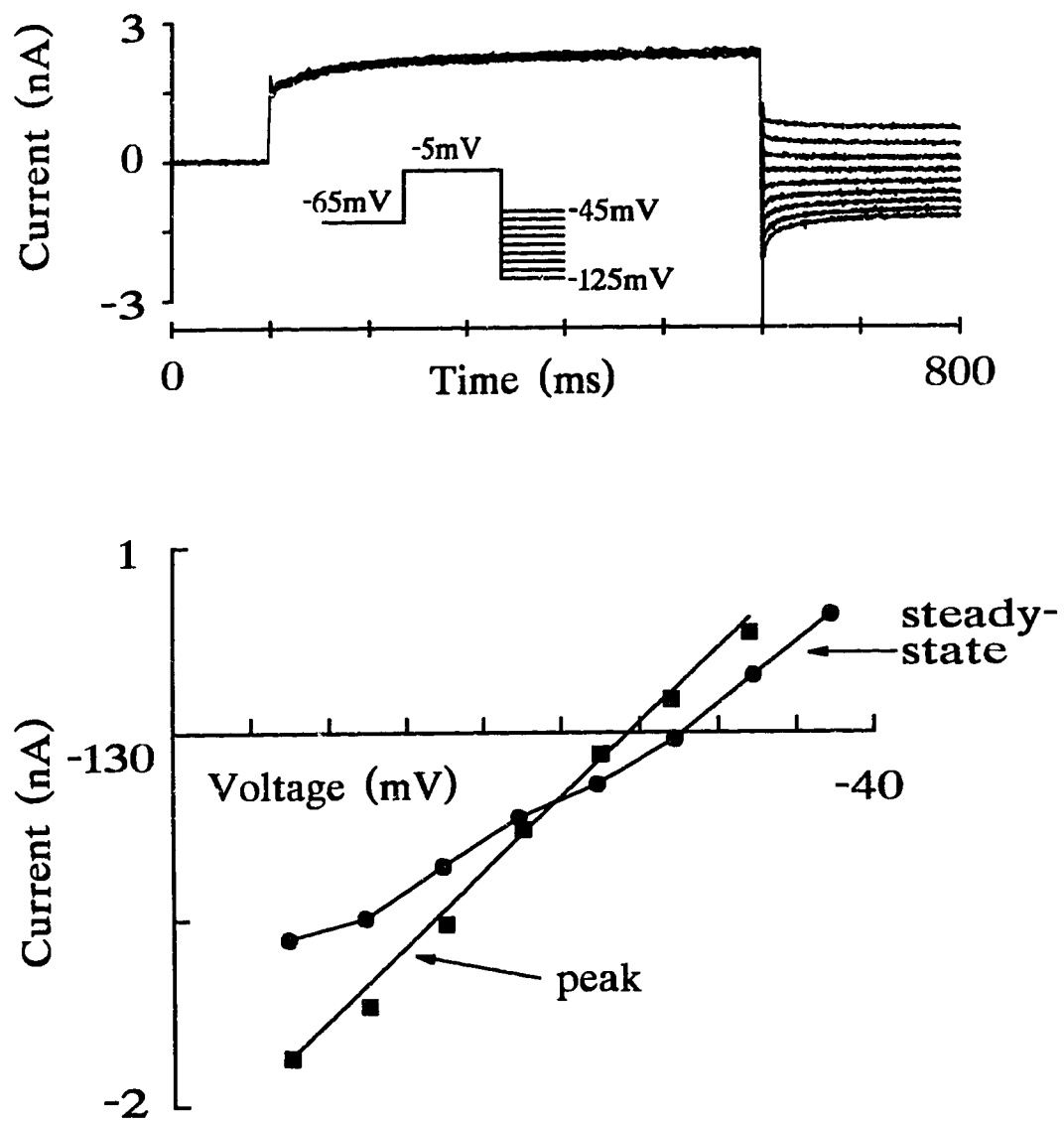
Figure 6.11. The tail currents (above) and reversal potential (below) for a TEA-insensitive current. In this cell the reversal potential of TEA resistant current was -80 mV.
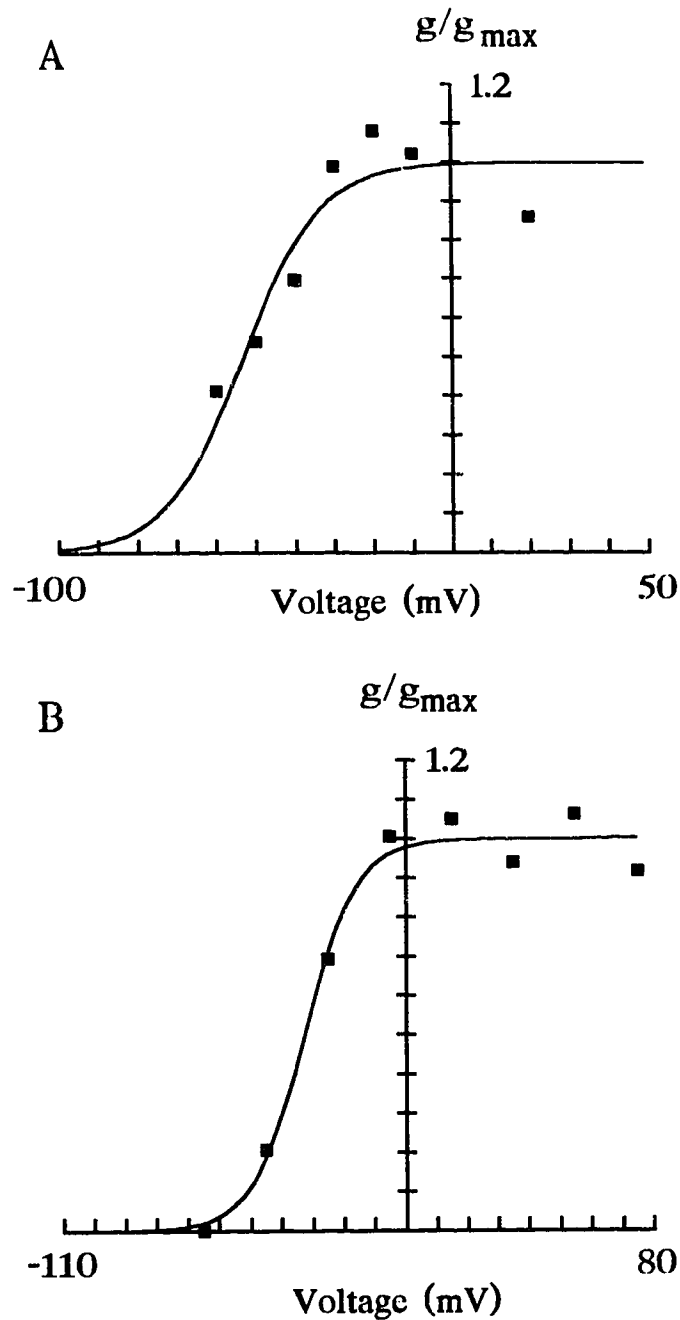
Figure 6.12. Voltage dependence of activation of **A** the Co^{2+}-insensitive and **B** TEA-insensitive outward currents. The relative conductances were measured form the chord conductance of the I_∞ using the reversal potential of the same cell (-105 mV in **A** and -80 mV in **B**). Boltzmann distributions fitted to the data gave the values **A**: V_{50} = -53.0 mV, s = 9.8 mV and g_{max} = 13 nS, and **B**: V_{50} -29.2 mV, s = 8.9 and g_{max} = 9 nS.

The voltage dependence of activation was defined from the I_∞ values that were obtained from the fits with equation (5.1). The activation data were fitted by the Boltzmann distribution (Fig. 6.12) using the measured reversal potentials for calculation of the conductance (Eqs. 5.2 and 5.3, page 88). Fitting was performed using the Levenberg-Marquardt general nonlinear algorithm (Press et al. 1990). The results obtained from a fit of four experiments with TEA-resistant currents were: V_{50} (half maximal activation) = -61.2 mV, s (the slope factor) = 4.0 mV and g_{max} (maximum conductance) = 20 nS. Three experiments with Co^{2+}-insensitive current gave values of V_{50} = -57.5 mV, the slope factor, s = 5.7 mV and g_{max} = 9 nS. The equivalent gating charge (z) for the activation could be calculated from the Eq. 5.4 (page 91). For the TEA-resistant current, z was 6.3 and for the Co^{2+}-resistant current, z was 4.4. The activation in both cases was clearly voltage dependent and followed a sigmoidal time course that indicates multiple gating particles (Hodgkin and Huxley 1952b).

Current-clamp

A typical recording of the effect of Co^{2+} on the voltage response of the tactile spine neuron is shown in Fig. 6.13. The threshold for action potentials in four different experiments where extracellular Ca^{2+} was replaced with Co^{2+} or Cd^{2+} decreased by about 80% (S.D. = ±20%, n = 4) from the original value and the resting potential was 13.2 mV (S.D. = ±4.3, n = 6) more negative than in the control saline. The action
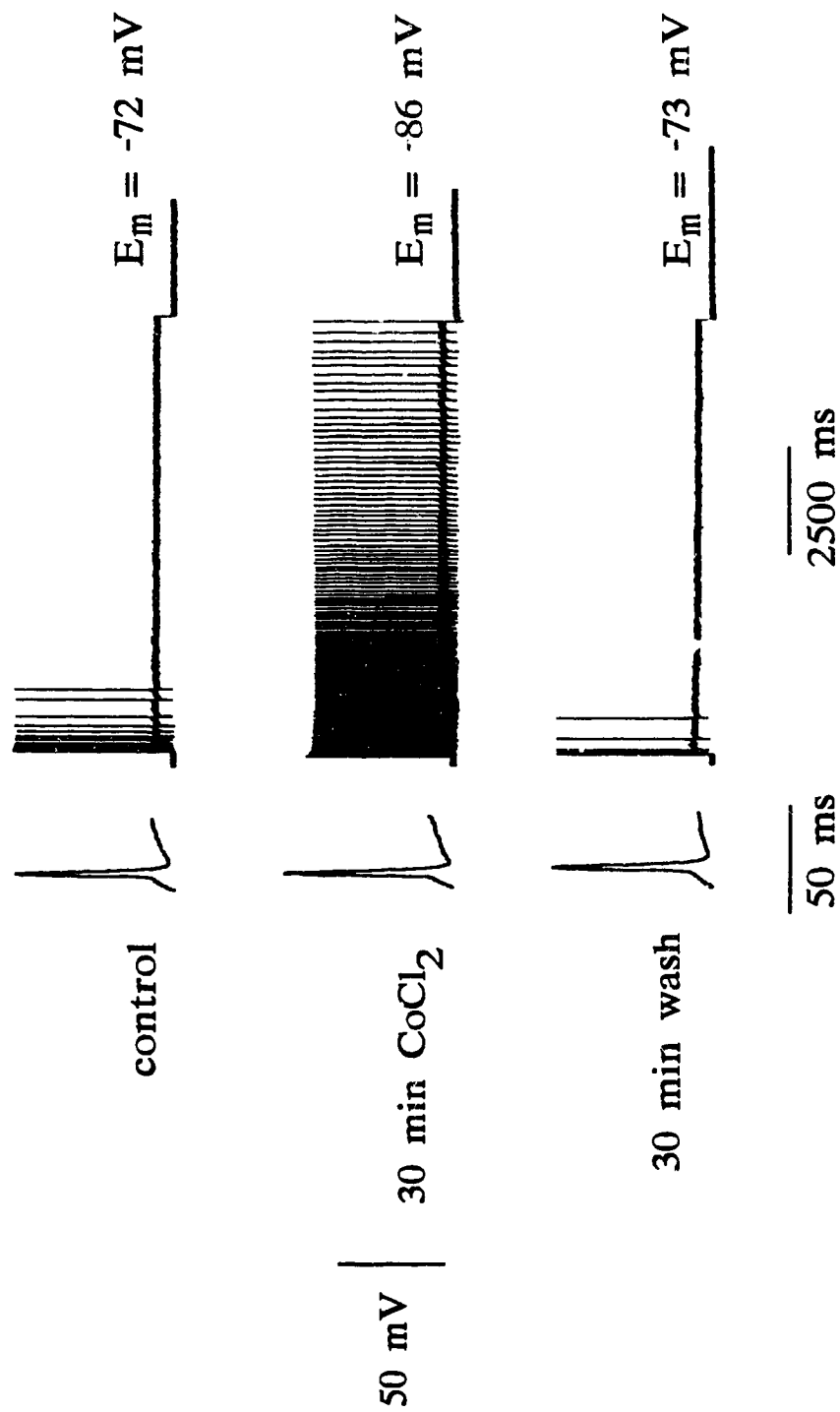
Figure 6.13. A current stimulus of 200 nA for 10 s elicited a rapidly, (< 2 s) adapting burst of action potentials in normal saline. The action potential frequency was significantly higher 30 min after replacement of Ca^{2+} with Co^{2+} in the saline. Ca^{2+} replacement did not affect the amplitude or duration of the individual action potentials.

127
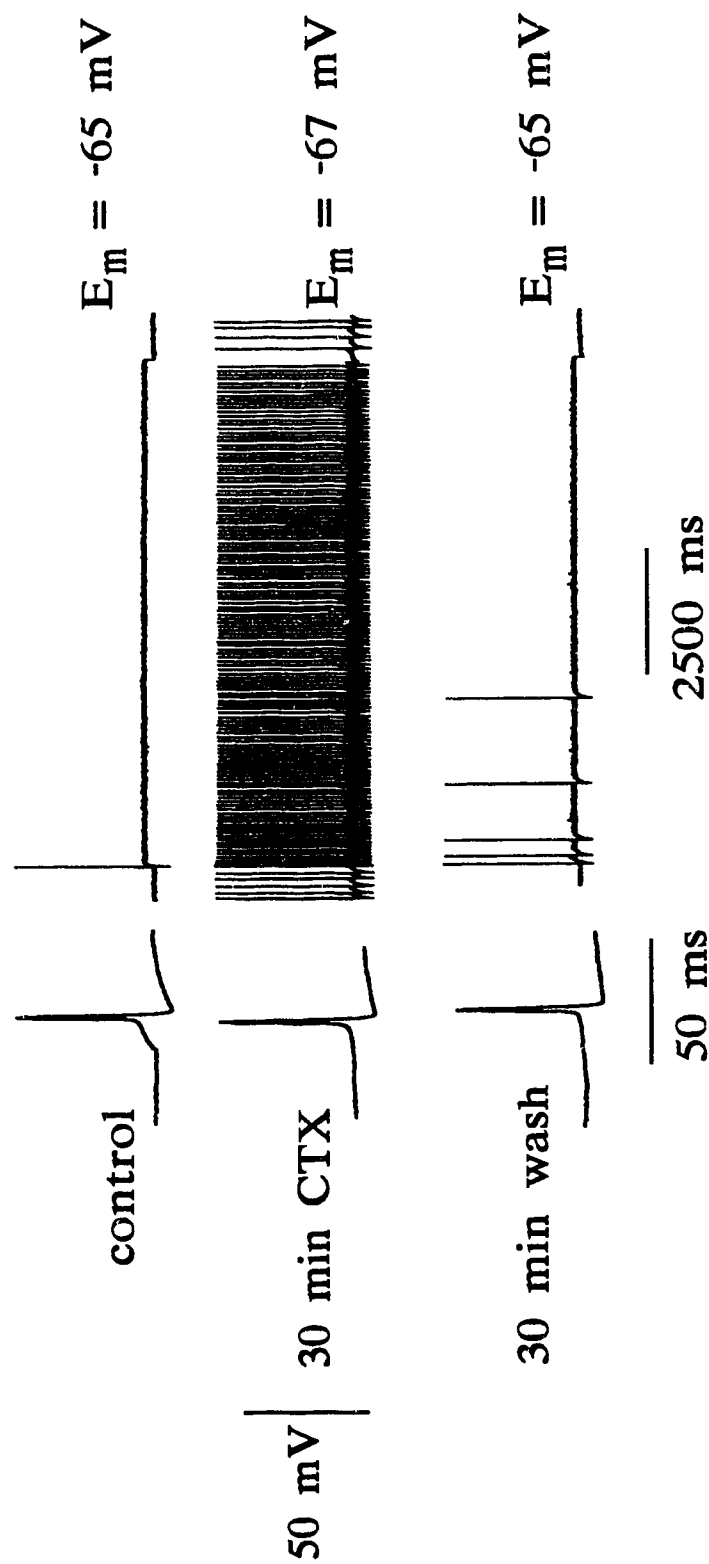
Figure 6.14. The effect of 30 nM CTX on the voltage response. A 100 pA current stimulus for 10 s elicited only one action potential in control saline, but application of CTX for 30 min made the cell fire spontaneously, the depolarizing pulse increasing the firing frequency. No changes in the shape or size of action potentials were observed.

128

potential frequency increased significantly in all four experiments after less than 30 min, and with longer observation times the cell usually started to fire spontaneously. No effect on the shape or amplitude of the action potentials was observed.

The effects of blockers of $I_{K(Ca)}$ on the voltage response were usually very slow. The experiment with 30 nM CTX shown in Fig. 6.14 was the only one that showed a very clear and rapid increase in the firing frequency, in other experiments CTX usually caused a small increase in the action potential frequency as well as in the threshold, but it usually took about two hours to develop. No significant changes in the resting potential or the size and shape of action potentials were detected. 5 or 10 μM apamin did not have any clear effect on the action potential frequency, amplitude or duration in four experiments up to two hours long, indicating an absence of SK-type Ca^{2+}-sensitive K^+-channels in the tactile spine neuron. This is consistent with the finding that there is no long lasting afterhyperpolarization following a burst of action potentials, as shown in Chapter 4.

TEA had a prominent effect on the size and shape of action potentials as shown in Fig. 6.15. The amplitude of the action potentials increased up to 30 mV and with longer TEA application times they did not repolarize totally before the end of the stimulus. There were no afterhyperpolarizations after individual action potentials or at the end of the burst. TEA also affected the resting potential, hyperpolarizing it 6.2 mV (S.D. $= \pm 4.6$, n $= 5$). Action potential frequency also increased at the beginning of the
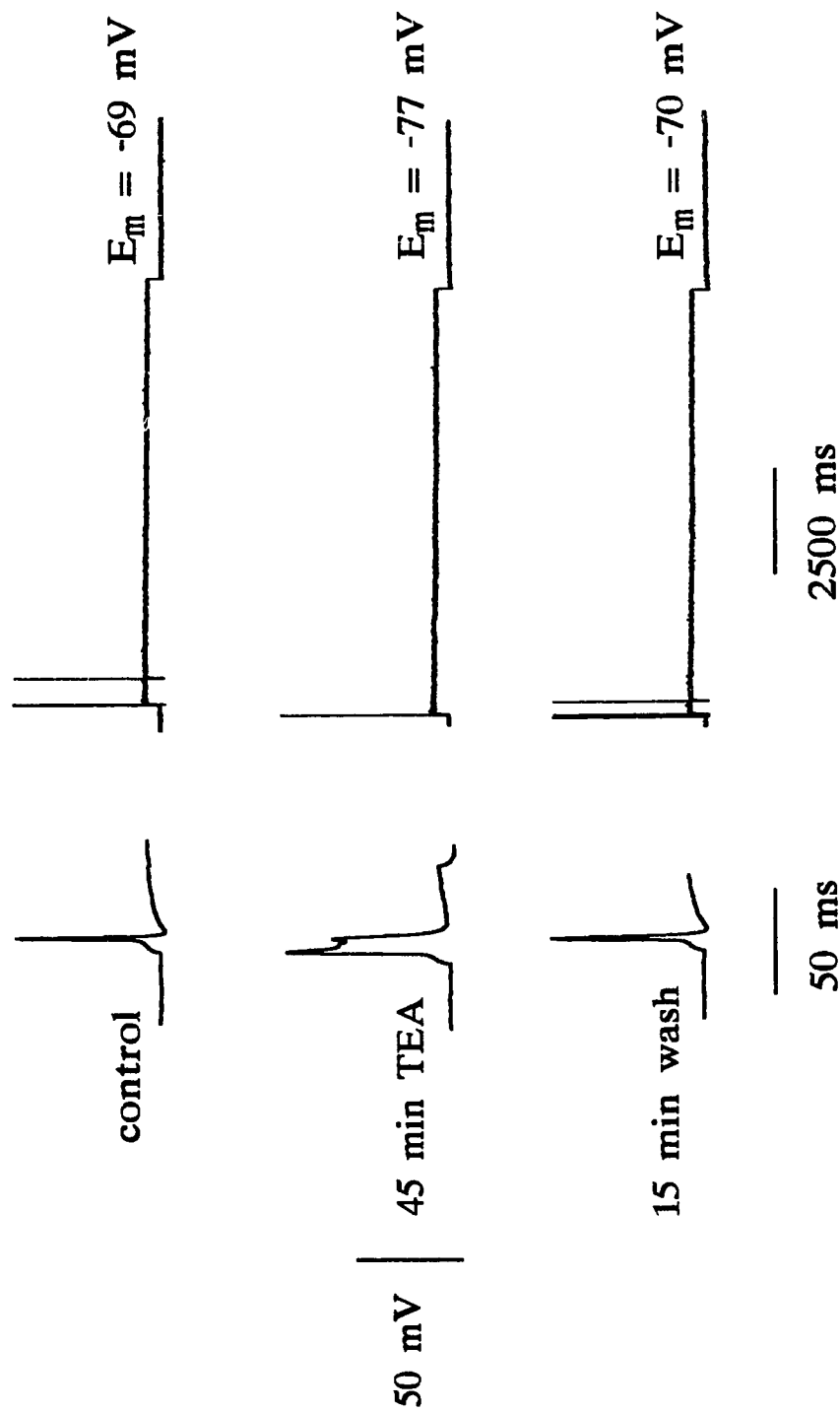
Figure 6.15. The effect of 50 mM TEA on the voltage response. A 120 pA current pulse for 10 s elicited a few action potentials and application of TEA significantly increased the duration and amplitude of these action potentials.

130

TEA effect before the repolarization became too long for proper observation of the frequency, and the threshold for production of action potentials decreased during the first half hour, but increased later.

6.3. Discussion

Two types of current profiles

The position of the electrode inside the tactile spine neuron could not be seen during the recordings. The fact that two different current patterns were observed in voltage-clamp suggests that the recording electrodes were in variable locations inside the cell. However, the only statistically significant difference (Table 6.1) in the electrophysiological properties of neurons with different outward current inactivation kinetics was the higher amplitude action potentials in those neurons whose outward current decayed with two exponential time constants. If some of the recordings had been made from the axon, the membrane resistance would have been significantly higher and the threshold for action potentials significantly lower than in the soma. Also, the narrow part of the dendrite would probably have had higher resistance. A similar difference was also found with I_A; it only existed in about half of the recordings, and its existence did not correlate with any other electrophysiological findings or with the other current profiles of the neurons.

Spatial differences in the ion channel populations of excitable cells have been observed previously. The functions of different parts of the neuron demand different types of channels. Axons mainly propagate the action potentials to the terminal, the cell body integrates input coming from the dendrites, either from presynaptic sources or from sensory stimulation. For example, the macroscopic K^+-currents in squid giant axons and cell bodies have similar time courses of activation, similar voltage dependencies and pharmacological sensitivities, but they differ in their inactivation kinetics. In the axon the inactivation time constant is over 1 s and in the soma only about 100 ms (Chabala 1984; Llano and Bookman 1986). It was shown in Chapter 3, that the only possible location where the electrode can impale the tactile spine neuron is the basal part of the dendrite or the soma. Therefore, the current recordings were most probably made from the same area.

Another explanation for these differences may be that the cells were not perfectly space-clamped. In insect photoreceptors it has been shown that the input resistance of the axon is much higher than that of the soma and the electrical properties of the soma are not affected by those of the axon (van Hateren 1986). The relationship between the sizes of the axon and soma in the tactile spine neuron is similar to that of photoreceptors, and this situation should allow a good space-clamp, especially when the propagating Na^+-currents are blocked.

The replacement of extracellular Ca^{2+}-ions with the same concentration of Co^{2+} left about one third of the outward current unaffected. The remaining part of the current showed faster activation and inactivation kinetics (Fig. 6.8) and its current-voltage curve (Fig. 6.6) was a simpler rising function than that of the total outward current. The persistent current was independent of intracellular Ca^{2+}-concentration and its reversal potential was -91.2 mV. The sigmoidal activation curve (Fig. 6.12A) was typical of a voltage-dependent K^+-current and the equivalent gating charge was estimated to be near four, which is the predicted value for K^+-current from Hodgkin-Huxley model. The current activated less than 10 mV above the resting potential and reached the half maximal activation at -57.5 mV. The fastest activation time constants at potentials above zero millivolts were less than one millisecond and the inactivation could be fitted with one exponential decay ranging from few hundred milliseconds to several seconds. The conductance of this current was about 9 nS. The slope conductance of the I_K in the solitary semicircular canal hair cells of the pigeon were estimated to be 6 - 7 nS (Lang and Correia 1989) and in blowfly second order photoreceptors about 20 nS (Hardie and Wecström 1990). All these findings fit well with the descriptions of the delayed rectifier type K^+-current, especially in other invertebrate preparations (Rudy 1988; Kolb 1990; Hille 1992).

The function of this current could be seen in the current-clamp recordings when TEA was added to the cockroach saline (Fig. 6.15). Although TEA obviously blocked part of the $I_{K(Ca)}$, as can be seen in the voltage-clamp recordings, the voltage response after TEA application was distinctly different than with any blockers of $I_{K(Ca)}$. TEA increased the duration and amplitude of action potentials which indicates the prevention of the repolarizing outward current. This is the classical function of I_K described by Hodgkin and Huxley (1952a) in the squid axon and later in several other neurons (Rudy 1988).

TEA-insensitive outward current

TEA-treatment decreased the outward current about one half from the control condi   Because only one third of the current remained after Co^{2+} treatment, it means that   A   o blocked part of the $I_{K(Ca)}$. The TEA-persistent current activated less than 10 mV above the resting potential in less than ten milliseconds and it did not inactivate at all during the recording period. It had a sigmoidal activation curve with a reversal potential of -86.8 mV, a maximal conductance of 20 nS and half maximal activation of -61.2 mV.

In several experiments with Co^{2+}, Cd^{2+} or CTX in the saline, the cell started to fire spontaneously, or the rate of adaptation decreased (Figs. 6.13 and 6.14). This treatment did not affect the afterhyperpolarization after individual action potentials, whose production is often described as one of the most important functions of the BK-channels,

neither did this treatment cause any effect on the AHP after a burst of action potentials. Apamin did not affect the voltage response and, because there is no long lasting AHP after the spike burst in the tactile spine neuron, there most probably are not any SK-channels either. These findings are somewhat different than those usually reported for the K_{Ca}-channels. CTX-sensitive BK-channels in most preparations have been shown to be involved in spike repolarization (Adams et al. 1982; Storm 1987; Gola et al. 1990) and to have a limited role in the spike frequency modulation. SK-channels are usually believed to be the ones responsible for spike frequency regulation because of their stronger Ca^{2+} sensitivity and small voltage dependency (Madison and Nicoll 1984; Lancaster et al. 1991). However, the experiments with the tactile spine neuron did not reveal the unitary conductance of the channels in question, and it is possible that more than one type of K_{Ca}-channel was contributing to the total current.

Comparison with other neurons

Significant $I_{K(Ca)}$ has previously been recorded from several other cockroach neurons. For example, in normally nonspiking motoneurons (Thomas 1984; Nightingale and Pitman 1989), blocking of $I_{K(Ca)}$ enabled the generation of Na^+-spikes. The patch-clamp recordings from these neurons have revealed channels with rather small unitary conductances (5 to 11 pS) that could be blocked by inorganic cations Cd^{2+} and Mn^{2+} as well as verapamil and TEA. However, TEA also blocked another component of the outward current that was dependent on voltage, but not on Ca^{2+} (Nightingale and Pitman

135

1989) indicating the presence of I_K in these neurons as well. From the dorsal unpaired median (DUM) neurons of cockroach, similar channels have been found among other K_{Ca}-channels with 34 and 110 pS unitary conductances (Dunbar and Pitman 1985). Christensen et al. (1988) found a number of outwardly rectifying channels in cultured embryonic brain cells of the cockroach. A similar variety of potassium channel types to the tactile spine neuron was found in nudibranch (*Tritonia*) nerve cell bodies by Thompson (1977): I_A, that was selectively blocked by 4-AP; I_K, that could be blocked by TEA and $I_{K(Ca)}$ that was inhibited with Co^{2+} or Mn^{2+}, and partly with high concentrations of TEA.

The current-clamp experiments showed that the $I_{K(Ca)}$ in the tactile spine neuron did not have any role in action potential repolarization, but had a strong effect on the regulation of action potential frequency. Crest and Gola (1993) described similar findings in *Helix* U neurons; the $I_{K(Ca)}$ was not involved in repolarizing Na^+-dependent action potentials, but was more active when the I_K progressively inactivated during firing. I_K has been shown to be the major current repolarizing the action potentials in molluscan soma (Aldrich et al. 1979; Adams et al. 1980) and in *Aplysia* bursting pacemaker neurons (Adams and Benson 1985). In vertebrates I_K is less important in spike repolarization (Storm 1987). For example, in frog sympathetic ganglia the $I_{K(Ca)}$ is the main repolarizing current (Adams et al. 1982) and in rat ganglia I_A has an important function in action potential repolarization (Beluzzi et al. 1985).

Great variability of K_{Ca}-channels has been found in neurons. In the same tissue, channels with different sensitivity to Ca^{2+}-concentration have been found, even though they have all been classified as BK-channels according to their toxin sensitivity and unitary conductance. In single-channel recordings the same BK-channel have even been shown to be able to undergo large changes in gating kinetics under steady-state conditions (McManus 1991).

Reversal potential and resting potential

The reversal potential obtained from the tail currents varied from -82 to -91 mV. The ratio for $[K^+]_{in}/[K^+]_{out}$ using the Nernst equation therefore varied from 26/1 to 37/1. The extracellular K^+-concentration in these experiments was 10 mM except in the experiments where TEA was added to the saline, and $[K^+]_{out}$ was lowered to 5 mM. Thomas and Treherne (1975) estimated the K^+-concentration of the cockroach hemolymph to be about 10 mM, but assumed that the strong glial barrier around the neurons would give a perineural K^+-concentration of about 3 to 5 mM, that is near the extracellular K^+-concentrations of several other insect species. The range of reversal potentials obtained in this work suggests an intracellular K^+-concentration of 78 - 185 mM if an extracellular concentration of 3 to 5 mM is used in the Nernst equation. Thomas (1984) evaluated the intracellular K^+-concentration in the cockroach central motoneurons to be about 180 mM.

In the experiments where pharmacological agents were added to the saline solution, changes in the resting membrane potential were often observed. In the experiments where TEA or 4-AP were added to the saline, the resting potential hyperpolarized 5 to 10 mV. In these experiments the external K^+-concentration was decreased from 10 to 5 mM, and this may explain the observed change in the resting potential. An even larger change, about 13 mV hyperpolarization, of the resting potential was detected, when Co^{2+} or Cd^{2+} were added to the saline. This suggests that closing of Ca^{2+}-channels, whose equilibrium potential is strongly positive, pulls the membrane to more negative potentials.

Previous extracellular recordings from the tactile spine neuron (French 1986a), did not produce clear evidence for the association of $I_{K(Ca)}$ with rapid adaptation. In that work extracellular Ca^{2+}-concentration was increased from 5 to 15 mM and it caused a rapid decrease in the action potential frequency. The same result was obtained with 15 mM Co^{2+} in the saline. This change was assumed to be caused by the divalent cation effect, which was probably the right conclusion. When external divalent ion concentration is increased, the threshold for excitation increases, because the divalent ions bind to the negatively charged sites on the membrane and neutralize the charges, thus preventing the intramembrane voltage sensor from detecting the membrane potential and Na^+-channels from opening (Hille 1992). Lowering the extracellular Ca^{2+}-concentration should have the opposite effect, but in the case of the tactile spine neuron, no such effect was detected (French 1986a). It has been very difficult to change the ion concentration around the neuron, for example in intracellular experiments, where external Na^+-ions were replaced

with choline ions, this change took usually more than three hours. This may be the reason why reduction of Ca^{2+}-concentration did not work in the earlier experiments. In the experiments of this chapter, the divalent cation concentration was kept constant by replacing the Ca^{2+} with equal concentration of Co^{2+} or Cd^{2+}, and therefore no divalent ion effect was observed.

In conclusion, the delay   tifier type of potassium current is the sole action potential repolarizing current in the tactile spine neuron. The most important function of the calcium-sensitive potassium current is modulation of action potential frequency. Both of these findings are typical for insect neurons. It is quite difficult to compare the time constants obtained from the voltage-clamp experiments to those recorded extracellularly using totally different recording methods, but if the $I_{K(Ca)}$ starts to modulate the action potential frequency as soon as it activates just above the threshold for firing, it may be the fastest component of adaptation detected in recordings of chapter 2. Its time constant of activation is in the same range (30 - 100 ms) as measured in Chapter 2 and earlier experiments in this laboratory. However, this challenges all the earlier findings that have indicated that this component is caused by the inactivation of Na^+-channels (French 1987; Basarsky and French 1991; Ramirez and French 1990). $I_{K(Ca)}$ stays activated a long time and it is possible that its function in adaptation is more cumulative and that it could form one or both of the slower components of adaptation described in Chapter 2. To confirm these results it would be useful to record the time course of adaptation intracellularly

using the same blockers as in the experiments of this chapter, and experimentally detect

the currents underlying the recorded components.

7. GENERAL DISCUSSION

Adaptation mechanisms

The main purpose of this research was to discover the ionic mechanisms underlying rapid adaptation in the cockroach femoral tactile spine neuron. This kind of information has not been obtained previously from any other insect cuticular mechanoreceptors or from the skin mechanoreceptors of vertebrates. Voltage-clamp measurements have been made from the hair cells of the vertebrate auditory system (Hudspeth 1986; Ashmore 1991) and stretch receptors of crustacea (Gestrelius and Grampp 1983; Rydqvist and Zhou 1989; Swerup and Rydqvist 1992; Purali and Rydqvist 1992). In crustacean stretch receptors, adaptation seems to involve several processes, including visco-elasticity, adaptation of the receptor channels, and two voltage-activated potassium currents (Swerup and Rydqvist 1992). However, calcium-activated potassium currents and A-currents do not seem to play important roles (Purali and Rydqvist 1992).

Adaptation in the tactile spine neuron

Previous research in this laboratory (reviewed in: French 1988; French 1992; French and Torkkeli 1994) revealed important aspects of the process of adaptation in this neuron and formed the direction for the research projects completed in this thesis. One of the most important previous findings was that rapid adaptation does not take place during the

141

transduction of the sensory stimulus into the receptor potential (French 1984a) but occurs

during action potential encoding. Therefore, visco-elastic movements or receptor current

adaptation are probably unimportant in controlling the cell's dynamic properties.

Identification of the mechanisms that make the cell stop firing during the encoding of

action potentials when a constant mechanical or electrical stimulus is used, were a major

subject of this thesis.

After the intracellular recording technique was developed to record electrical activity

from the tactile spine neuron (Basarsky and French 1991), suspicions about the accuracy

of the power-law theory (Chapman and Smith 1963) in describing the adaptation behavior

of the tactile spine neuron began to accumulate. In the first project that I contributed to

after starting to work in this laboratory (Stockbridge et al. 1991) we showed that the

frequency response function could be fitted by a model using a pair of exponential filters.

All the voltage-clamp experiments gave exponential rise and decay times for the currents

that participate in the modulation of the action potential frequency. Because techniques

for mechanical stimulation during intracellular recording in this neuron have not yet been

developed and are probably very difficult, the power-law behavior was re-examined using

extracellular recording techniques (Chapter 2). The long (up to 30 s) recording times

combined with the use of the log binning method (Sigworth and Sine 1987) revealed that

the sum of two or three exponential decays gave an accurate fit of the adaptation over

the 30 s period of response duration. This finding fits with one of the original theories

explaining the adaptation, that the power-law is only an estimation of a more complicated

combination of many exponential decays with varying time constants spread over the time course of the response (Chapman and Smith 1963; Thorson and Biederman-Thorson 1974).

Sodium-dependent processes

French (1989a) discovered that the threshold for action potentials during adaptation in the tactile spine neuron was labile, increasing with membrane depolarization and decreasing when the membrane was hyperpolarized. This threshold change occurred with two separate components. The faster component had a time constant of 60 - 70 ms depending on the recording techniques (French 1989a; French and Patrick 1994), and it was linked to slow sodium inactivation because of its sensitivity to agents that block this process (French 1987; Ramirez and French 1990; Basarsky and French 1991). The second component was considerably longer, varying from 500 ms (French and Patrick 1994) to more than 1,000 ms (French 1989a), and its origin has never been established, although it was suggested to be caused by an electrogenic Na^+-pump (French 1989b).

It was not possible to study the Na^+-current under voltage-clamp. Even though the space-clamp appeared to be good locally, the action potentials propagating along the axon interfered with the recording even when the repolarizing outward current was blocked by TEA. Under subthreshold conditions a small inward current could be recorded, and it always had at least two components of inactivation. However, it was very difficult to

143

interpret these results, because the contributions of outward currents to the decay of the inward currents may have been significant. Therefore, I did not succeed in revealing the contribution of Na^+-channel inactivation to adaptation. The fact that TEA often totally prevented the repolarization of action potentials and significant[l] increased their amplitude, indicates that the inactivation of Na^+-current does not produc[e] the repolarization, but also that the amplitude of the action potentials is par[tly] regulated by the delayed rectifier K^+-current.

When the membrane fires action potentials, the K^+-ions flowing through the voltage- and Ca^{2+}-sensitive ion channels accumulate on the extracellular side, and Na^+-ions that come via the voltage sensitive channels accumulate inside the cell. This ion accumulation normally increases the activity of an electrogenic Na^+-pump, which has been suggested to be an important component of adaptation in some neurons (Sokolove and Cooke 1971; Scriven 1981). Attempts to study the function of the electrogenic Na^+-pump in the tactile spine neuron using the cardiac glycoside ouabain as a blocking agent, showed that the pump has an important function in this cell. The block rapidly caused spontaneous action potentials that were followed by a large depolarization and a decrease of action potential size and frequency. Inhibition of the pump function has been shown to lead to accumulation of K^+-ions in the extracellular space, which in turn leads to the activation of Na^+-channels and significant depolarization of the membrane (Läuger 1991). In the tactile spine neuron this depolarization occurred rapidly (in less than 10 ms), and made it impossible to study the pump function under voltage-clamp. However, these

experiments showed that the function of the electrogenic Na$^+$-pump in the tactile spine neuron is probably important, and it could form one of the components of adaptation.

Potassium currents

Here, it was shown that both I_A and $I_{K(Ca)}$ had important, but separate, roles in adaptation. I_A increased the interval between action potentials, activating rapidly when the cell hyperpolarized following the repolarization. I_A also inactivated rapidly, in 10 to 20 ms, and it could only prevent the cell from firing action potentials when rather small depolarizations were used for stimulation. The higher the depolarization the smaller the effect of I_A, because not enough hyperpolarization would follow the spike repolarization to release the inactivation of A-channels. I_A did not cause an afterhyperpolarization following the action potential, but opposed membrane depolarization.

The only current that caused action potential repolarization was I_K. The finding that TEA increased the amplitude of the spikes as well as their duration suggests that this current turned on before the Na$^+$-channels were inactivated. The repolarizing effect of I_K was strong enough to produce an AHP after the spikes as well as the small and fast AHP after a burst of spikes. In the tactile spine neuron there was no long-lasting AHP after the spike burst, and no indication of SK-type Ca^{2+}-sensitive K$^+$-channels were found in the voltage- or current-clamp experiments. In several other preparations, an $I_{K(C}$, that causes a long AHP has been shown to be an important component of adaptation.

145

$I_{K(Ca)}$ had a strong effect on the action potential frequency. However, it is difficult to relate the results obtained under voltage-clamp to those from current-clamp recordings. Under voltage-clamp, command voltage steps from 10 to 150 mV above rest lasting 100 - 500 ms were used to elicit the current response, while under current-clamp, current stimuli that varied from 100 to 500 pA were used, corresponding to voltages of 5 to 20 mV, if the membrane resistance is assumed to be about 50 MΩ. All the outward currents decayed rapidly after the depolarization was terminated. It is not clear what happens to these currents in the real situation when the membrane, in response to a relatively small depc 'arization, fires an action potential whose amplitude is about 80 mV and then repolarizes in a few milliseconds to below the resting potential. The peak depolarization of an action potential is strong enough to fully activate $I_{K(Ca)}$, which opposes the tendency of the cell to fire more action potentials. The activation and inactivation of $I_{K(Ca)}$ would alternate between turning fully on at the peak of the spike and turning off when the membrane returns to rest.

The potassium currents contributing to adaptation in the tactil' spine neuron are significantly different to those in the crustacean stretch receptors. Although the rapidly and slow! adapting stretch receptor neurons of crayfish were shown to have at least two different types of outward current. neither of them was sensitive to extracellular Ca^{2+} id neither had an A-current (Rydqvist and Zhou 1989; Purali and Rydqvist 1992). A-current and Ca^{2+}-activated K^+-currents have been found in the hair cells of vertebrate

146

auditory and vestibular systems, although their contributions to the adaptation have not been described (Hudsbeth 1986; Ashmore 1991).

If it is difficult to compare the results from the voltage-clamp and current-clamp recordings, it is even more complicated to relate the results obtained extracellularly to those from voltage-clamp recordings. The function of I_A could probably not have been detected in the ext   ar recordings, because its time constants of activation and inactivation are far too fast to explain any of the three components described in Chapter 2 when mechanical stimulation was used to study the time course of adaptation. In the experiments performed earlier in this laboratory (French 1989a), neither of the components causing the threshold change could be I_A, because a conditioning depolarization enhanced both of these components, and I_A would be inactivated under these conditions. $I_{K(Ca)}$ could explain part of the threshold change, because a conditioning depolarization would activate $I_{K(Ca)}$ and increase the threshold. French (1987) also found that a conditioning hyperpolarization decreased the action potential threshold. This can be explained as a removal of inactivation of Na^+-channels. A similar effect was seen in Fig. 4.3 where the release of hyperpolarization caused an anodal break action potential. I_A would also activate when the hyperpolarization is followed by depolarization, and its effect in reducing the action potential frequency under these conditions would be stronger than normal.

147

Therefore, $I_{K(Ca)}$ is probably responsible for at least one of the extracellularly recorded components of adaptation. Although its activation time constants suggest that it might be the faster component of adaptation, all the previous work has indicated that this component is caused by slow Na^+ inactivation (French 1989a; Ramirez and French 1990; Basarsky and French 1991). However, the role of slowly inactivating Na^+-channels was mainly inferred from the effects of chloramine-T and other mild oxidizing agents, which have recently been shown to also affect K^+-channels (Dubois and Rouzaire-Dubois 1991). Therefore, these toxins may be too unspecific to separate the roles of sodium inactivation and potassium currents in the adaptation of the tactile spine neuron. Similarly, the effect of phentolamine in decreasing the action potential frequency has never been clearly linked to the inactivation of Na^+-channels.

Future directions

It would be worthwhile to examine the contribution of the ionic currents to the time course of adaptation by repeating the work in Chapter 2 using intracellular electrical stimulation to reveal the time constants of adaptation. The ionic currents could then be blocked using the agents that were effective here, while observing the changes in the rate of adaptation. The exchange of extracellular solutions is easier during electrical stimulation, and intracellular recordings allow complete separation of activity in the tactile spine neuron from other neurons.

A more ambitious project would be to voltage-clamp the neuron while tying the axon via a hole in the femur. This would give a better space-clamp and possibly allow investigation of the kinetics of the inward Na^+-currents. However, this may be very difficult, because the binding would probably have to be done when the electrode is already inside the neuron, since impalement is achieved by detecting the extracellular action potentials from the axon to locate the neuron.

The receptor current or voltage has never been recorded intracellularly from any insect mechanosensillum, given the location and size of these sensilla. However, it is worth trying to perform intracellular recording during mechanical stimulation from the tactile spine neuron, using basically the same dissection method to that in the experiments here, but holding the wall of the tactile spine with a similar kind of pusher as used in the experiments of Chapter 2. I believe that the electrode would stay inside the cell during the small movements (a few nanometers) that are needed to elicit the receptor current. This would be a very interesting research project because of the arrangement of the potassium rich environment around the dendrite of the neuron described in Chapter 1. Receptor currents and potentials have already been recorded from spider slit sensilla in this laboratory (Juusola et al. 1994), but the composition of the receptor lymph space of slit sensilla differs from that of insect cuticular mechanoreceptors by being rich in Na^+-ions, and thus its receptor potential is probably driven by sodium.

149

It would be difficult to study the kinetics of the outward currents in the tactile spine neuron better than was done here without using patch-clamp techniques. The same is true for the usually very small Ca^{2+}-currents. The subdivision and functions of the different K^+-currents, especially the Ca^{2+}-sensitive K^+-currents, in the tactile spine neuron seem to be different than those of vertebrate neurons or insect central neurons, and patch clamp research could provide new information about the evolution of these channels. Research into the functions of the electrogenic ion pump would also need complete control of the constitution of the ions inside and outside the membrane. However, making a cell culture from tactile spine neurons would probably be too difficult, and for patch-clamp research a better idea might be to use some other cockroach tissue that has more mechanosensilla than the leg. For example, the antenna on the head of the cockroach or the cerci at the back might be used. Some progress has already been made with culturing chordotonal antennal mechanoreceptors in this laboratory (Stockbridge and French 1989) but this must be improved to remove the glia from around the neurons.

Conclusions

Although rapid adaptation is a widespread feature of sensory receptors, its ionic basis has not been clearly established in any preparation because the small sizes of most mechanoreceptors have severely restricted the range of experiments that can be performed to examine the mechanisms of adaptation. The cockroach tactile spine is an unusual example of an insect mechanoreceptor from which intracellular recordings are

possible and this thesis described the first voltage-clamp recordings from his neuron. The results indicate that different processes contribute to adaptation in different sensory cells such as the crayfish stretch receptor neurons and tactile spine neuron. However, more similar potassium currents have been recorded in the hair cells of vertebrate auditory and vestibular systems, so that similar type of adaptation may occur in these functionally related structures. The potassium currents that were observed in the tactile spine neuron were relatively selective to the different blocking agents used, so that the tactile spine neuron, or other insect cuticular receptors, may provide useful preparations for future work on sensory transduction and adaptation.

APPENDIX I

Constructing log time histograms

Linear histograms

Consider a receptor in which the rate of action potential discharge after a step stimulus, y, follows an exponential decay: $y = a.e^{-t/\tau}$, where a is the initial rate in action potentials per second (ap/s), t is time, and τ is the time constant. If the action potentials are counted into a histogram bin (Fig. 1) that starts at time t_1 and ends at time t_2, then the number of action potentials in the bin will be given by:

$$b = \int_{t_1}^{t_2} y\,dt \tag{1}$$

The indefinite integral of the exponential decay is given by:

$$\int y\,dt = \int ae^{-t/\tau}\,dt = -a\tau e^{-t/\tau} + c \tag{2}$$

where c is a constant of integration. Since the integral is zero at time zero, $c = a\tau$ and:

$$\int y\,dt = a\tau - a\tau e^{-t/\tau} = a\tau(1-e^{-t/\tau}) \tag{3}$$

From equations (1) and (3):

152

$$b = a\tau(1 - e^{-t_2/\tau} - 1 + e^{-t_1/\tau})$$
(4)

or:

$$b = a\tau(e^{-t_1/\tau} - e^{-t_2/\tau})$$
(5)

If the histogram bins are equally spaced in time so that the nth. bin starts at $t_1 = n\Delta t$ and ends at $t_2 = (n+1)\Delta t$, its contents will be:

$$b_n = a\tau(e^{-n\Delta t/\tau} - e^{-(n+1)\Delta t/\tau})$$
(6)

or:

$$b_n = a\tau(1 - e^{-\Delta t/\tau})e^{-n\Delta t/\tau}$$
(7)

Therefore, the histogram has the form of a simple exponential decay in n with time constant $\tau/\Delta t$.

Log histograms

Following Sigworth and Sine (1987) we construct a log histogram by defining a new abscissa x, where:
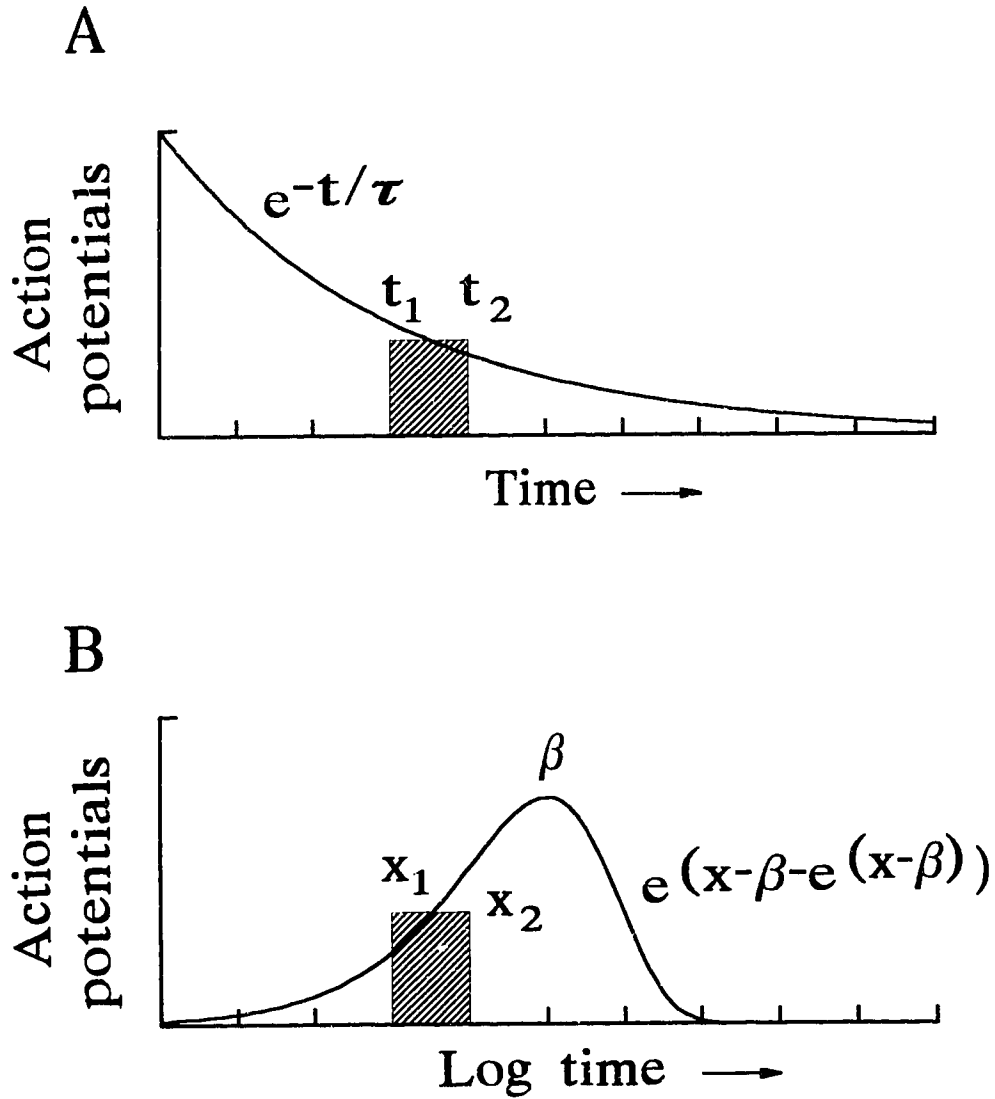
Figure 1. Constructing linear and log time step response histograms. **A** When action potentials are counted into bins that are linearly spaced in time following the step, so that $t_1 = n\Delta t$, $t_2 = (n+1)\Delta t$, an exponentially decaying rate gives bin heights that also follow an exponential decay (equation 7). **B** If the time axis, t, is replaced with a log time axis, $x = \ln t$, the same exponentially falling rate of action potentials produces a histogram whose form is the exponential of an exponential, as shown. The shape, but not the amplitude, of this function is independent of the decay time constant, τ, and it reaches a maximum at $\beta = \ln \tau$.

154

$$x = \ln t, \quad t = e^x, \quad \beta = \ln \tau, \quad \tau = e^\beta \tag{8}$$

Then the distribution of equation (3) becomes:

$$G(x) = a e^\beta (1 - e^{-e^{(x-\beta)}}) \tag{9}$$

and the rate function is obtained by differentiating $G(x)$ with respect to x:

$$g(x) = a e^\beta e^{x - \beta - e^{(x-\beta)}} \tag{10}$$

If we define a generic function (Sigworth and Sine, 1987) of the same form:

$$g_0(x) = e^{z - e^z} \tag{11}$$

then:

$$g(x) = g_0(x - \beta) \tag{12}$$

From equation (12) it is seen that $g(x)$ has a shape which is independent of ß (and hence of τ). It has a maximum at $x = $ ß ($t = \tau$) and it slides along the abscissa, x, with changes in ß (τ). The form of $g(x)$ is also shown in Fig. 1.

Therefore, if the rate of action potentials per second follows the sum of several exponentials:

155

$$y = \sum_{i=0}^{n} a_i e^{-t/\tau_i}$$ (13)

Then the log histogram will consist of the sum of a set of similarly shaped functions (equation 11) with peaks at the log time constants, β_i.

BIBLIOGRAPHY

Adams DJ, Smith SJ & Thompson SH 1980: Ionic currents in molluscan soma. *Annu Rev Neurosci* 3:141-167.

Adams P 1982: Voltage-dependent conductances of vertebrate neurones. *Trends Neurosci* 5:116-119.

Adams PR, Constanti A, Brown DA & Clark RB 1982: Intracellular Ca^{2+} activates a fast voltage-sensitive K^+ current in vertebrate sympathetic neurones. *Nature* 296:746-749.

Adams PR & Galvan M 1986: Voltage-dependent currents of vertebrate neurons and their role in membrane excitability. *Adv Neurol* 44:137-170.

Adams WB & Benson JA 1985: The generation and modulation of endogenous rhythmicity in the *Aplysia* bursting pacemaker neurone R15. *Prog Biophys Molec Biol* 46:1-49.

Aldrich RW, Getting PA & Thompson SH 1979: Mechanisms of frequency-dependent broadening of molluscan neurone soma spikes. *J Physiol* (Lond) 291:531-544.

Andersen M & Hablitz JJ 1992: Kinetic properties of a transient outward current in rat neocortical neurons. *J Neurophysiol* 68:1133-1142.

Armstrong CM 1971: Interaction of tetraethylammonium ion derivatives with the potassium channels of giant axons. *J Gen Physiol* 58:413-437.

Ashmore JF 1991: The electrophysiology of hair cells. *Annu Rev Physiol* 53:465-476.

Baker M, Howe JR & Ritchie JM 1993: Two types of 4-aminopyridine-sensitive potassium currents in rabbit Schwann cells. *J Physiol* (Lond) 464:321-342.

Barrett EF & Barrett JN 1976: Separation of two voltage-sensitive potassium currents, and demonstration of a tetrodotoxin-resistant calcium current in frog motoneurones. *J Physiol* (Lond) 255:737-774.

Barrett EF & Barrett JN 1982: Intracellular recording from vertebrate myelinated axons: Mechanism of the depolarizing afterpotential. *J Physiol* (Lond) 323:117-144.

Barth FG 1981: Strain detection in the arthropod exoskeleton. In: Laverack MS & Cosens DJ (eds.) *Sense organs*. Chapter VII. Blackie, pp. 112-141.

Basarsky TA & French AS 1991: Intracellular measurements from a rapidly adapting sensory neuron. *J Neurophysiol* 65:49-56.

Beluzzi O, Sacchi O & Wanke E 1985: A fast transient outward current in the rat sympathetic neurones studied under voltage-clamp conditions. *J Physiol* 358:91-102.

Bernard J, Guillet JC & Coillot JP 1980: Evidence for a barrier between blood and sensory terminal in an insect mechanoreceptor. *Comp Biochem Physiol A* 67:573-579.

Biederman-Thorson M & Thorson J 1971: Dynamics of excitation and inhibition in the light-adapted *Limulus* eye in situ. *J Gen Physiol* 58:1-19.

Blatz LA & Magleby KL 1986: Single apamin-blocked Ca-activated K^+ channels of small conductance in cultured rat skeletal muscle. *Nature* 323:718-720.

Blight AR & Someya S 1985: Depolarizing afterpotentials in myelinated axons of mammalian spinal cord. *Neuroscience* 15:1-12.

Bohnenberger J 1981: Matched transfer characteristics of single units in a compound slit sense organ. *J Comp Physiol* 142:391-402.

Brown MC & Stein RB 1966: Quantitative studies on the slowly adapting stretch receptor of the crayfish. *Kybernetik* 3:175-185.

Chabala LD 1984: The kinetics of recovery and development of potassium channel inactivation in perfused squid (*Loligo Pealei*) giant axons. *J Physiol* (Lond) 356:193-220.

Chapman KM 1965: Campaniform sensilla on the tactile spines of the legs of the cockroach. *J Exp Biol* 41:191-203.

Chapman KM & Smith RS 1963: A linear transfer function underlying impulse frequency modulation in a cockroach mechanoreceptor. *Nature* 197:699-701.

Chesler M & Fourtner CR 1981: Mechanical properties of a slow muscle in the cockroach. *J Neurobiol* 12:391-402.

Christensen BN, Larmet Y, Shimahara T, Beadle D & Pichon Y 1988: Ionic currents in neurones cultured from embryonic cockroach (*Periplaneta americana*) brains. *J Exp Biol* 135:193-214.

Connor JA 1975: Neural repetitive firing: a comparative study of membrane properties of crustacean walking leg axons. *J Neurophysiol* 38:922-932.

Connor JA & Stevens CF 1971: Voltage clamp studies of a transient outward membrane current in gastropod neural somata. *J Physiol* 213:21-30.

Cres M & Gola M 1993: Large conductance Ca^{2+}-activated K^+ channels are involved in both spike shaping and firing regulation in *Helix* neurones. *J Physiol* 465:265-287.

Dubois JM 1982: Properties and physiological roles of K^+ currents in frog myelinated nerve fibers as revealed by 4-aminopyridine. In: Lechat P, Thesleff S & Bowman WC (eds.) *Advances in the biosciences, Vol 35, Aminopyridines and similarly acting drugs.* Pergamon, Oxford, pp. 43-51.

Dubois J-M & Rouzaire-Dubois B 1991: Interactions of 4-aminopyridine with normal and chloramine-T-modified K channels of neuroblastoma cells. *Pflügers Arch* 419:93-100.

Dunbar SJ & Pitman RM 1985: Unitary currents recorded from the soma of identified cockroach neurones using the patch clamp technique. *J Physiol* (Lond) 367:88P.

Edman A, Gestrelius S & Grampp W 1983: Intracellular ion control in lobster stretch receptor neuron. *Acta Physiol Scand* 118:241-252.

Erler G 1983: Reduction of mechanical sensitivity in an insect mechanoreceptor correlated with destruction of its tubular body. *Cell Tissue Res* 23:451-61.

Erler G & Thurm U 1981: Dendritic impulse initiation in an epithelial sensory neuron. *J Comp Physiol* A 142: 237-249.

Erxleben C 1989: Stretch-activated current through single ion channels in the abdominal stretch receptor organ of the crayfish. *J Gen Physiol* 94:1071-1083.

Finkel AS & Redman S 1984: Theory and operation of a single microelectrode voltage clamp. *J Neurosci Meth* 11:101-127.

Frankenhaeuser B 1963: A quantitative description of potassium current in myelinated nerve fibres of *Xenopus laevis*. *J Physiol* (Lond) 169:424-430.

Frankenhaeuser B & Huxley AF 1964: The action potential in the myelinated nerve fibre of *Xenopus laevis* computed on the basis of voltage clamp data. *J Physiol* (Lond) 171:02-315.

French AS 1980: Sensory transduction in an insect mechanoreceptor: linear and nonlinear properties. *Biol Cybernetics* 38:115-123.

French AS 1984a: The receptor potential and adaptation in the cockroach tactile spine. *J Neurosci* 4:2063-2068.

French AS 1984b: Dynamic properties of the action potential encoder in an insect mechanosensory neuron. *Biophys J* 46:285-290.

French AS 1984c: After-hyperpolarization and receptor potential attenuation following bursts cf action potentials in an insect mechanoreceptor. *Can J Physiol Pharmacol* 63:18-22.

French AS 1984d: Action potential adaptation in the femoral tactile spine of the cockroach, *Periplaneta americana*. *J Comp Physiol* A 155: 803-812.

French AS 1985: The effects of ter ¬erature on action potential encoding in the cockroach tactile spine. *J Comp Physio. .*1 156:817-821.

French AS 1986a: The role of calcium in the rapid adaptation of an insect mechanoreceptor. *J Neurosci* 6:2322-2326.

French AS 1986b: Strength-duration properties of a rapidly adapting insect sensory neuron. *J Comp Physiol* A 159:757-764.

French AS 1987: Removal of rapid sensory adaptation from an insect mechanoreceptor neuron by oxidizing agents which affect sodium channel inactivation. *J Comp Physiol* A 161:275-282.

French AS 1988: Transduct ¬n mechanisms of mechanosensilla. *Annu Rev Entomol* 33:39-58.

French AS 1989a: Two cc ¬ponents of rapid sensory adaptation in a cockroach mechanoreceptor neuron. *J N. rophysiol* 62:768-777.

French AS 1989b: Ouabain selecti. ely affects the slow component of sensory adaptation in an insect mechanoreceptor. *Brain Res* 504:112-114.

French AS 1992: Mechanotransduction. *Annu Rev Physiol* 54:135-152.

French AS, Holden AV & Stein RB 1972: The estimation of the frequency response function of a mechanoreceptor. *Kybernetik* 11: 15-23.

French AS & Sanders EJ 1981: The mechanosensory apparatus of the femoral tactile spine of the cockroach, *Periplaneta americana*. *Cell Tissue Res* 219:53-68.

French AS & Kuster JE 1981: Sensory transduction in an insect mechanoreceptor: extended bandwidth measurements and sensitivity to stimulus strength. *Biol Cybern* 42:87-94.

French AS & Kuster JE 1982: The effects of temperature on mechanotransduction in the cock. ach tactile spine. *J Comp Physiol* A 147:251-258.

French AS & Sanders EJ 1983: The mechanosensory apparatus of the femoral tactile spine of the cockroach *Periplaneta americana*. *Cell Tissue Res* 219:53-68.

French AS, Klimaszewski AR & Stockbridge LL 1993a: The morphology of the sensory neuron in the cockroach femoral tactile spine. *J Neurophysiol* 69:669-673.

French AS, Sanders EJ, Dyszyk E, Prasad S, Torkkeli PH, Haskins J & Murphy RA 1993b: Immunocytochemical localization of sodium channels in an insect central nervous system using a site-directed antibody. *J Neurobiol* 24:939-948.

French AS & Patrick SK 1994: A nonlinear model of step responses in the cockroach tactile spine neuron. *Biol Cybern* 70:435-441.

French AS & Torkkeli PH 1994: The basis of rapid adaptation in mechanoreceptors. *News in Physiological Sciences* 9:158-161.

Gestrelius S & Grampp W 1983: Impulse firing in the slowly adapting stretch receptor neurone of lobster and its numerical simulation. *Acta Physiol Scand* 118:253-261.

Glynn IM 1957: The action of cardiac glycosides on sodium and potassium movements in human red cells. *J Physiol* (Lond) 136:148-173.

Gola M, Ducreux & Chaneux H 1990: Ca^{2+}-activated K^+ current involvement in neuronal function revealed by *in situ* single-channel analysis in *Helix* neurones. *J Physiol* (Lond) 420:73-109.

Grampp W 1966: The impulse activity in different parts of the slowly adapting stretch receptor neuron of the lobster. *Acta Physiol Scand* 66 Suppl 262, pp. 36.

Guharay & Sachs F 1984: Stretch-activated single ion channel currents in tissue cultured embryonic chick skeletal muscle. *J Physiol* (Lond) 352:685-701.

Guillet JC, Bernard J, Coillot JP & Callec JF 1980: Electrical properties of the dendrite in an insect mechanoreceptor: effects of antidromic or direct electrical stimulation. *J Insect Physiol* 26: 755-762.

Hagiwara S, Kusano K & Saito N 1961: Membrane changes of *Onchidium* nerve cell in potassium rich media. *J Physiol* (Lond) 155:470-489.

Hamill OP & McBride DW Jr 1994: Molecular mechanisms of mechanoreceptor adaptation. *NIPS* 9:53-59.

Hamon A, Guillet JC & Callec JJ 1988: Initiation and conduction of impulses in mechanosensory neurons: effects of hypoxia. *Comp Biochem Physiol* 91A: 797-805.

Hardie RC & Weckström M 1990: Three classes of potassium channels in large monopolar cells of the blowfly *Calliphora vicina*. *J Comp Physiol* A 167:723-736.

Hille B 1992: *Ionic channels of excitable membranes*. Sinauer, Sunderland, pp. 667.

Hobbs A 1982: Comparative effects of external monovalent cations on sodium pump activity and ouabain inhibition rates in squid giant axon. *J Pysiol* (Lond) 331:567-576.

Hodgkin AL & Hyxley AF 1952a: The components of membrane conductance in the squid giant axon of *Loligo*. *J Physiol* (Lond) 116:473-496.

Hodgkin AL & Huxley AF 1952b: A quantitative description of membrane current and its application to conduction and excitation in nerve. *J Physiol* (Lond) 117:500544.

Howard J, Roberts WM & Hudspeth AJ 1988: Mechanoelectrical transduction by hair cells. *Annu Rev Biophys Biophys Chem* 17:99-124.

Hudspeth AJ 1986: The ionic channels of a vertebrate hair cell. *Hearing Res* 22:21-27.

Ito F & Komatsu Y 1979: Calcium-dependent regenerative responses in the afferent nerve terminal of the frog muscle spindle. *Brain Res* 175:160-164.

Ito F, Komatsu Y & Fujitsuka N 1982: GK(Ca)-dependent cyclic potential changes in the sensory nerve terminal of frog muscle spindle. *Brain Res* 252:39-50.

Juusola M, Seyfarth E-A & French AS 1994: The sodium-dependent receptor current in a new mechanoreceptor preparation *J Neurophysiol* (In press).

Karnovsky MJ 1965: A formaldehyde-glutaraldehyde fixative of high osmolarity for use in electron microscopy. *J Cell Biol* 27:138A.

Kolb H-A 1990: Potassium channels in excitable and nonexcitable cells. *Rev Physiol Biochem Pharmacol* 115:51-91.

Kuffler SW, Nicholls JG & Martin AR 1984: *From neuron to brain. A cellular approach to the function of the nervous system*. Sinauer, Sunderland. pp. 651.

Küppers J 1974: Measurements of the ionic milieu of the receptor terminal in mechanoreceptive sensilla of insects. In Schwartzkopff J (ed.) *Mechanoreception*. Rhein-Westf Akad Wiss 53:387-394.

Kuster JE & French AS 1983: Sensory transduction in a locust multipolar joint receptor: the dynamic behavior under a variety of stimulus conditions. *J Comp Physiol* A 150:207-215.

Kuster JE, French AS & Sanders EJ 1983: The effects of microtubule dissociating agents on the physiology and cytology of the sensory neuron in the femoral tactile spine of the cockroach, *Periplaneta americana* L. *Proc R Soc London* Ser B 219:397-412.

Lancaster B & Adams PR 1986: Calcium-dependent current generating the aterhyperpolarization of hippocampal neurons. *J Neurophysiol* 55:1268-1282.

Lancaster B, Nicoll RA & Perkel DJ 1991: Calcium activates two types of potassium channels in rat hippocampal neurons in culture. *J Neurosci* 11:23-30.

Landolt JP & Correia MJ 1980: Neurodynamic response analysis of anterior semicircular canal afferents in the pigeon. *J Neurophysiol* 43:1746-1770.

Lang DG & Correia MJ 1989: Studies of solitary semicircular canal hair cells in the adult pigeon. II Voltage-dependent ionic conductances. *J Neurophysiol* 62:935-945.

Lansman JB, Hallam TJ & Rink TJ 1987: Single stretch-activated ion channels in vascular endot··ir·   . ·· mechanotransducers. *Nature* 325:811-813.

Latorre R, Coronad· ·t ·   ·.rgara C 1984: K$^+$ channels gated by voltage and ions. *Annu Rev Physiol* 46 ·'·· ··

Läuger P 1991: *Electrogenic ion pumps.* Sinauer, Sunderland, pp. 313.

Lewis DV & Wilson WA 1982: Calcium influx and post-stimulus current during early adaptation in *Aplysia* giant neurons. *J Neurophysiol* 48:202-216.

Linden TM & Palka J 1992: A student apparatus for recording action potentials in cockroach legs. *Am J Physiol* 262:S18-S22.

Llano I & Bookman RJ 1986: Ionic conductances of squid giant fiber lobe neurons. *J Gen Physiol* 88:543-569.

Loewenstein WR & Mendelson M 1965: Components of receptor adaptation in a Pacinian Corpuscle. *J Physiol* (Lond) 177:377-397.

MacDermott AB & Weight FF 1982: Action potential repolarization may involve a transient, Ca^{2+}-sensitive outward current in a vertebrate neurone. *Nature* 300:185-188.

Madison DV & Nicoll RA 1982: Noradrenaline blocks accommodation of pyramidal cell discharge in the hippocampus. *Nature* 299:636-638.

Madison DV & Nicoll RA 1984: Control of the repetitive discharge of rat CA1 pyramidal neurones *in vitro*. *J Physiol* 354:319-331.

Madison DV & Nicoll RA 1986: Cyclic adenosine 3',5'-monophosphate mediates beta-receptor actions of noradrenaline in rat hippocampal pyramidal cells. *J Physiol* 372:245-259.

Martinac B, Adler J & Kung C 1990: Mechanosensitive ion channels of *E coli* activated by amphipaths. *Nature* 348:261-263.

McIver SB 1985: Mechanoreception. In: Kerkut GA & Gilbert LI (eds.) *Comprehensive insect physiology, biochemistry and pharmacology*. Vol 6. Pergamon, Oxford UK, pp. 71-132.

McIver S & Siemicki R 1975: Campaniform sensilla on the palps of *Anopheles stephensi* Lisotn (Diptera; Culicidae). *Int J Insect Morph Embryol* 4:127-130.

McManus OB 1991: Calcium-activated potassium channels: regulation by calcium. *J Bioenerget Biomembr* 23:537-560.

Mellon D Jr & Kennedy D 1964: Impulse origin and propagation in a bipolar sensory neuron. *J Gen Physiol* 47:487-499.

Mendelson M & Loewenstein WR 1964: Mechanisms of receptor adaptation. *Science* 144:554-555.

Miller C, Moczydlowski E, Latorre R, Phillips M 1985: Charybdotoxin, a protein inhibitor of single Ca^{2+}-activated K^+ channels from mammalian skeletal muscle. *Nature* 313:316-318.

Mirolli M 1981: Fast inward and outward current channels in a non-spiking neurone. *Nature* (Lond) 292:251-253.

Moore RK 1960: *Travelling-Wave Engineering*. McCraw-Hill, New York, Toronto, London, pp. 360.

Moran DT & Varela FG 1971: Microtubules and sensory transduction. *Proc Natn Acad Sci* U.S.A. 68:757-760.

Mountcastle VB, LaMotte RH & Carli G 1972: Detection threshold for stimuli in humans and monkeys: comparison with threshold events in mechanoreceptive afferent nerve fibres innervating the monkey hand. *J Neurophysiol* 35:122-136.

Nakajima S & Takahashi K 1966: Post-tetanic hyperpolarization and electrogenic Na pump in stretch receptor neurone of crayfish. *J Physiol* (Lond) 187:105-127.

Nakajima S & Onodera K 1969a: Adaptation of the generator potential in the crayfish stretch receptors under constant length and constant tension. *J Physiol* (Lond) 200:187-204.

Nakajima S & Onodera K 1969b: membrane properties of the stretch receptor neurones of crayfish with particular reference to mechanisms of sensory adaptation. *J Physiol* (Lond) 200:161-185.

Narahashi T 1964: Restoration of action potential by anodal polarization in lobster giant axons. *J Cell Comp Physiol* 64:73-96.

Nicklaus R, Lundqvist PG & Wersäll J 1967: Electronmikroskopie am sensorischen Apparat de Fadenhaare auf den Cerci der Schabe *Periplaneta americana*. *Z Vergl Physiol* 56:412-415.

Nightingale WD & Pitman RM 1989: Ionic currents in the soma of an identified cockroach motoneurone recorded under voltage-clamp. *Cop Biochem Physiol* 93A:85-93.

Norris CH, Ricci AJ, Housley GD & Guth PS 1992: The inactivating potassium currents of hair cells isolated from the crista ampullaris of the frog. *J Neurophysiol* 68:1642-1653.

Oldham KB & Spanier J 1974: *The Fractional Calculus*. Academic Press, New York and London, pp. 234.

Ottoson D & Swerup C 1985a: Ionic dependence of early adaptation in the crustacean stretch receptor. *Brain Res* 336:1-8.

Ottoson D & Swerup C 1985b: Effects of intracellular injection on early adaptation of crustacean stretch receptor. *Brain Res* 336:9-17.

Pallotta BS, Magleby KL & Barrett JN 1981: Single channel recordings of Ca^{2+}-activated K^+ current in rat muscle cell culture. *Nature* 293:471-474.

Pennefather P, Lancaster B, Adams PR & Nicoll RA 1985: Two distinct Ca-dependent K currents in bullfrog sympathetic ganglion cells. *Proc Natl Acad Sci USA* 82:3040-3044.

165

Polder H-R & Swandulla D 1990: Design and optimal tuning of single and double electrode voltage clamp systems using methods of optimization by modulus hugging. *Pflügers Arch* 415:S77.

Poppele RE & Chen WJ 1972: Repetitive firing behavior of mammalian muscle spindle. *J Neurophysiol* 35:357-367.

Press WH, Flannery BP, Teukolsky SA & Vetterling WT 1990: *Numerical recipes in C*. Cambridge University Press, Cambridge UK, pp. 735.

Pringle JWS & Wilson VJ 1952: The response of a sense organ to a harmonic stimulus. *J Exp Biol* 29:220-234.

Pumphrey RJ 1936: Slow adaptation of a tactile receptor in the leg of the common cockroach. *J Physiol* (Lond) 87:6P.

Purali N & Rydqvist B 1992: Block of potassium outward currents in the crayfish stretch receptor neurons by 4-aminopyridine, tetraethylammonium chloride and some other chemical substances. *Acta Physiol Scand* 146:67-77.

Quinta-Ferreira ME, Rojas E & Arispe N 1982: Potassium currents in the giant axon of the crab *Carcinus maenas*. *J Membrane Biol* 66:171-181.

Ramirez J-M & French AS 1990: Phentolamine selectively affects the fast sodium component of sensory adaptation in an insect mechanoreceptor. *J Neurobiol* 21:893-899.

Reinhart PH, Chung S & Levitan IB 1989: A family of calcium-dependent potassium channels from rat brain. *Neuron* 2:1031-1041.

Rennie KJ & Ashmore JF 1991: Ionic currents in isolated vestibular hair cells from the guinea-pig crista ampullaris. *Hearing Res* 51:279-292.

Rice MJ, Galun R & Finlayson LH 1973: Mechanotransduction in insect neurones. *Nature New Biol* 241:286-288.

Ritchie AK 1987: Two distinct calcium-activated potassium currents in a rat anterior pituitary cell line. *J Physiol.* (Lond) 385:591-609.

Rogawski MA 1985: The A-current: how ubiquitous a feature of excitable cells is it? *Trends Neurosci* 8:214-219.

Romey G & Lazduski M 1984: The coexistence in rat muscle cells of two distinct classes of Ca^{2+}-dependent K^+ channels with different pharmacological properties and different physiological functions. *Biochem Biophys Res Commun* 118:669-674.

166

Rudy B 1988: Diversity and ubiquity of K channels. *Neuroscience* 25:729-749.

Ruppersberg JP, Frank R, Pongs O & Strocker M 1991: Cloned $I_K(A)$ channels reopen during recovery from inactivation. *Nature* (Lond) 353.

Rydqvist B & Zhou J-Y 1989: Potential-dependent potassium currents in the slowly adapting stretch receptor neuron of the crayfish. *Acta Physiol Scand* 137:409-419. 336.

Schafer R & Reagan PD 1981: Colchicine reversibly inhibits electrical activity in arthropod mechanoreceptors. *J Neurobiol* 12:155-166.

Scriven DRL 1981: Modelling repetitive firing and bursting in a small unmyelinated nerve fiber. *Biophys J* 35:715-730.

Seyfarth E-A, Bohnenberger J & Thorson J 1982: Electrical and mechanical stimulation of a spider slit sensillum: outward current excites. *J Comp Physiol* 147:423-432.

Seyfarth E-A & French AS 1994: Intracellular characterization of identified sensory cells in a new spider mechanoreceptor preparation. *J Neurophysiol* 71:1422-1427.

Sigworth FJ & Sine SM 1987: Data transformations for improved display and fitting of single-channel dwell time histograms. *Biophys J* 52:1047-1054.

Sokolove PG & Cooke IM 1971: Inhibition of impulse activity in a sensory neuron by an electrogenic pump. *J Gen Physiol* 57:125-.

Solc CK & Aldrich RW 1988: Voltage-gated potassium channels in larval CNS neurons of *Drosophila*. *J Neurosci* 8:2556-2570.

Stanfield PR 1983: Tetraethylammonium ions and the potassium permeability of excitable cells. *Rev Physiol Biochem Pharmacol* 97:1-67.

Stockbridge LL & French AS 1989: Ion channels in isolated mechanosensory neurons from the connective chordotonal organ in the pedicel of the American cockroach. *Soc Neurosci Abstr* 15:1287.

Stockbridge LL & French AS 1991: The morphological basis of intracellular measurements in the cockroach tactile spine neuron. *J Comp Physiol* A 169:471-477.

Stockbridge LL, Torkkeli PH & French AS 1991: Intracellular nonlinear frequency response measurements in the cockroach tactile spine neuron. *Biol Cybern* 65:181-187.

Storm JF 1987: Action potential repolarization and a fast after-hyperpolarization in rat hippocampal pyramidal cells. *J Physiol* 385:733-759.

Swerup C & Rydqvist B 1992: The abdominal stretch receptor organ of the crayfish. *Comp Biochem Physiol* 103A:423-431.

Tempel BL, Papazian DM, Schwarz TL, Jan YN & Jan LY 1987: Sequence of a probable potassium channel component encoded at *Shaker* locus of *Drosophila*. *Science* 237:770-775.

Teorell T 1971: A biophysical analysis of mechano-electrical transduction. In: Loewenstein WR (ed.) *Handbook of sensory physiology* Vol 1. Springer-Verlag, Berlin, pp. 291-339.

Thomas MV 1984: Voltage-clamp analysis of a calcium-mediated potassium conductance in cockroach (*Periplaneta americana*) central neurones. *J Physiol* (Lond) 350:159-178.

Thomas MV & Treherne JE 1975: An electrophysiological analysis of extra-axonal sodium and potassium concentrations in the central nervous system of the cockroach (*Periplaneta americana* L.). *J Exp Biol* 63:801-811.

Thompson S 1982: Aminopyridine block of transient potassium current. *J Gen Physiol* 80:1-18.

Thompson SH 1977: Three pharmacologically distinct potassium channels in molluscan neurones. *J Physiol* 265:465-488.

Thompson SH & Aldrich RW 1980: Membrane potassium channels. In: Cotman CW, Poste G & Nicolson GL (eds.) *The cell surface and neuronal function*. Elsevier, Amsterdam, pp. 49-85.

Thorson J & Biederman-Thorson M 1974: Distributed relaxation processes in sensory adaptation. *Science* 183:161-172.

Thurm U 1965 An insect mechanoreceptor. Part II: Receptor potentials. *Cold Spring Harbor Symp Quant Biol* 30:83-94.

Tomko DL, Peterka RJ, Schor RH & O'Leary DP 1981: Response dynamics of horizontal canal afferents in barbiturate-anesthetized cats. *J Neurophysiol* 45:376-396.

Ulbricht W & Wagner H-H 1976: Block of potassium channels of the nodal membrane by 4-aminopyridine and its partial removal on depolarization. *Pflügers Arch* 367:77-87.

Vallbo AB 1964: Accommodation related to inactivation of the sodium permeability in single myelinated nerve fibres from *Xenopus laevis*. *Acta Physiol Scand* 61:429-444.

van Hateren JH 1986: An efficiet algorithm for cable theory, apllied to blowfly photoreceptor cells and LMCs. *Biol Cybern* 54:301-311.

Wagoner PK & Oxford GS 1987: Cation permeation through voltage-dependent potassium channels in the squid axon. Characteristics and mechanisms. *J Gen Physiol* 90:261-290.

Weckström M, Kouvalainen E & Juusola M 1992: Measurement of cell impedance in frequency domain using discontinuous current clamp and white-noise-modulated current injection. *Pflügers Arch* 421:469-472.

Wilson WA & Goldner MM 1975: Voltage clamping with a single microelectrode. *J Neurobiol* 6:411-422.

Wolbarsht ML 1960: Electrical characteristics of insect mechanoreceptors. *J Gen Biol* 44:105-122.

Yarom Y, Sugimori M & Llinas R 1985: Ionic currents and firing patterns of mammalian vagal motoneurons *in vitro*. *Neuroscience* 16:719-737.

Zhang L & Krnjevic K 1987: A... depresses selectively the afterhyperpolarization of cat spinal motoneurons. *Neuro. ... ... 74:58-62.